การให้ความร้อนด้วยคลื่นไมโครเวฟและกระตุ้นด้วยโพแทสเซียมไฮดรอกไซต์เพื่อเปลี่ยน
ผักตบชวาให้เป็นถ่านกัมมันต์

นางสาวภูริชญา คุปตจิต

วิทยานิพนธ์นี้เป็นส่วนหนึ่งของการศึกษาตามหลักสูตรปริญญาวิศวกรรมศาสตรมหาบัณฑิต
สาขาวิชาวิศวกรรมเคมี ภาควิชาวิศวกรรมเคมี
คณะวิศวกรรมศาสตร์ จุฬาลงกรณ์มหาวิทยาลัย
ปีการศึกษา 2560

MICROWAVE HEATING WITH POTASSIUM HYDROXIDE ACTIVATION FOR CONVERTING WATER HYACINTH INTO ACTIVATED CARBON

Miss Purichaya Kuptajit

จุฬาลงกรณ์มหาวิทยาลัย
CHULALONGKORN UNIVERSITY
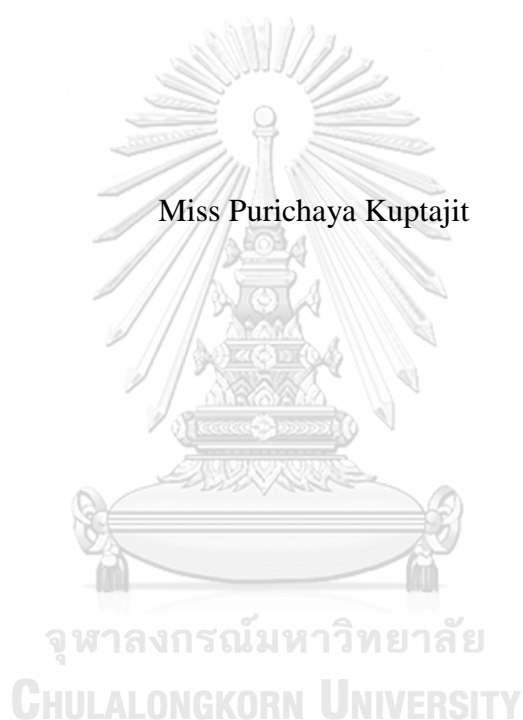
A Thesis Submitted in Partial Fulfillment of the Requirements
for the Degree of Master of Engineering Program in Chemical Engineering
Department of Chemical Engineering
Faculty of Engineering
Chulalongkorn University
Academic Year 2017

Thesis Title	MICROWAVE HEATING WITH POTASSIUM HYDROXIDE ACTIVATION FOR CONVERTING WATER HYACINTH INTO ACTIVATED CARBON
By	Miss Purichaya Kuptajit
Field of Study	Chemical Engineering
Thesis Advisor	Associate Professor Tawatchai Charinpanitkul, D.Eng.
Thesis Co-Advisor	Professor Noriaki Sano, D.Eng.

Accepted by the Faculty of Engineering, Chulalongkorn University in Partial Fulfillment of the Requirements for the Master's Degree

⋯⋯⋯⋯⋯⋯⋯⋯⋯⋯ Dean of the Faculty of Engineering
(Associate Professor Supot Teachavorasinskun, D.Eng.)

THESIS COMMITTEE

⋯⋯⋯⋯⋯⋯⋯⋯⋯⋯ Chairman
(Chalida Klaysom, Ph.D.)

⋯⋯⋯⋯⋯⋯⋯⋯⋯⋯ Thesis Advisor
(Associate Professor Tawatchai Charinpanitkul, D.Eng.)

⋯⋯⋯⋯⋯⋯⋯⋯⋯⋯ Thesis Co-Advisor
(Professor Noriaki Sano, D.Eng.)

⋯⋯⋯⋯⋯⋯⋯⋯⋯⋯ Examiner
(Professor Artiwan Shotipruk, Ph.D.)

⋯⋯⋯⋯⋯⋯⋯⋯⋯⋯ External Examiner
(Kajornsak Faungnawakij, D.Eng.)

ภูริชญา คุปตจิต : การให้ความร้อนด้วยคลื่นไมโครเวฟและกระตุ้นด้วยโพแทสเซียมไฮดรอกไซต์เพื่อเปลี่ยนผักตบชวาให้เป็นถ่านกัมมันต์ (MICROWAVE HEATING WITH POTASSIUM HYDROXIDE ACTIVATION FOR CONVERTING WATER HYACINTH INTO ACTIVATED CARBON) อ.ที่ปรึกษาวิทยานิพนธ์หลัก: รศ. ดร. ธวัชชัย ชรินพาณิชกุล, อ.ที่ปรึกษาวิทยานิพนธ์ร่วม: ศ. ดร. โนริเอกิ ซะโน, หน้า.

วิทยานิพนธ์ฉบับนี้ประสบความสำเร็จในการสังเคราะห์ถ่านกัมมันต์จากผักตบชวาโดยใช้การกระตุ้นด้วยโพแทสเซียมไฮดรอกไซต์และให้ความร้อนด้วยคลื่นไมโครเวฟ จากการศึกษาพบว่าการนำคลื่นไมโครเวฟเข้ามาช่วยในขั้นตอนการกระตุ้นยังช่วยลดเวลาที่ใช้เหลือเพียง 1 นาที จากระบบปกติที่ทำในเตาไฟฟ้าจะต้องใช้เวลาในการกระตุ้นถึง 1 ชั่วโมง เพราะการกระตุ้นด้วยคลื่นไมโครเวฟก่อนให้เกิดความร้อนอย่างสม่ำเสมอในวัตถุที่ให้ความร้อน อีกทั้งอัตราการให้ความร้อนยังเร็วกว่าการให้ความร้อนด้วยเตาไฟฟ้าแบบทั่วไป นอกจากนี้จากการศึกษายังพบว่าปริมาณของถ่านกัมมันต์และอัตราส่วนของธาตุคาร์บอนในถ่านกัมมันต์ที่ได้ยังลดลงตามเวลาที่ใช้ในการกระตุ้นและปริมาณโพแทสเซียมไฮดรอกไซต์ที่เพิ่มขึ้น และพบว่าถ่านกัมมันต์ที่ได้จากการให้ความร้อนด้วยคลื่นไมโครเวฟเป็นเวลา 1 นาที และใช้อัตราส่วนโดยมวลของโพแทสเซียมไฮดรอกไซต์กับผักตบชวาที่ผ่านการคาร์บอไนเซชั่นที่ 3 ต่อ 1 มีพื้นที่ผิวจำเพาะเป็น 1,073 ตารางเมตรต่อกรัมคาร์บอน กระบวนการเติมน้ำเข้าสู่ระบบในขั้นตอนกระตุ้นเป็นอีกปัจจัยที่ถูกนำมาศึกษาและพบว่าถ่านกัมมันต์ที่เตรียมได้จากการให้ความร้อนด้วยคลื่นไมโครเวฟและเติมน้ำด้วยการเตรียมให้แก็สไนโตรเจนมีความชื้นร่วมกับการแช่ในสารละลายโพแทสเซียมไฮดรอกไซต์มีพื้นที่ผิวจำเพาะเป็น 208 ตารางเมตรต่อกรัมคาร์บอน

ภาควิชา	วิศวกรรมเคมี	ลายมือชื่อนิสิต	
สาขาวิชา	วิศวกรรมเคมี	ลายมือชื่อ อ.ที่ปรึกษาหลัก	
ปีการศึกษา	2560	ลายมือชื่อ อ.ที่ปรึกษาร่วม	

5970396221 : MAJOR CHEMICAL ENGINEERING

KEYWORDS: ACTIVATED CARBON / WATER HYACINTH / POTASSIUM HYDROXIDE ACTIVATION / MICROWAVE IRRADIATION

PURICHAYA KUPTAJIT: MICROWAVE HEATING WITH POTASSIUM HYDROXIDE ACTIVATION FOR CONVERTING WATER HYACINTH INTO ACTIVATED CARBON. ADVISOR: ASSOC. PROF. TAWATCHAI CHARINPANITKUL, D.Eng., CO-ADVISOR: PROF. NORIAKI SANO, D.Eng., pp.

Activated carbon was successfully synthesized form dried water hyacinth via KOH activation with microwave irradiation. Resultant activated carbon with large specific surface area can be produced using microwave irradiation for 1 minute which was consumed less time than conventional heating method that consumed 1 hour. Microwave irradiation can be a strategic way to improve uniform and quick heating to prepare porous carbons by inducing dipole rotation in atomic scale and creating a frictional force between atoms and molecules within heated material so that volumetric heating inside the heated material is realized. The BET analysis shown that the activated carbon, derived by KOH activated with microwave irradiation for 1 minute with mass radio of potassium hydroxide to carbonized water hyacinth at 3:1, possessed a large specific surface area of 1,073 $m^2\,g^{-1}$-carbon. Furthermore, methods for adding water into activation system was also studied. Specific surface area of activated carbon prepared by using both wet nitrogen gas and wet impregnation possessed specific surface area of 208 $m^2\,g^{-1}$-carbon.

Department:	Chemical Engineering	Student's Signature	....
Field of Study:	Chemical Engineering	Advisor's Signature	....
Academic Year:	2017	Co-Advisor's Signature	....

ACKNOWLEDGEMENTS

CONTENTS

จุฬาลงกรณ์มหาวิทยาลัย

CHULALONGKORN UNIVERSITY

LIST OF TABLES

จุฬาลงกรณ์มหาวิทยาลัย

CHULALONGKORN UNIVERSITY

LIST OF FIGURES

จุฬาลงกรณ์มหาวิทยาลัย
CHULALONGKORN UNIVERSITY

CHAPTER 1

INTRODUCTION

1.1 Motivation

Recently, energy storage technology has been developed continuously to serve the increasing energy demand (Chen et al. 2009). Among various energy storage alternatives, capacitor is a simple way to store electricity. It basically consists of two electrodes separated by a separator. It can be charged and discharged more than 1,000 times with high efficiency and high energy density which makes capacitors charging period shorter than conventional batteries (Chen et al. 2014). Since capacitors store energy using ion adsorption, electrode materials with desired pore size and ultrahigh surface area is a key to high capacitance and superb power delivery rate (Zhang et al. 2011).

Activated carbon is a promising carbonaceous material for fabricating capacitor-electrode owing to its high porosity, low cost, and easy processability (Zhang et al. 2011). The production of activated carbon involves with three individual steps which are pretreatment, carbonization, and activation. Hydrothermal pretreatment has been studied wildly since it could enhance yield and propertied of the products. In hydrothermal pretreatment, a feedstock is firstly heated with water within a temperature range of 180 to 250 ℃ under an autogenously pressurized condition to remove some amorphous structure including some of hemicellulose and lignin (Gao et al. 2013). Then, solid residuals from hydrothermal pretreatment step is heated at temperature in

the range of 400 to 1000 °C under inert atmosphere to produce carbonized powder. Then, the carbonized powder is transferred to another reactor to perform activation.

Activation step aims to increase surface activity of a certain material with activating agents at high temperature ranging between 400 and 900 °C (Sayğılı, Güzel, and Önal 2015) for a designated long process time (for example 1-7 h) (Baccar et al. 2009). Potassium hydroxide activation is a potential method because it could provide activated carbon with microporous structure and extremely large specific surface area. Though the reaction mechanism of carbon with potassium hydroxide has not been clearly studied, simple reaction can be described as follows:

$$6KOH + 2C \rightarrow 2K + 3H_2 + 2K_2CO_3.$$

H_2, CO and CO_2 could be produced from redox reactions between potassium compounds and carbon because this activation occurred at high temperature resulting in activated carbon with micropores and mesopores in their structures (Wu et al. 2016).

In electric furnace, heat transfer is slow since heat needs to be transferred from heated coils to container before being received by surface of heating materials. Microwave irradiation has been considered as a promising choice to overcome the heat transfer limitation in conventional electric furnace. When microwave irradiation is applied, microwave energy can create frictional force in atomic scale resulting in rapidly generating of volumetric heat within heating materials (Russell et al. 2012).

There are various kinds of material that could be used as a feedstock to produce activated carbon. Water hyacinth is vastly widespread and cause countless ecology-

issues. Notably, this plant has thin cell walls and large intercellular spaces. The cell walls are mostly made from cellulose which basically composed from carbon element. Therefore, water hyacinth could be a good feedstock for synthesizing activated carbon that has large specific surface area and high capacitance (Wu et al. 2016).

In this work, activated carbon was synthesized from water hyacinth using hydrothermal pretreatment, carbonization, and potassium hydroxide activation with microwave irradiation. Operating variables regulated in potassium hydroxide activation with microwave irradiation were investigated their effects on characteristics of resultant activated carbon.

1.2 Objectives

Synthesize activated carbon from water hyacinth using potassium hydroxide activation with microwave irradiation.

1.3 Scopes of the research

To achieve desired objectives, following scope of experimental work in potassium hydroxide activation with microwave irradiation had been considered. Two operating variables were investigated their effects on characteristics of resultant activated carbon as described in **Table 1-1**.

Table 1-1 Operating variables regulated in potassium hydroxide activation step with microwave irradiation

Operating variables			
Microwave irradiation time (min)	1	2	3
Mass ratio of potassium hydroxide to carbonized water hyacinth	1:1	3:1	6:1

In addition, methods of adding water into activation system which are wet impregnation, wet nitrogen gas, and wet impregnation together with wet nitrogen gas were studied.

1.4 Expected benefits

This study provided an insight to roles of some permanent variables used in synthesis of activated carbon from water hyacinth using potassium hydroxide activation with microwave irradiation.

Effects of the operating variables which are microwave irradiation time, mass ratio of potassium hydroxide to carbonized water hyacinth, and methods of adding water into activation system on characteristics of the resultant activated carbon was obtained.

CHAPTER 2

FOUNDAMENTAL KNOWLEDGE

To produce activated carbon from water hyacinth and utilized it as a capacitor electrode material, basic knowledge and understanding in relevant issues are important. Therefore, basic knowledge of capacitor, activated carbon, and properties of water hyacinth are briefly summarized in this chapter.

2.1 Capacitors
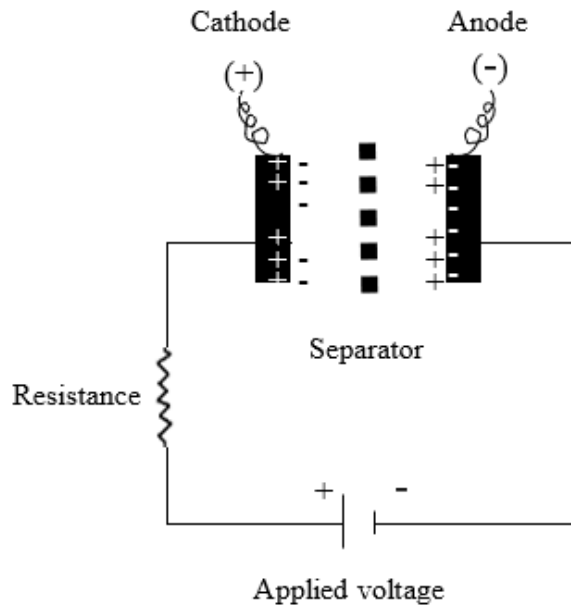
Figure 2-1 Illustration of double-layer capacitor

There are two types of capacitor which are double layer and pseudo capacitors. Double layer capacitors consist of two electrodes separated by insulator as shown in **Figure 2-1**. They store energy charges by non-faradaic reactions which means that there is no charge transfer at interface of electrode and electrolyte. In contrast, faradaic charge transferring at electrode-electrolyte interface is observed in pseudo-capacitors resulting in the charge stored electrostatically. On the other hand, transition metal oxides (Lin et al. 2008) and conducting polymers are used as electrode materials for pseudo-capacitors (Yan et al. 2010). In this research, electrical double-layer capacitors would be an ultimate goal which would be started from production of activated carbon with acceptable characteristics.

Charge/discharge method could be employed to analyze capacitor. This method would be performed at a supporting electrolyte between initial potential to final potential at a specific current density. The charge/discharge curve is shown in **Figure 2-2.**
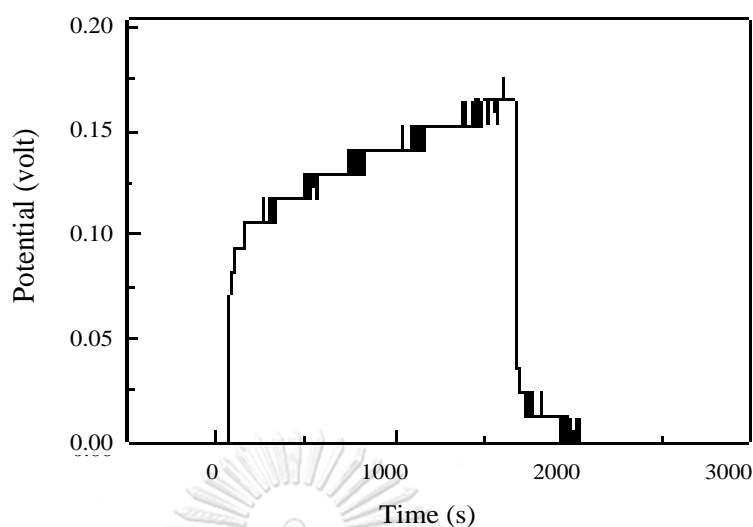
Figure 2-2 Charge/discharge curves of carbon-based electrode derived from

water hyacinth using carbon dioxide activation

Average specific capacitance of electrode materials can be evaluated using **Equation 2-1** (Yang, Chen, and Chang 2011).

$$C_{cp} \ (F \ g^{-1}) = \frac{I \times \Delta t}{\Delta V \times m}$$ **Equation 2-1**

Whereas, I refers to discharging current (A), Δt represents discharging time, ΔV represents discharging voltage and m is the electrode mass.

Normally, an electrode material which was tested by charge/discharge method and its capacitance decreased in a range of 40 – 50 % is considered as a not stable electrode material. In the case of electrodes derived from carbon materials, the charge/discharge test can be done more than 1,000 cycles while specific capacitance decreased only 10%. This could be implied that carbon materials have good electrode stability (Wang, Wang, and Xia 2005).

2.2 Activated carbon

Activated carbon has been used widely as electrode materials owing to its ultrahigh specific surface area, low cost, and easy processability.

Generally, activated carbon possesses large specific surface area of $1000 \text{ m}^2 \text{ g}^{-1}$ but electrodes fabricated from such activated carbon shown a capacitance less than 10 μF cm^{-2} which is lower than the theoretical value ($15–25 \text{ μF cm}^{-2}$). This could be implied that not every pores are possible to accumulating charges (Kierzek et al. 2004). Structure of activated carbon basically comprises of micro-, meso-, and macro-pores. Previous studies reported that capacitance of electrode derived from activated carbon in aqueous electrolytes (in the range of 100 F g^{-1} to 300 F g^{-1}) is higher than in organic electrolytes (less than 150 F g^{-1}). It should be note that electrolyte ion cannot access into pores that is smaller than the ion. The pores which can be accessible by the ion have no contribution to the charge stored. Since size of organic electrolyte ion is larger than size of aqueous electrolyte ion, organic electrolyte ion has less chance to be stored in the pores of porous carbonaceous electrode than aqueous electrolyte ion. Optimal pore size for storing electrons in double-layer capacitance is 0.7 nm (Raymundo-Piñero et al. 2006). It should be noted that specific surface area is not only important parameter for evaluating capacitive properties but also pore size distribution.

Surface functional groups are one of the key factors in capacitance because they have an effect on wettability at the surface of electrode and electrolyte solution (Pandolfo and Hollenkamp 2006). Types of surface functional groups, found on carbon electrodes, normally depend on preparation method. Oxygen-and nitrogen-containing groups are the most common functional groups that was found on the surface of carbon electrodes. Previous work shown that acidic oxygenated surface groups can elevate the

capacitive performance of carbon electrode by improving wettability of the surface (Hsieh and Teng 2002). Furthermore it could be observed that in acidic media system, capacitance of carbon electrodes trend to increase with an increase in nitrogenate functional groups (Frackowiak 2007). The increasing of capacitance in acidic electrolyte cause by interaction of nitrogen species with protons of the electrolyte (Hulicova, Kodama, and Hatori 2006).

Normally activated carbon can be synthesized via carbonization and activation. In addition, hydrothermal pretreatment could be employed to remove volatile content from precursor to produce activated carbon. Hydrothermal pretreatment is a thermal process aims to converting organic materials into solid products with high carbon content. This method can be done by mixing organic materials with water and heating them in close system in temperature range of 180 to 250 ℃ (Gao et al. 2013). Pressure in the system depends on autogenous step due to saturated vapor pressure of subcritical water according to system-temperature. Hydrothermal pretreatment is an exothermal reaction leading to formation of oxygenate functional group on surface of hydrothermal pretreatment powder which could enhance capacitive properties of carbon-base materials.

Carbonization is a method for converting biomass resources into solid products with high carbon content (Hu, Ma, and Li 2015). Carbonized water hyacinth powder produced from carbonization step could be activated via several methods to produce activated carbon.

2.3 Potassium hydroxide activation with microwave irradiation

Generally, a carbon precursor can be activated with various activation agents including steam, air, and potassium hydroxide. Potassium hydroxide has been using widely to produce activated carbon in industrial section because activated carbon produced from potassium hydroxide activation posse ultrahigh surface area with suitable pore structure. During activation step, the following reactions summarized in **Equation 2-2** take place (Lillo-Ródenas, Cazorla-Amorós, and Linares-Solano 2003).

$$
\left.
\begin{aligned}
C + 2KOH &\rightarrow 2K + H_2 + CO_2 \\
C + 2KOH &\rightarrow 2K + H_2O + CO \\
CO_2 + 2KOH &\rightarrow K_2CO_3 + H_2O
\end{aligned}
\right\} \quad \textbf{Equation 2-2}
$$
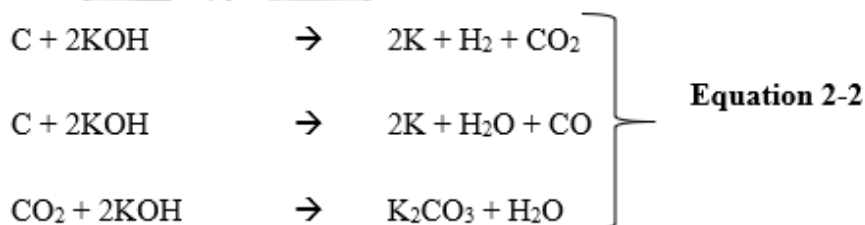
Previous study reported that in potassium hydroxide activation, potassium carbonate was produced and make carbon precursor burn-off resulting in good value in produce yield and good pore developing (Abechi et al. 2013). When temperature is higher than 700 °C in potassium hydroxide activation, yield of activated carbon trends to increase with an increase in temperature because carbon atoms at the surface of carbon precursor was oxidized leaded to pore formation (Abdul Khalil et al. 2010).

In commercial scale, electric furnace has been employed to be a heating source for potassium hydroxide heating method because it is easy to use and to monitor the temperature inside the furnace. In contrast, heating by electric furnace required long heating period leaded to lots of energy consuming. Microwave irradiation could be

employed to overcome those disadvantages of electric furnace. Microwave could consume shorter activating time and less energy than electric furnace.

Microwave irradiation under inert atmosphere has been used to prepared activated carbon from many organic materials likes bamboo sawdust (Dai et al. 2017), orange peel (Lam et al. 2017), and coffee shell (Li et al. 2016). Surface structure of activated carbon derived from potassium hydroxide activation with microwave irradiation is different from those of electric furnace. It could be observed that activated carbon derived from microwave irradiation possess a larger specific surface area than activated carbon derived from electric furnace and the specific surface area increases with increasing reaction temperature, and microwave power level (Huang, Chiueh, and Lo 2016).

Normally, thermal decomposition of lignocellulosic materials at constant temperature is consisted with Arrhenius equation as described in **Equation 2-2.**

$$\frac{dx}{dT} = \frac{A}{\beta} \exp\left(-\frac{E}{RT}\right)(1\text{-}x)^n \qquad \textbf{Equation 2-2}$$

Hereby, x is the conversion fraction of carbonized powder obtained from carbonization step: $\frac{\text{weight of dried water hyacinth - weight of activated carbon}}{\text{weight of dried water hyacinth}}$, T is the temperature, β is the heating rate, A is the pre-exponential or frequency factor, E is the activation energy, and R is the universal gas constant. **Equation 2-3** can be integrated into **Equation 2-3** and **Equation 2-4** (Huang, Chiueh, and Lo 2016).

$$\ln\left[\frac{-\ln(1\text{-}x)}{T^2}\right] = \ln\left[\frac{AR}{\beta E}\left(1\text{-}\frac{2RT}{E}\right)\right] - \frac{E}{RT} \quad \text{(for n=1)} \qquad \textbf{Equation 2-3}$$

$$\ln\left[\frac{1-(1-x)^{1-n}}{T^2(1-n)}\right] = \ln\left[\frac{AR}{\beta E}\left(1-\frac{2RT}{E}\right)\right] - \frac{E}{RT} \quad \text{(for } n\neq1) \qquad \textbf{Equation 2-4}$$

Assuming 2RT/E << 1, **Equation 2-3** and **Equation 2-4** can be simplified to **Equation 2-5** and **Equation 2-6.**

$$\ln\left[\frac{-\ln(1-x)}{T^2}\right] = \ln\left(\frac{AR}{\beta E}\right) - \frac{E}{RT} \quad \text{(for } n=1) \qquad \textbf{Equation 2-5}$$

$$\ln\left[\frac{1-(1-x)^{1-n}}{T^2(1-n)}\right] = \ln\left(\frac{AR}{\beta E}\right) - \frac{E}{RT} \quad \text{(for } n\neq1) \qquad \textbf{Equation 2-6}$$

A plot of $\ln\left[\frac{-\ln(1-x)}{T^2}\right]$ versus 1/T for n = 1 from **Equation 2-5** or $\ln\left[\frac{1-(1-x)^{1-n}}{T^2(1-n)}\right]$ versus 1/T for n ≠1 from **Equation 2-6** shown a linear trend when -E/R represented a slope and ln(AR/βE) represented an intercept, then E and A can be determined.

Microwave irradiation provides many advantages over heat irradiation and convection occurred in electric furnace. The hot spot phenomenon occur in microwave heating method would have significant influence on the yield and characteristics of resultant powder. The activation energy and pre-exponential factor of product from microwave heating method are much lower than those of conventional heating method, revealing that the reaction kinetics for the two heating methods are different. Microwave heating method might have a high potential for converting lignocellulosic biomass into valuable products (Huang, Chiueh, and Lo 2016).

2.4 Water activation with microwave irradiation

Nitrogen and water vapor-mixture could be used in activation step. It could be prepared by bubbling nitrogen gas into water. This system could be considered as a vapor liquid equilibrium and could be assumed that the vapor is an ideal gas and the liquid phase is an ideal solution. In the reactor, there is nitrogen (1) and water vapor (2) in system, compositions of the vapor and liquid phase in a sealed can be calculated as described follows.

Pressure in the system is equal to atmospheric pressure which is 0.99 bar. To calculate compositions of vapor and liquid phase in this system, temperature must be specified. Base on a steady state assumption with a temperature of 40 ˚C (313.15 K).

Henry's law described by **Equation 2-7** can be applied for nitrogen.

$$y_1 P \quad = \quad x_1 k_{h1} \qquad \qquad \textbf{Equation 2-7}$$

where y_1 is mole fraction of nitrogen in vapor phase, P is system pressure, x_1 is mole fraction of nitrogen in liquid phase, and k_{h1} is Henry's law coefficient.

Henry's law coefficient is a function of temperature. It can be described using **Equation 2-8**,

$$k_H = k_H^{\Theta} \times \exp\left\{\frac{-d\ln k_H}{d(1/T)}\left(\frac{1}{T} - \frac{1}{T^{\Theta}}\right)\right\} \qquad \textbf{Equation 2-8}$$

Where k_H^{Θ} is Henry's law coefficient at standard condition, $\frac{-d\ln k_H}{d(1/T)}$ is temperature dependence, T is system temperature, and T^{Θ} is temperature at standard condition which is 25 ˚C (298.15 K).

Therefore, Henry's law coefficient of nitrogen is:

$$k_H = (6.5 \times 10^{-4}) \times e^{\left(1300\left(\frac{1}{313.15} - \frac{1}{298.15}\right)\right)}$$ (Smith and Van Ness 1987)

$$k_H = 3.69 \times 10^{-3}$$ M/atm

$$k_H = 15,183$$ bar

Raoult's law described by **Equation 2-9** can be applied for water and can be written:

$$y_2 P = x_2 P_{sat2}$$ **Equation 2-9**

where y_2 is mole fraction of water in vapor phase, P is system pressure, x_2 is mole fraction of water in liquid phase, and P_{sat2} is vapor pressure of water at the temperature of system which can be calculated by Antoine equation as described in **Equation 2-10**.

$$\log_{10} P_{sat2} = A - \frac{B}{C+T}$$ **Equation 2-10**

$$\log_{10} P_{sat2} = 8.07131 - \frac{1730.63}{233.426+40}$$ **(Smith and Van Ness 1987)**

$$P_{sat2} = 55.19$$

$$P_{sat2} = 0.70$$ bar

Mole fraction of nitrogen in liquid phase can be evaluated using **Equation 2-7** and **Equation 2-9** as show in **Equation 2-11,**

$$(y_1 + y_2) \times P = x_1 k_{h1} + x_2 P_{sat2}$$ **Equation 2-11**

Since $y_1 + y_2 = 1$, Equation 2-12 can be simplified into **Equation 2-12**:

$$x_1 \quad = \quad \frac{P-Psat_2}{k_{h1} - Psat_2} \qquad \textbf{Equation 2-12}$$

$$x_1 \quad = \quad \frac{0.99-0.70}{15,183-0.70} \quad = \quad 6.02\times10^{-5}$$

$$x_2 \quad = \quad 1 - 6.02\times10^{-5} \quad = \quad 0.99994$$

Composition in vapor phase can be calculated from **Equation 2-7,**

$$y_1 \quad = \quad \frac{x_1\ k_{h1}}{P}$$

$$y_1 \quad = \quad \frac{6.02\times10^{-5} \times15,183}{0.99} \quad = \quad 0.92545$$

$$y_2 \quad = \quad 1 - 0.92545 \quad = \quad 0.07455$$

Compositions of liquid and vapor phase at various temperatures used in this research are described in **Table 2-1**.

Table 2-1 Compositions in liquid and vapor phase at various temperatures

Mole fraction	Temperature (°C)	
	40	60
Nitrogen in liquid phase	6×10^{-5}	3×10^{-5}
Water in liquid phase	0.99994	0.99997
Nitrogen in vapor phase	0.92545	0.79867
Water in vapor phase	0.07455	0.20133

2.5 Water Hyacinth

Water hyacinth (Eichhorniacrassipes) is floating plant recognized as invasive aquatic species. Since water hyacinth's stem is like spongy, it can spread widely and makes serious problems on biological and ecological system. Generally, water hyacinth composes of lignocellulosic materials which are cellulose, hemicellulose, and lignin.

Cellulose is composed from a homo-polymer compound. It can be found in starch, glycogen, and other carbohydrates. Cellulose consists of D-glucose ($C_6H_{10}O_5$) units linked by β-1,4 glycosidic bond via hydrogen bonds and van der Waals forces. Both crystalline and amorphous structures can be found in structure of cellulose. The amorphous structures are more easily to decomposed than the crystalline structure in subcritical water condition. Cellulose could be hydrolyzed with de-ionized water at temperature of 180 °C which is normally used in hydrothermal pretreatment.

Hemicellulose is another lignocellulosic compound that could be found in every plant. Hemicellulose consists of sugars with five or six carbon atoms which are pentose, hexoses, mannose, glucose, and sugar acids. Each sugar is linked by (1→4)-glycosidic or α(1→2)-bonded 4-O-methylglucoronic acids. Random amorphous structures including 500-3,000 shorter chains sugar units could be found in hemicellulose structure. The hemicellulos can be hydrolyzed at 160 °C in the presented of water as known as hydrothermal pretreatment.

Lignin is a complex hydrocarbon structure. It can be found in structures of cell wall. Lignin is mostly composed of amorphous structures consisted of 10,000 units of cross-linked macromolecule.

Notedly, water content of water hyacinth is up to 95% wt leading to high energy consumption in drying process (Rezania et al. 2015). Hydrothermal pretreatment is one way to treat water hyacinth using less energy consumption than drying process.

2.6 Literature reviews

There were several researches presented that water hyacinth has been used as raw materials for producing activated carbon. Huang, et al. reported that activated carbon with meso-porous structure and oxygenate functional groups could be prepared from water hyacinth using phosphoric acid activation to eliminate lead(II) ion in water. Activated carbon possessed high meso-porosity (93.9%) with surface area of $424 \, m^2 \, g^{-1}$ (Huang et al. 2014). El-Wakil et al. explored the synthesis of activated carbon from dried water hyacinth stems by chemical activation with phosphoric acid. They were produced with a reasonable yield about 75% and have a remarkable surface area $864.52 \, m^2 \, g^{-1}$ well-developed pore structure (El-Wakil and Awad 2014).

Potassium hydroxide activation with microwave irradiation for producing activated carbon has been studies owing to shorter process time and effective energy use. Ji, et al. reveal that activated carbon with large specific surface area can be prepared via potassium hydroxide activation with microwave irradiation. The influences of potassium hydroxide to meso-carbon microbeads weight ratio and activating time on pore development of the activated carbon has been studied. Activated carbon prepared using microwave irradiation possessed larger specific surface area than those by heat convection. The microwave irradiation can shortened the activation time considerably (Ji et al. 2007). Kubota, et al. used potassium hydroxide activation with microwave

irradiation to prepare activated carbon from phenolic resin. The most developed porosity of activated carbon was obtained when potassium hydroxide was mixed with phenolic resin at weight ratio of 4 and activated using microwave irradiation at total input power of 0.39 kW. Mesoporous structures can be developed under microwave irradiation owing to the rapid heating rate of the heating materials. It should be noted that temperature of heating materials heated by microwave irradiation is rose extremely faster than those heated by electric furnace (Kubota, Hata, and Matsuda 2009). Furthermore, activated carbon can be prepared from oil palm empty fruit bunch using potassium hydroxide activation with microwave irradiation operated at 2.45 GHz. Microwave oven was used at total input power of 360 W with irradiation time of 15 minutes. The resultant activated carbon shown a large specific surface area of 807.54 m^2 g^{-1}. (Foo and Hameed 2011). Ahmad and Theydanb presented that pomegranate peel can be converted into activated carbon using potassium hydroxide activation with microwave heating method. The activated carbon powder was characterized educing nitrogen-adsorption surface area which gave remarkable increase in specific surface area (941.02 m^2 g^{-1}) (Ahmed and Theydan 2013).

CHAPTER 3

EXPERIMENTAL

According to literature reviews related to the production of activated carbon from water hyacinth, experimental methodology and configuration of the reactor used in hydrothermal pretreatment, carbonization and potassium hydroxide activation with microwave irradiation will be briefly summarized in this chapter.

3.1 Raw Materials and Chemicals

Fresh water hyacinth was gathered from Maha Sawat canal, Nakhon Pathom, Thailand. Potassium Hydroxide with 85.0 % purity had been purchased from Wako Pure Chemical Industries, Ltd and Nitrogen gas with 99.999 % purity was purchased from Linde (Thailand) Public Co, LTD.

3.2 Equipment and Reactor

3.2.1 Stainless steel autoclave reactor

50 ml of stainless steels autoclave reactor with Teflon liner was used in a series of experiment of hydrothermal pretreatment as shown in **Figure 3-1**. Diameter and height of the reactor are 3.5 and 5.5 cm, respectively.

Figure 3-1 Stainless steel autoclave reactor

3.2.2 Horizontal reactor equipped with Microwave oven

This reactor was used in potassium hydroxide activation with microwave irradiation. The reactor consisted of quartz tube which its diameter and length are 3.4 and 91 cm respectively. The quartz tube was placed in home-used microwave oven (R-216, Sharp) and connected to a vapor inlet which was consisted of nitrogen gas and water vapor as demonstrated in **Figure 3-2.**

Figure 3 2 Reactor used in potassium hydroxide activation heating by microwave

Heating oven used in hydrothermal pretreatment step was from Memmert and electric furnace used in carbonization step was Nabertherm High Temperature Furnace (HTCT 03/16/P330 LC030H6SN, Nabertherm).

3.3 Experimental Procedures

3.3.1 Preparation of water hyacinth

After being gathered from Maha Sawat canal, Nakhon Pathom, Thailand. Every part of water hyacinth including lefts, bodies, and roots was chopped and washed to remove sludge. Then, it was sun-dried for 3 days to remove moisture.

3.3.2 Hydrothermal pretreatment

Afterward, dried water hyacinth and de-ionized water was mixed at mass ratio of 1:10 before being load into the autoclave reactor. The reactor was heated in the oven at 180 °C for 8 hours before being quenched immediately by water at room temperature. Solid product was separated by filtration then it was dried at 110 °C overnight before being used in carbonization step.

3.3.3 Carbonization

1 kg of resultant solid obtained from hydrothermal pretreatment step was putted into a quartz tube before being loaded into a furnace. The pre-carbonization was performed at 450 ˚C (5 ˚C min^{-1}) in for 2 hours under ambient N_2. Carbonized water hyacinth was obtained by annealing the pre-carbonized product at 800 ˚C for 2 hours under N_2 (Wu et al. 2016). After being cooled to room temperature naturally, carbonized water hyacinth was collected for using in activation step.

3.3.4 Activation

In the activation step, the carbonized water hyacinth was mixed with potassium hydroxide flakes at the desired mass ratio before being grinded into fine powders using mortar. The mixture was put in a quartz boat hosted in a glass tube for safety protection, and it was heated to 200 °C with a heating rate of 10 °C min^{-1} and a holding time of 13 min before being transferred into microwave reactor. The microwave reactor was built by making holes on a home-use microwave oven (2.45 GHz, 800 Watts), through which a quartz tube was inserted. The activation reaction was carried out in this quartz tube, and the microwave irradiation time was set for 1 min. N_2 gas was supplied to this quartz tube at 300 ml min^{-1} and atmospheric pressure. The resultant activated carbon was filtrated and washed by distilled water until the pH value of the washing solution became neutral. Afterward, activated carbon was dried at 110 °C overnight.

In activation step, three difference methods for adding water were performed to study effects of water transfer on activated carbon properties. The first method: wet impregnation, carbonized water hyacinth had been soaking the prepared potassium hydroxides solutions for 24 h. The influence of chemical impregnation was examined over a range of impregnation ratio (i.e. weight of potassium hydroxide: weight of carbonized water hyacinth) ranging from 1:1 to 6:1. After being soaking for 24 h, solid product was separated by filtration and loaded into quartz tube equipped into modified microwave oven. Remaining among of water left in the separated solid can be determined by titration. For the second method, water was added by wet nitrogen gas. Carbonized water hyacinth grounded with potassium hydroxide pellet at desire portion was loaded into quartz tube equipped with microwave oven. Wetting nitrogen gas was prepared by bubbling nitrogen gas into water as shown in **Figure 3-2**. Mixture of water

and nitrogen gas was lined to the quartz tube. Composition of water can be calculated as descripted in **Table 2-1.** The third method had done by preparing wet impregnation and wet nitrogen gas at the same time. The quartz tube was equipped with microwave oven. To perform activation, the oven was adjusted to 800 W and used for desired period. The carrier gas will be fed with a flow rate of 300 ml min^{-1}. Resultant activated carbon was filtrated and washed by distilled water until the pH value of the washed solution is between 6 and 7 before being dried at 110 °C overnight.

To comparison the effect of heating methods, the carbonized powders were mixed with potassium hydroxide flakes grinded into fine particles at mass ratio of 1:3. The mixture was put on nickel foil placed in ceramic boat. Then, the boat was loaded into a stainless-steel tubular reactor located inside an electric furnace and connected with gas line. The reactor was heated to 700 °C with 10 °C min-1 and held at 700 °C for 1 h. Nitrogen was flowed through the reactor at 300 ml min-1 during the activation step. Afterwards, the potassium hydroxide activated carbon powders were filtrated and washed by distilled water until the pH value of the washed solution was between 6 and 7 before being dried at 110 °C overnight.

To comparison the effect of activating agent, carbon dioxide activation was studied. 0.3 g of dried water hyacinth were pressed using a hydraulic pressing machine with a regulated pressure of 4 MPa. The pellets with a nominal size of 10 mm in diameter and 2 mm in thickness could be consolidated without using any binders. The consolidated pellets of dried water hyacinth were placed in a container and loaded into a quartz tubular reactor, which was situated in a programmable electric furnace. The consolidated water hyacinth pellets were carbonized. Then the carbonized water

hyacinth pellets were activated by filling the reactor with mixture of carbon dioxide and nitrogen with volumetric ratio of 1:2 at the same temperature for 1 h. Finally, the activated carbon pellets were collected after the furnace had cooled to room temperature naturally under a pure nitrogen flow.

3.3.5 Capacitance measurement

To measure the capacitance of the resultant activated carbon pellets, two identical pellets were used as electrodes dipped in a 6 M KOH electrolyte. The electrodes were connected to charge-discharge circuit unit. This unit was built using constant-current diodes and a programable relay by which the charge-discharge direction was alternately switched between two targeted values of inter-electrode voltage. The potential data was collected using a data logger for estimating the capacitive properties of each electrode set.

3.4 Product Characterization

Morphology and surface composition of the activated carbon were studied by Scanning Electron Microscope and Energy Dispersive X-ray Spectrometer (SEM-EDS, JSM-6610LV, JEOL and X-MaxN 50, Oxford). Raman spectroscopy (MicroRAM-300OL, Lambda Vision) was used to investigate surface crystallinity and morphology. The specific surface area was determined by the Brunauer–Emmett–Teller (BET) method using an automated chemisorption/physisorption surface area analyzer (BELSORP-miniII-S, MicrotracBEL) at 77 K and estimated using N_2 gas isothermal adsorption. Elemental analyzer (FLASH 2000 HT, Thermo Scientific) was used to explore composition of the activated carbon. X-ray photoelectron spectroscopy (XPS;

PHI5000 Versaprobe II, ULVAC-PHI) has been employed to study the chemical states and compositions at the surface of activated carbon. The capacitance measurement circuit was controlled by a programable relay (ZEN-10C1DR-D-V2, Omron). The potential data was collected using a data logger (PCS10, Velleman).

CHAPTER 4

RESULTS AND DISSCUSSION

As the first step, elemental composition, and biopolymer components of dried water hyacinth before being hydrothermal pretreated, carbonized and activated with potassium hydroxide using microwave irradiation were determined. Typical sample of water hyacinth are composed of 40% of cellulose, 6% of hemicellulose, 7% of lignin, 37% of ash and 10% of moisture. Elemental analysis of dried water hyacinth powder revealed that the powder consisted of 33.95% of carbon, 4.85% of hydrogen, 2.16% of nitrogen, 0.08% of sulfur and 58.96% of others.

4.1 Effect of hydrothermal pretreatment and carbonization

Dried water hyacinth was hydrothermal pretreated at 180 °C for 8 hours before being carbonized at 800 °C for 2 hours under nitrogen flow. Particle size of dried, hydrothermal, and carbonized water hyacinth is in the range of 20 – 30 μm as shown in **Figure B-1** to **Figure B -3**.

4.1.1 Scanning Electron Microscope (SEM)

Figure 4-1 displays an SEM image of the dried water hyacinth and a sheet-like product with a large uniform surface was observed. The surface of the dried water hyacinth containing intercellular structure which was relatively smooth and consisted of a certain amount macro pores. Morphology of hydrothermal and carbonized water

hyacinth were presented in **Figure 4-2** and **Figure 4-3.** After being hydrothermally pretreated and carbonized, intercellular structures were still observed. However, it could be clearly observed that carbonized water hyacinth contained much more portion of smaller pores with broader distribution. Comparison of such microscopic structure would suggest that the elevated temperature in carbonization steps would result in the collapse of cellulose and hemicellulose structure within the activated carbon (Molina-Sabio et al. 1996).
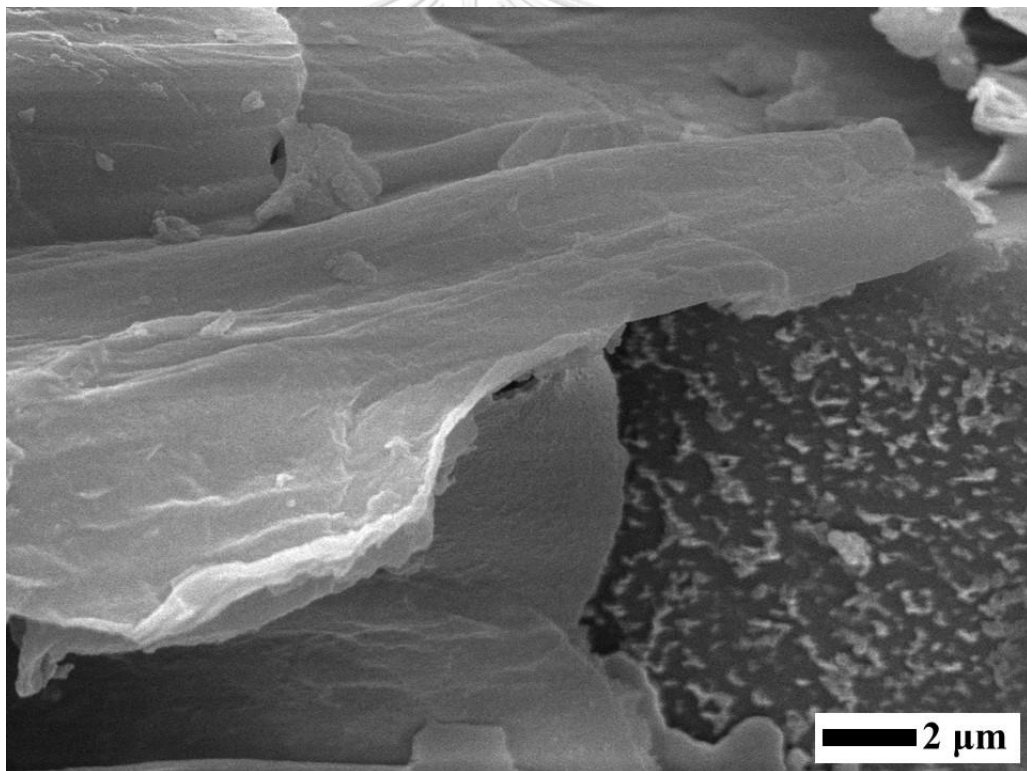
Figure 4-1 SEM images of dried water hyacinth
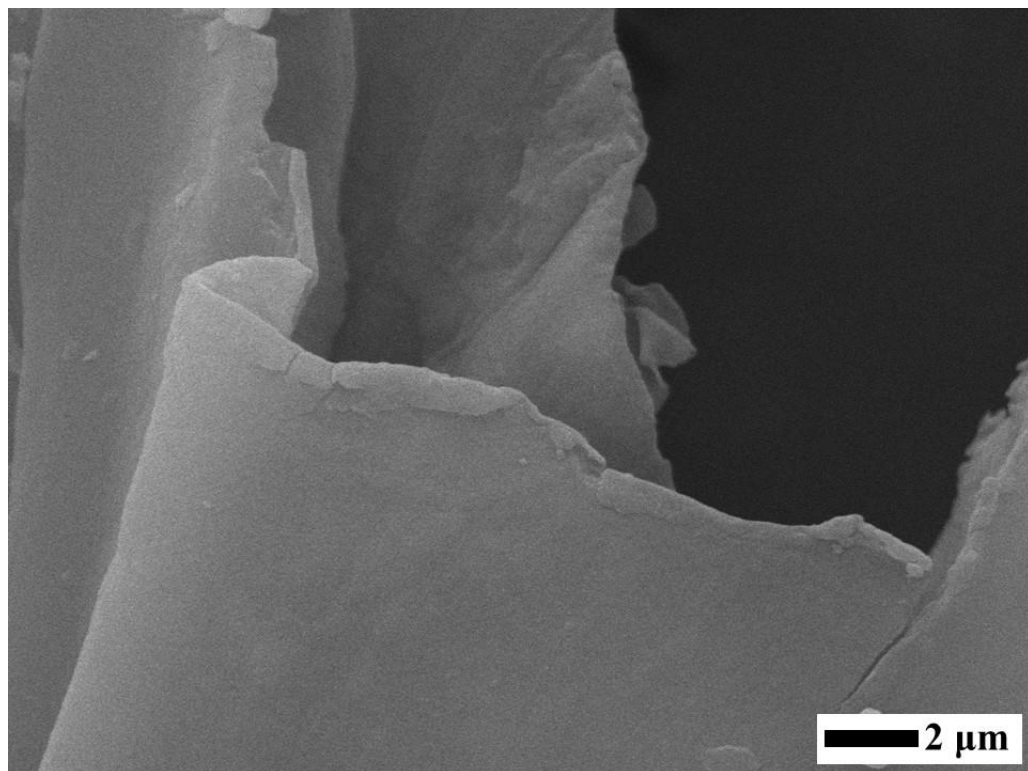
Figure 4-2 SEM images of hydrothermal water hyacinth
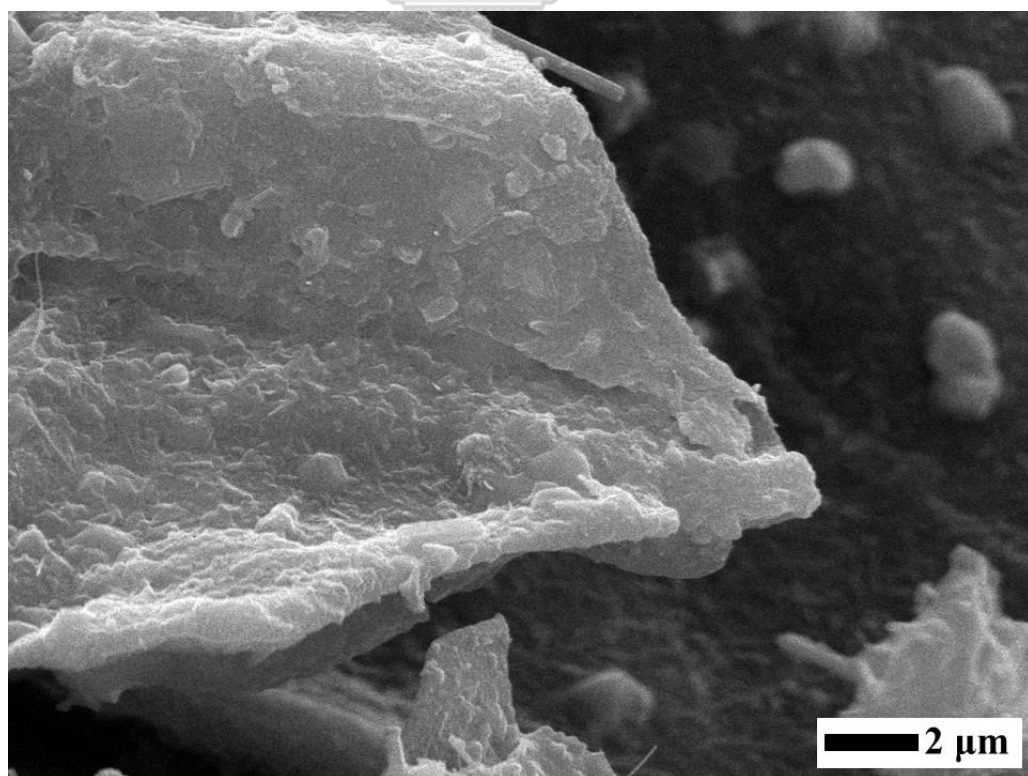
Figure 4-3 SEM images of carbonized water hyacinth

4.1.2 Elemental analysis

Thermal processes including hydrothermal pretreatment and carbonization can improve the properties of dried water hyacinth like the coalification process. Cellulose, which is the main component in water hyacinth, is known to have high H/C and O/C ratios, similar to other biomass materials (Funke and Ziegler 2010). The H/C and O/C ratios of dried water hyacinth decreased when it was hydrothermally pre-treated and carbonized because the cellulose was converted into carbonaceous products by chemical dehydration during hydrothermal pretreatment and carbonization (Funke and Ziegler 2010):

$$4(C_6H_{10}O_5)_n \rightarrow 2(C_{12}H_{10}O_5)_n + 10n\ H_2O).$$

Consequently, hydrothermal pretreatment can enhance carbon content of hydrothermal and carbonized water hyacinth from dried water hyacinth by reducing the hydrogen and oxygen contents of hydrothermal and carbonized water hyacinth as presented in **Figure 4-4.**
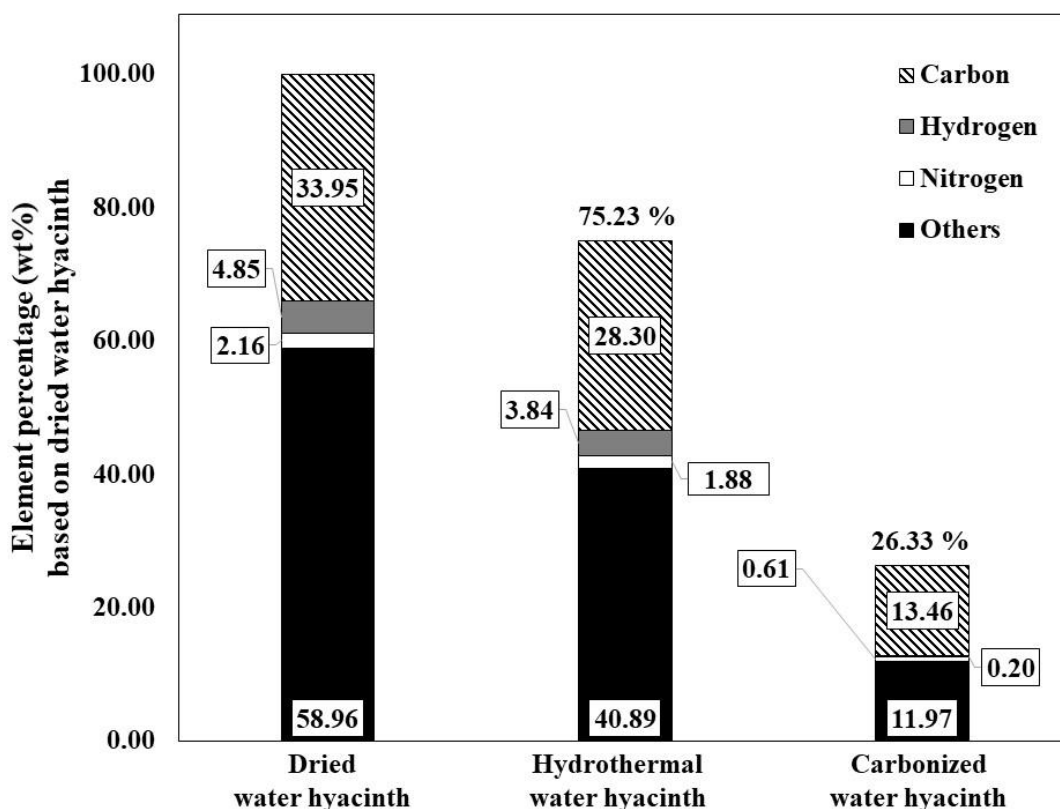
Figure 4-4 Elemental contents of dried, hydrothermal and carbonized water hyacinth on mass basis

Average mass yield percentage of hydrothermal and carbonized water hyacinth were determined using **Equation 4-1** and **Equation 4-2.** The mass yield percentage of hydrothermal and carbonized water hyacinth are 75.23 and 26.33 respectively. Weight of hydrothermal and carbonized water hyacinth dramatically decreased from dried water hyacinth. It could imply that some volatile compounds including humidity in dried water hyacinth structures were vaporized at rising temperature in hydrothermal and carbonization step leading to weight reduction in carbonization and activation step.

% yield of hydrothermal water hyacinth $= \dfrac{\text{weight of hydrothermal water hyacinth}}{\text{weight of dried water hyacinth}}$ x 100   **Equation 4-1**

% yield of carbonized water hyacinth = $\frac{\text{weight of carbonized water hyacinth}}{\text{weight of dried water hyacinth}}$ x 100   **Equation 4-2**

Due to limitation of elemental analysis used in this experiment, compositions of oxygen could not be measured directly. Compositions of oxygen, presented in **Figure 4-4** and **Figure 4-5**, were calculated by mass balance. Compositions of oxygen, obtained by mass balance, consisted with EDS and XPS results as shown in **Table 4-1** and **Table 4-2** respectively.

4.1.3 Energy dispersive x-ray spectroscopy analysis (EDS)

The EDS results of dried water hyacinth as shown in **Table 4-1** demonstrated that majority components in dried water hyacinth were carbon and oxygen which were consisted with elemental analysis results. Carbon and oxygen are the main component of cellulose which was a majority composition in water hyacinth. EDS spectrum of dried water hyacinth was provided in **Figure C-1.**

Table 4-1 Composition of dried water hyacinth obtained from EDS

	C	O	Mg	Si	Cl	K	Ca
% Composition by mass	46.81	34.75	0.35	0.05	7.10	9.76	1.19
% Composition by mole	59.30	33.04	0.22	0.03	3.11	3.86	0.45

4.2 Effect of activating agents

The color of water hyacinth changed from green to brown in drying step and then, it turned to black in the carbonization and activation steps. After dried water hyacinth was hydrothermally pretreated, resultant hydrothermal product was carbonized under nitrogen atmosphere.

Carbonized water hyacinth was mixed with potassium hydroxide at mass ratio of 1:6 and activated using electric furnace heated at 700 °C for 1 h. For comparison, carbonized water hyacinth was activated with carbon dioxide using electric furnace heated at 700 °C for 1 h.

4.2.1 Raman spectroscopy analysis

The surface structures of carbonized water hyacinth and activated carbon from potassium hydroxide and carbon dioxide activation with heat irradiation using electric furnace were studied using Raman scattering in the range of 1100 to 2000 cm^{-1} to confirm their graphitic and disorder carbon structure. As shown in **Figure 4-5**, carbonized water hyacinth and the activated carbons exhibited the Raman shift with detectable signals of disorder-induced D-band (1330 cm^{-1}) and in-plane graphitic vibrational G-band (1590 cm^{-1}) (Pimenta et al. 2007). D band represented the disordered carbonaceous structures which is linked to the breathing modes of disordered graphite rings while G band represents vibrations of sp^2 carbon atoms found in graphitic materials and double bonds (Chia et al. 2012). Raman spectrum of each samples was fitted using two Lorentz functions and a linear baseline to achieve an adequate match to the experimental data. The match of carbonized water hyacinth and activated carbon from potassium hydroxide activation with microwave irradiation,

potassium hydroxide activation with heat irradiation using electric furnace and carbon dioxide activation with heat irradiation using electric furnace presented R^2 values at 0.89, 0.94, and 0.98 respectively.

Figure 4-5 (a) demonstrated the G-band peak of carbonizeded water hyacinth which are stronger than the D-band with a higher intensity ratio of the D band to the G band (I_D/I_G) ratio of 0.81. This result indicated that there are both the disordered structures and graphitic structure in the structure of carbonized water hyacinth.

Figure 4-5 (b) demonstrated the G-band peak of activated carbon derived from potassium hydroxide activation with heat irradiation using electric furnace which are significantly stronger than the D-band with a higher intensity ratio of the D band to the G band (I_D/I_G) ratio of 0.87. It could be observed that activated carbon derived from potassium hydroxide activation using heat irradiation ocurred in electric furnace exhibited a higher I_D/I_G (0.87) than that of carbonized water hyacinth (0.81) indicating lower degree of graphitic ordering (Pimenta et al. 2007). The lower degree of graphitic ordering in the activated carbon derived from potassium hydroxide activation using heat irradiation might cause by some graphitic structures were destroyed during activation with potassium hydroxide for a long period.

Figure 4-5 (c) demonstrated the G-band peak of activeted carbon dereved from carbon dioxide activation using heat irradiation ocurred in electric furnace which are significantly stronger than the D-band with a higher intensity ratio of the D band to the G band (I_D/I_G) ratio of 1.11. Experimental results demonstrated that the activated carbon derived from carbon dioxide activation with heat irradiation exhabited a higher I_D/I_G than that of carbonized water hyacinth (0.81) and and activated carbon from potassium

hydroxide activation (0.87) indicating lower degree of graphitic ordering (Pimenta, et al., 2006). The lower degree of graphitic ordering in the activated carbon derived from carbon dioxide activation with heat convection might cause by some graphitic structures were destroyed during activation with carbon dioxide for a long period.
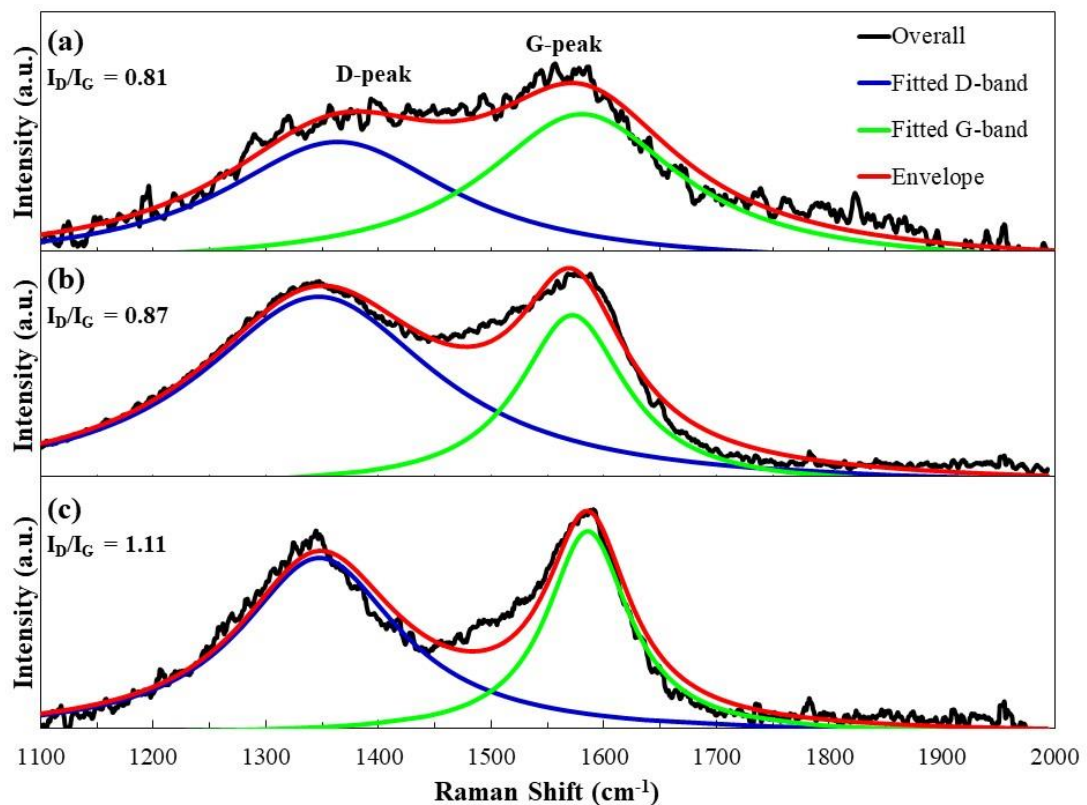
Figure 4-5 Raman spectrum and fitting results of (a) carbonized water hyacinth and activated carbon from (b) potassium hydroxide activation with heat irradiation and (c) carbon dioxide activation with heat irradiation

4.2.2 Brunauer–Emmett–Teller (BET) analysis

Otowa mechanism (Wang, et al., 2012) as described in **Equation 4-4** to **4-7** can be used to explain potassium hydroxide activation reaction that occurred on the surface of the carbonized water hyacinth (at below 700 °C).

2KOH	$\rightarrow$	K_2O+H_2O	**Equation 4-3**
$C + H_2O$	$\rightarrow$	$CO +H_2$	**Equation 4-4**
$CO + H_2O$	$\rightarrow$	CO_2+H_2	**Equation 4-5**
$CO_2 + K_2O$	$\rightarrow$	K_2CO_3	**Equation 4-6**
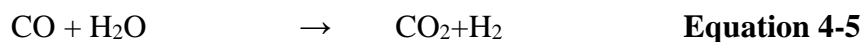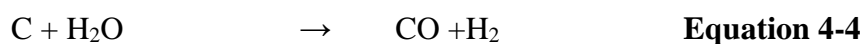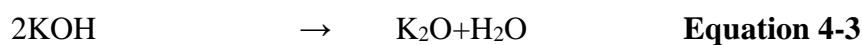
The reaction between potassium hydroxide and carbonized water hyacinth during the chemical activation step is similar to the scheme proposed by the Linares-Solano group, which can be expressed as follows (Lillo-Ródenas, Cazorla-Amorós, and Linares-Solano 2003):

$6KOH + 2C$	$\rightarrow$	$2K + 2 K_2CO_3+3H_2$	**Equation 4-7**

According to Sodtipinta, et al., the reduction reactions of CO_2, K_2O, and K_2CO_3 by carbon that produces CO and potassium metal occurred at high temperatures as shown in **Equation 4**-**10** - **Equation 4**-**12**, respectively (Sodtipinta et al. 2017). Therefore, there were three main KOH activation mechanisms:

(a) reactions between potassium hydroxide and carbonized water hyacinth that lead to the collapse of the carbon framework (**Equation 4**-**8**),

(b) the physical activation through gasification of carbon (**Equation 4**-**5**) via the formation of H_2O (**Equation 4**-**4)** and CO_2 (**Equation 4**-**6**) that was responsible for introducing the microporosity in the carbon matrix,

(c) the intercalation process of potassium metal (**Equation 4**-**8**) in the carbon lattices of the carbonized water hyacinth that volumetrically expands the carbon

framework. After the intercalated potassium metal, K_2CO_3, and K_2O were removed by washing, a large specific surface area (1,642 m^2 g^{-1}-carbon) with high micro- and meso-porosity was obtained as presented in **Figure 4-7 (a).**
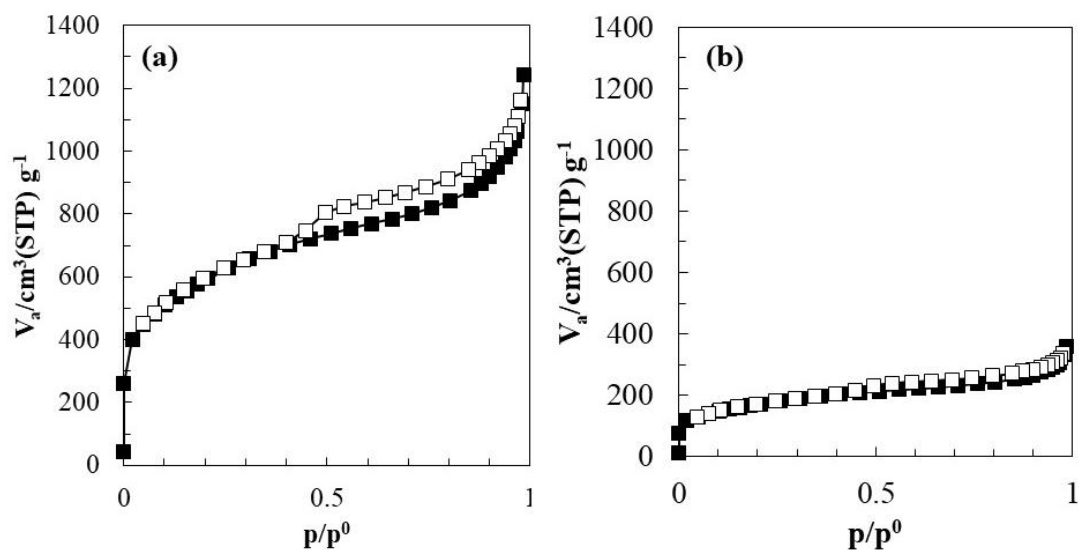
Figure 4-6 N_2 sorption isotherms (filled symbols mean adsorption isotherm, and open symbols mean desorption isotherm) of (a) activated carbon derived from potassium hydroxide activation and (b) activated carbon derived from carbon dioxide activation with heat irradiation using electric furnace

For comparison, activated carbon derived from carbon dioxide activation was prepared. The reaction of carbon dioxide with carbon material is heterogeneous, and numerous problems are encountered in attempting to explain its mechanism. **Equation 4-10** explained reaction between carbon dioxide and carbonaceous materials consisted with mechanism suggested by Ergun (Ergun 1956). The mechanism demonstrated the ability of certain carbon atoms to detach an oxygen atom from a carbon dioxide

molecule. In another word, oxygen retained on the surface can be removed by carbon monoxide. These reactions may be expressed as **Equation 4-13.**

$$CO_2 + C_f \quad \rightleftharpoons \quad CO + C_o \qquad \textbf{Equation 4-8}$$
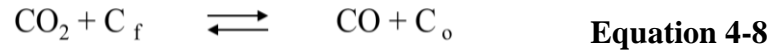
Where C_f represented a free site, which is capable of reaction, and C_o was an occupied site, i.e., a site possessing an oxygen atom. **Equation 4-13** expresses the oxygen exchange phenomenon, not the carbon transfer from solid to gas phase. The transfer of carbon from solid phase to gas phase originates from the occupied sites and may be expressed as shown in **Equation 4-14.**

$$C_o \quad \longrightarrow \quad CO \qquad \textbf{Equation 4-9}$$

Where n is an integer having a value of 0, 1 or 2, when occupied sites are considered individually. When the reaction of a macroscopic carbon sample is considered, n can have any statistical value between 0 and 2; but the most likely value appears to be 1. The reverse of the above reaction, **Equation 4-13**, and the reactions shown in **Equation 4-13** would result in carbon transfer from gas to solid phase and to carbon deposition when the concentration of CO exceeds that required by thermodynamic equilibrium between CO_2 and CO. According to the reaction presented in **Equation 4-13**, it could imply that carbon dioxide activation mainly causes the creation of microporosity. (Molina-sabio, et al., 1996). In this research, experimental results shown that the activated carbon derived from carbon hydroxide activation

possessed a nominal specific surface area (599 m^2 g^{-1}-carbon) with micro- and meso-porosity was obtained as presented in **Figure 4-7 (b)**.

To compare the effects of activating agent, activated carbon were prepared using two difference activating agents which are potassium hydroxide and carbon dioxide. The experimental results show that porosity of activated carbon derived from potassium hydroxide activation was larger than that of carbon dioxide activation because potassium hydroxide reacted with carbonized water hyacinth and generated various activating agents that could enhance activation process.

4.2.3 Elemental analysis

Average mass yield percentage of activated carbon was calculated using **Equation 4-14.** The mass yield percentage of activated carbon, shown in **Figure 4-7**, from potassium hydroxide activation using microwave oven, potassium hydroxide activation using electric furnace and carbon dioxide activation using electric furnace are 40.70 and 55.92 respectively.

$$\% \text{ yield of activated carbon} = \frac{\text{weight of activated carbon}}{\text{weight of carbonized water hyacinth}} \times 100 \quad \textbf{Equation 4-10}$$

Since weight of activated carbon dramatically decreased from carbonized water hyacinth, it could imply that some parts of carbonized powder were reacted with activating agents and produced some compounds that were vaporized in activation step as described in **Equation 4-4** to **Equation 4-13**. Those reasons lead to weight reduction in activation step
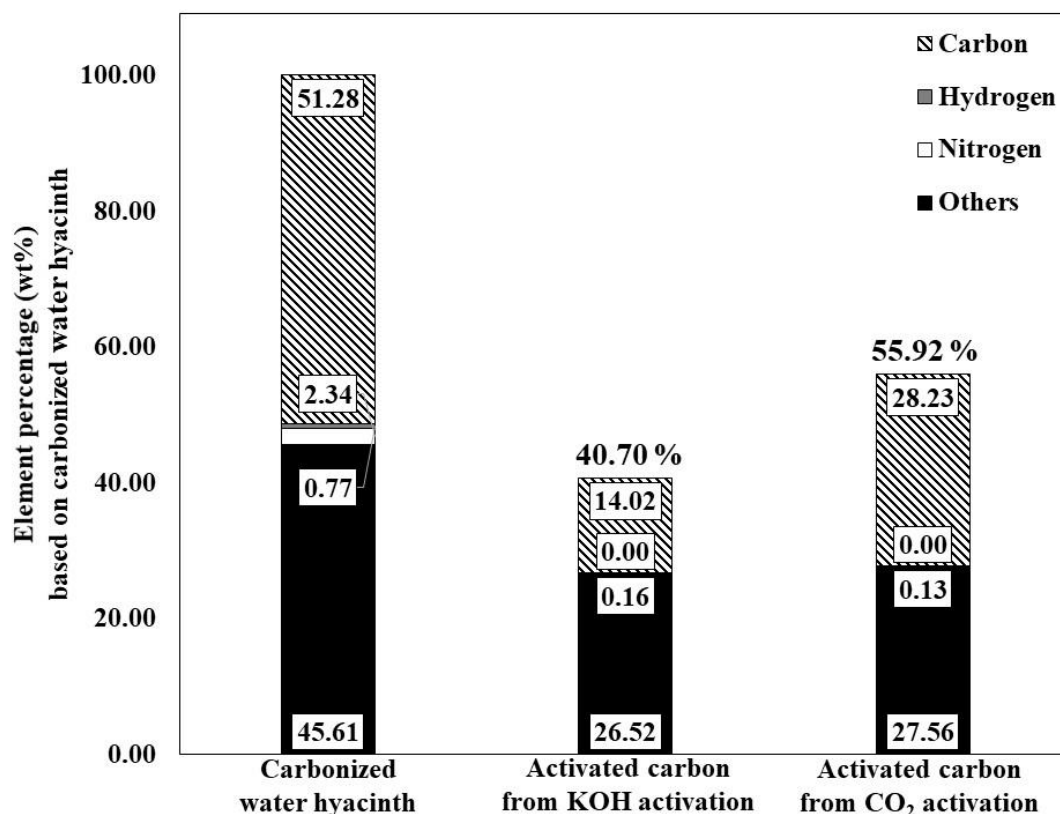
Figure 4-7 Mass yield percentage and elemental contents of (a) carbonized water hyacinth and activated carbon from (b) potassium hydroxide activation and (c) carbon dioxide activation with heat irradiation using electric furnace

จุฬาลงกรณ์มหาวิทยาลัย
CHULALONGKORN UNIVERSITY

4.3 Effect of heating methods

Carbonized water hyacinth was mixed with potassium hydroxide at mass ratio of 1:6 and activated using microwave irradiated at 800 watts for 3 minutes. For comparison, the mixture of carbonized water hyacinth and potassium hydroxide was heated with electric furnace heated at temperature of 700 °C for 1 h.

4.3.1 Raman spectroscopy analysis

The surface structures of carbonized water hyacinth and activated carbon from potassium hydroxide activation with microwave irradiation and with heat irradiation

using electric furnace were studied using Raman scattering from 1100 to 2000 cm^{-1} to confirm their graphitic and disorder carbon structure. As shown in **Figure 4-8**, carbonized water hyacinth and the activated carbons exhibited the Raman shift with detectable signals of disorder-induced D-band (1330 cm^{-1}) and in-plane graphitic vibrational G-band (1590 cm^{-1}) (Pimenta et al. 2007). D band represented the disordered carbonaceous structures which is linked to the breathing modes of disordered graphite rings while G band represents vibrations of sp^2 carbon atoms found in graphitic materials and double bonds (Chia et al. 2012). Raman spectrum of each samples was fitted using two Lorentz functions and a linear baseline to achieve an adequate match to the experimental data. The match of carbonized water hyacinth and activated carbon from potassium hydroxide activation with microwave irradiation and potassium hydroxide activation with heat irradiation using electric furnace presented R^2 values at 0.89, 0.94, and 0.95 respectively.

Figure 4-10 (a) demonstrated the G-band peak of carbonizeded water hyacinth which are stronger than the D-band with a higher intensity ratio of the D band to the G band (I$_D$/I$_G$) ratio of 0.81. This result indicated that there are both the disordered structures and graphitic structure in the structure of dried water hyacinth.

Figure 4-10 (b) demonstrated the G-band peak of activated carbon derived from potassium hydroxide activation using heat irradiation occurred in electric furnace which are significantly stronger than the D-band with a higher intensity ratio of the D band to the G band (I$_D$/I$_G$) ratio of 0.87. It could be observed that activated carbon derived from potassium hydroxide activation using heat irradiation ocurred in electric furnace exhabited a higher I$_D$/I$_G$ (0.87) than that of carbonized water hyacinth (0.81)

indicating lower degree of graphitic ordering (Pimenta et al. 2007). The lower degree of graphitic ordering in the activated carbon derived from potassium hydroxide activation using heat irradiation occurred in electricfurnace might cause by some graphitic structures were destroyed during activation with potassium hydroxide for a long period.

Figure 4-10 (c) demonstrated the G-band peak of activated carbon from potassium hydroxide activation with microwave irradiation which are significantly stronger than the D-band with a higher intensity ratio of the D band to the G band (I_D/I_G) ratio of 0.65. The activated carbon from potassium hydroxide activation with microwave irradiaiton possesed a lower I_D/I_G (0.65) than that of carbonized water hyacinth (0.81) and activated carbon from potassium hydroxide activation with heat irradiation (0.87) indicating higher degree of graphitic ordering (Pimenta et al. 2007). From this result, the resultant activated carbon can be expected to possess the high electric conductivity, which is necessary property for application of the capacitor.
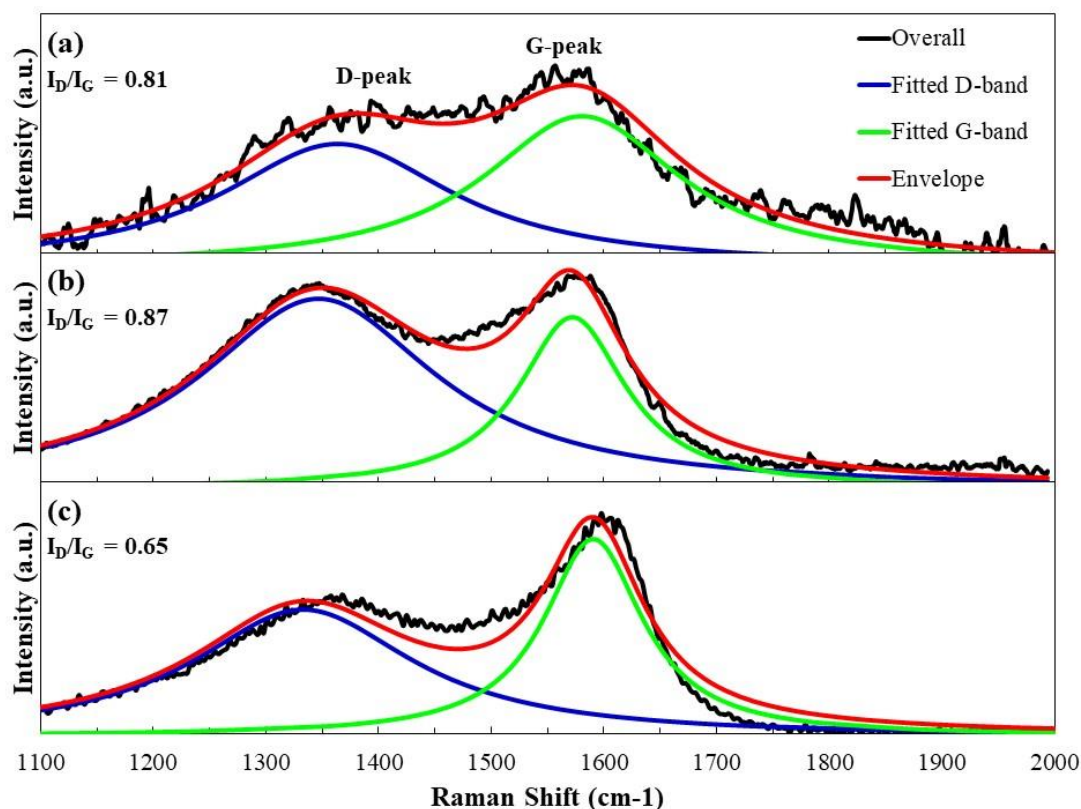
Figure 4-8 Raman spectrum and fitting results of (a) carbonized water hyacinth and activated carbon from (b) potassium hydroxide activation with heat irradiation, (c) potassium hydroxide activation with microwave irradiation

4.3.2 Brunauer–Emmett–Teller (BET) analysis

Potassium hydroxide activation with microwave irradiation can provides many benefits over heat irradiation occurred in electric furnace. The hot spot phenomenon occurred in microwave irradiation could have influence on resultant activated carbon. The activation energy and pre-exponential factor of product from microwave irradiation were much lower than those of the heat irradiation occurred in electric furnace, revealing that the reaction kinetics for the two heating methods were different. Since activation energy, used in the activation with microwave irradiation, was lower than

those of the heat irradiation occurred in electric furnace, activation time used in the activation with microwave irradiation was shorter than those of the heat irradiation occurred in electric furnace. In this research, the activated carbon, derived from and activated with microwave irradiation for 3 minutes, possessed a nominal specific surface area (868 m^2 g^{-1}-carbon) with micro- and meso-porosity as presented in **Figure 4-9**.
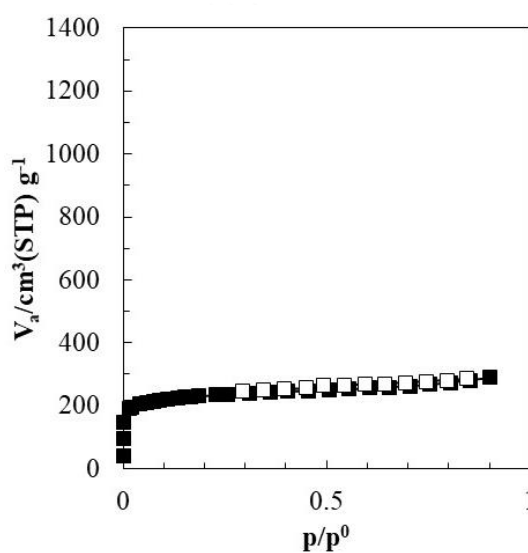
Figure 4-9 N$_2$ sorption isotherms (filled symbols mean adsorption isotherm, and open symbols mean desorption isotherm) of activated carbon derived from potassium hydroxide activation with microwave irradiation

To compare the effects of heating method, activated carbon derived from potassium hydroxide activation were prepared using two difference heating methods which are microwave irradiation and heat irradiation using electric furnace. To synthesize activated carbon with norminal specific surface area, both heating methods could be used but microwave irradiation (3 minutes) consumed less time than heat convection (1 hours). The hot spot phenomenon occurred in microwave irradiation

could have significant influence on resultant activated carbon. According to Arrhenius equation in Equation 2-3, the activation energy and pre-exponential factor of product from microwave heating method are much lower than those of heat irradiation method resulting in shorten activation time (Huang, Chiueh, and Lo 2016).

4.3.3 Elemental analysis

Average mass yield percentage of activated carbon was calculated using **Equation 4-3.** The mass yield percentage of activated carbon, shown in **Figure 4-6**, from potassium hydroxide activation using microwave oven and potassium hydroxide activation using electric furnace are 59.28 and 55.92 respectively.

$$\% \text{ yield of activated carbon} = \frac{\text{weight of activated carbon}}{\text{weight of carbonized water hyacinth}} \times 100 \qquad \textbf{Equation 4-11}$$

Since weight of activated carbon dramatically decreased from carbonized water hyacinth, it could imply that some parts of carbonized powder were reacted with activating agents and produced some compounds that were vaporized in activation step as described in **Equation 4-4** to **Equation 4-12**. Those reasons lead to weight reduction in activation step as shown in **Figure 4-10**.

Figure 4-10 Mass yield percentage and elemental contents of (a) carbonized

water hyacinth and activated carbon from potassium hydroxide activation with

(b) heat irradiation and (c) microwave irradiation

4.4 Effect of microwave irradiation time

This research focused on activated carbon derived from water hyacinth using potassium hydroxide activation with microwave irradiation. Potassium hydroxide was mixed with carbonized water hyacinth at mass ratio of 1:1 and irradiated by microwave at 800 watts in the range of 1-3 minutes.

4.4.1 Raman spectroscopy analysis

The surface structures of activated carbon from potassium hydroxide activation using microwave irradiation in the range of 1-3 minutes were studied using

Raman scattering from 1100 to 2000 cm^{-1} to confirm their graphitic and disorder carbon structure. As shown in **Figure 4-11**, carbonized water hyacinth and the activated carbons exhibited the Raman shift with detectable signals of disorder-induced D-band (1330 cm^{-1}) and in-plane graphitic vibrational G-band (1590 cm^{-1}) (Pimenta et al. 2007). D band represented the disordered carbonaceous structures which is linked to the breathing modes of disordered graphite rings while G band represents vibrations of sp^2 carbon atoms found in graphitic materials and double bonds (Chia et al. 2012). Raman spectrum of each samples was fitted using two Lorentz functions and a linear baseline to achieve an adequate match to the experimental data. The match of activated carbon from potassium hydroxide activation using microwave irradiation in the range of 1-3 minutes presented R^2 values at 0.95, and 0.96 respectively.

Figure 4-11 (a) demonstrated the G-band peak of carbonizeded water hyacinth which are significantly stronger than the D-band with a higher intensity ratio of the D band to the G band (I_D/I_G) ratio of 0.81. This result indicated that there are both the disordered structures and graphitic structure in the structure of dried water hyacinth.

Figure 4-11 (b) demonstrated the G-band peak of activated carbon from potassium hydroxide activation using microwave irradiation for 1 minutes which are significantly stronger than the D-band with a higher intensity ratio of the D band to the G band (I_D/I_G) ratio of 0.65. The activated carbon from potassium hydroxide activation with microwave irradiaiton for 1 minutese possesed a lower I_D/I_G (0.65) than that of carbonized water hyacinth (0.81) indicating higher degree of graphitic ordering (Pimenta et al. 2007). From this result, the resultant activated carbon can be expected

to possess the high electric conductivity, which is necessary property for application of the capacitor.

Figure 4-11 (c) demonstrated the G-band peak of activated carbon from potassium hydroxide activation using microwave irradiation for 3 minutes which are significantly stronger than the D-band with a higher intensity ratio of the D band to the G band (I_D/I_G) ratio of 0.65. The activated carbon from potassium hydroxide activation with microwave irradiaiton for 1 minutese possesed a lower I_D/I_G (0.65) than that of carbonized water hyacinth (0.81) indicating higher degree of graphitic ordering (Pimenta et al. 2007). In addition, I_D/I_G of activated carbon from potassium hydroxide activation using microwave irradiation for 3 minutes is the same as that of activated carbon from potassium hydroxide activation using microwave irradiation for 1 minutes. It could be imply that microwave irradiation time in the range of 1 – 3 minutes did not make significantly different on surface crystallinity of activated carbon presented by Raman scattering.
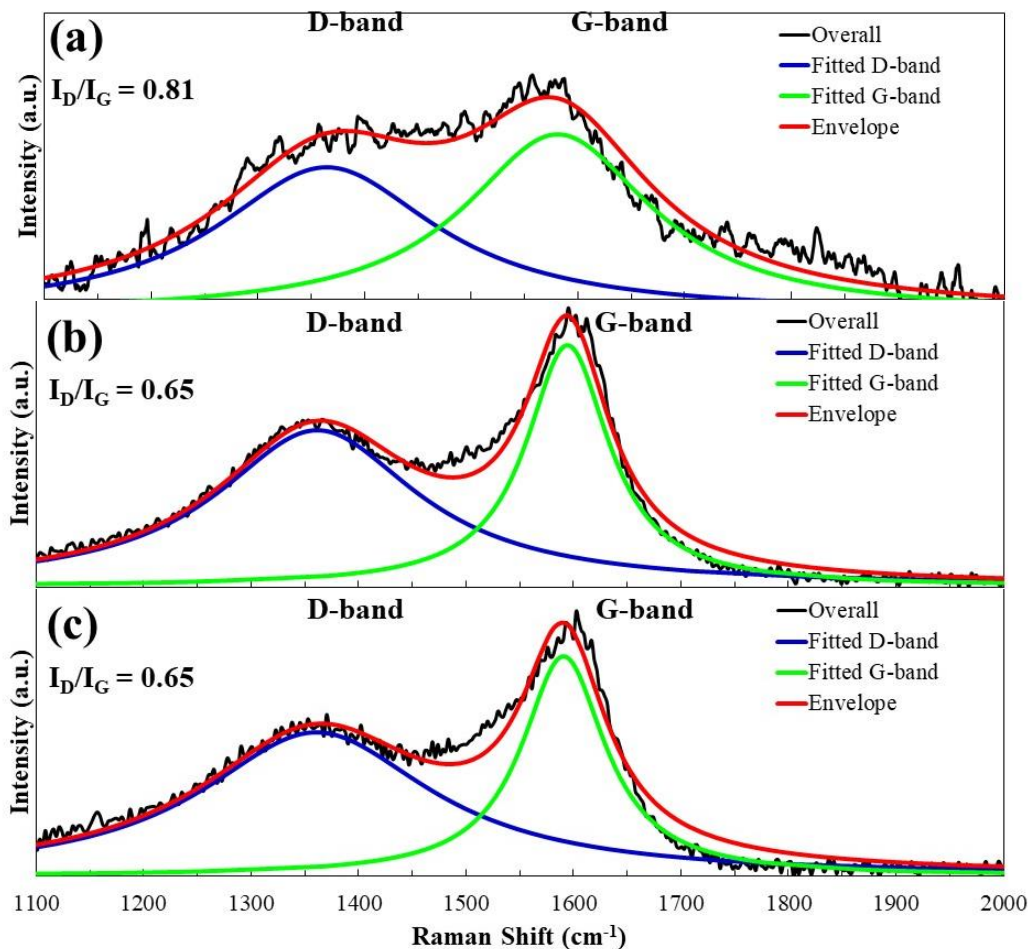
Figure 4-11 Raman spectrum and fitting results of (a) carbonized water hyacinth and activated carbon prepared from potassium hydroxide activation with microwave irradiation for (b) 1 minutes and (c) 3 minutes using mixture of potassium hydroxide to carbonized water hyacinth at mass ratio of 1:1

4.4.2 Elemental analysis

It found that the yield of activated carbon, which was calculated using **Equation 4-3**, and percentage of carbon content slightly decreased with an increasing of irradiation time as shown in **Figure 4-12**. The reaction rate directly related to temperature, which increase with increasing of irradiation time, resulting in decreased of carbon yield when irradiation time is longer (Huang, Chiueh, and Lo 2016).
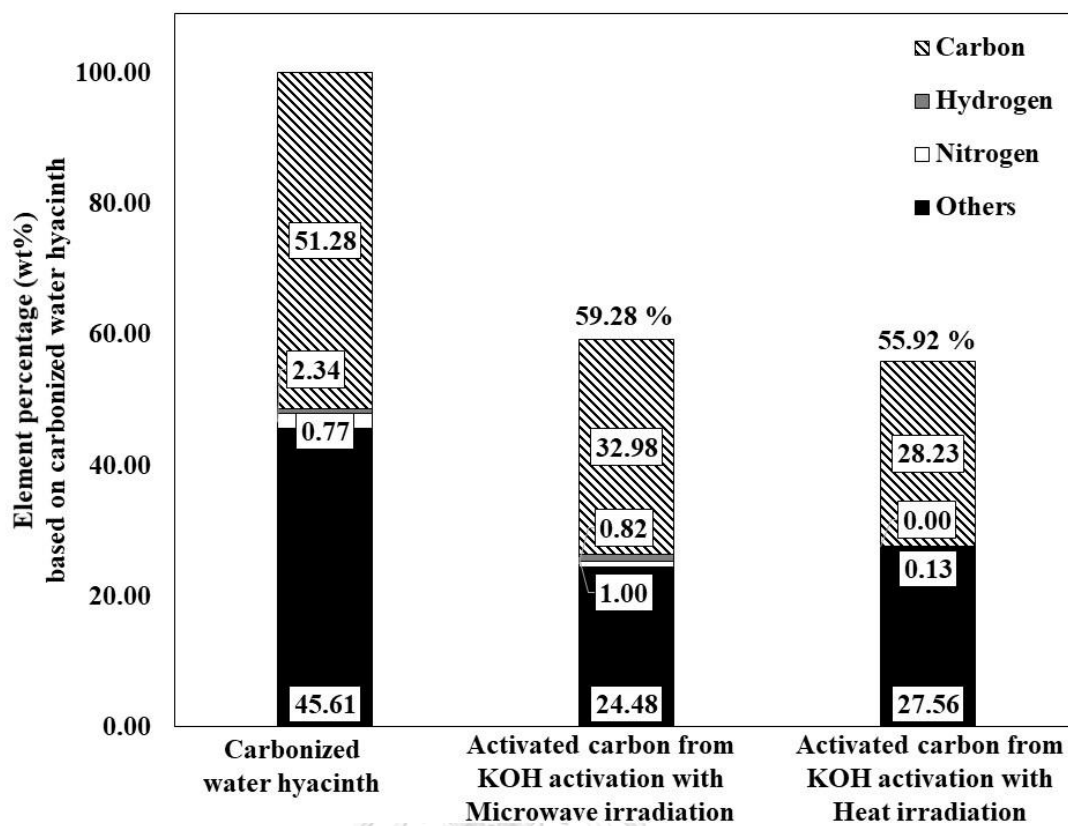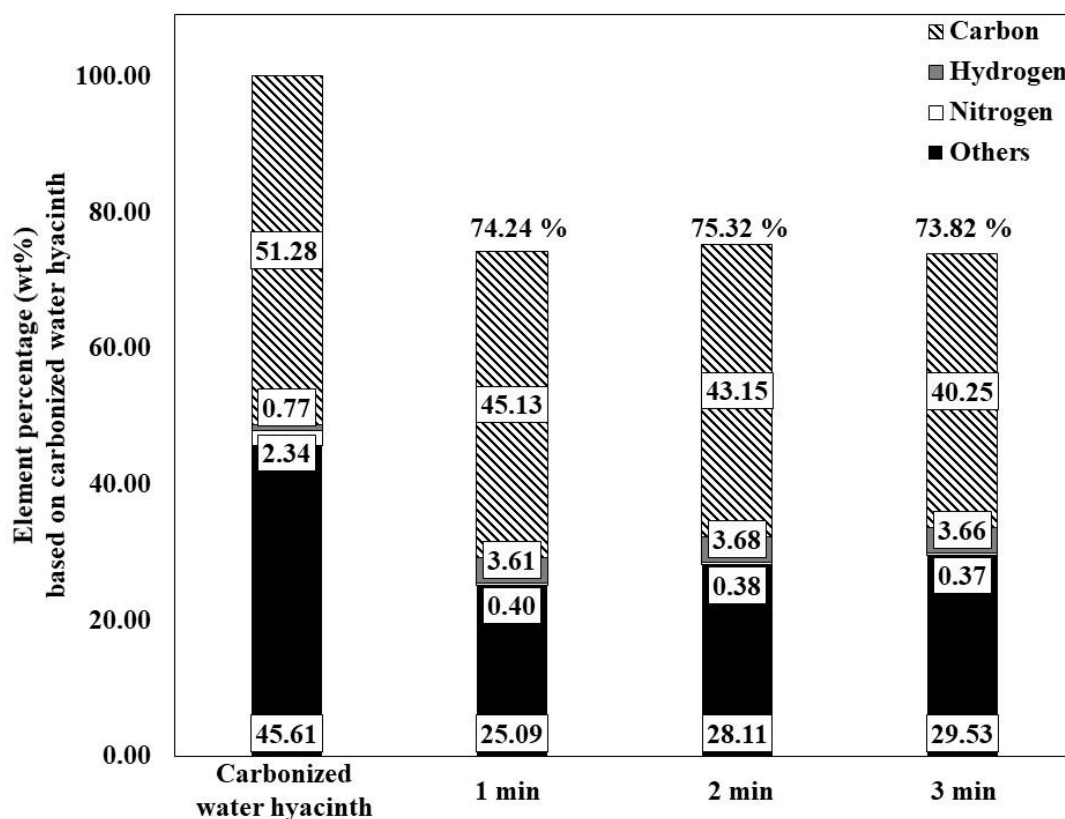
Figure 4-12 Elemental contents of (a) carbonized water hyacinth and activated carbon derived from potassium hydroxide activation with microwave irradiation time of (b) 1, (c) 2, and (d) 3 minutes

4.4.3 X-ray photoelectron spectroscopy analysis (XPS)

Due to limitation of elemental analysis used in this experiment, compositions of oxygen could not be measured directly. Compositions of oxygen can be obtained by XPS as shown in **Table 4-3**. The results shown that majority components in activated carbon were carbon and oxygen which were consisted with elemental analysis results. XPS spectrum of the activated carbon were provided in **Figure D-3** and **Table D-1**.

Table 4-2 Composition of activated carbon derived from potassium hydroxide activation with microwave irradiation at 3 minutes obtained from XPS

	C	O	K
% Composition by mass	43.47	56.53	0
% Composition by mole	36.58	63.42	0

4.5 Effect of potassium hydroxide to carbonized water hyacinth mass ratio

This part of thesis focusing on effect of potassium hydroxide to carbonized water hyacinth mass ratio on activated carbon derived from potassium hydroxide activation with microwave irradiation. Potassium hydroxide was mixed with carbonized water hyacinth at mass ratio of 1:1, 3:1, and 6:1 and irradiated by microwave at 800 watts in the range of 1-3 minutes.

4.5.1 Scanning Electron Microscope (SEM)

Figure 4-13 displays an SEM image of activated carbon activated carbon, derived from potassium hydroxide activation using microwave radiation at 3 minutes and potassium hydroxide to carbonized water hyacinth mass ratio of 6:1 which is considered as the most severe condition studied in this thesis, a sheet-like product with a large uniform surface was observed. After being activated, the morphology of the products' structure changed slightly compared with dried, hydrothermal, and carbonized water hyacinth's structures as presented in **Figure 4-1** to **Figure 4-3**.
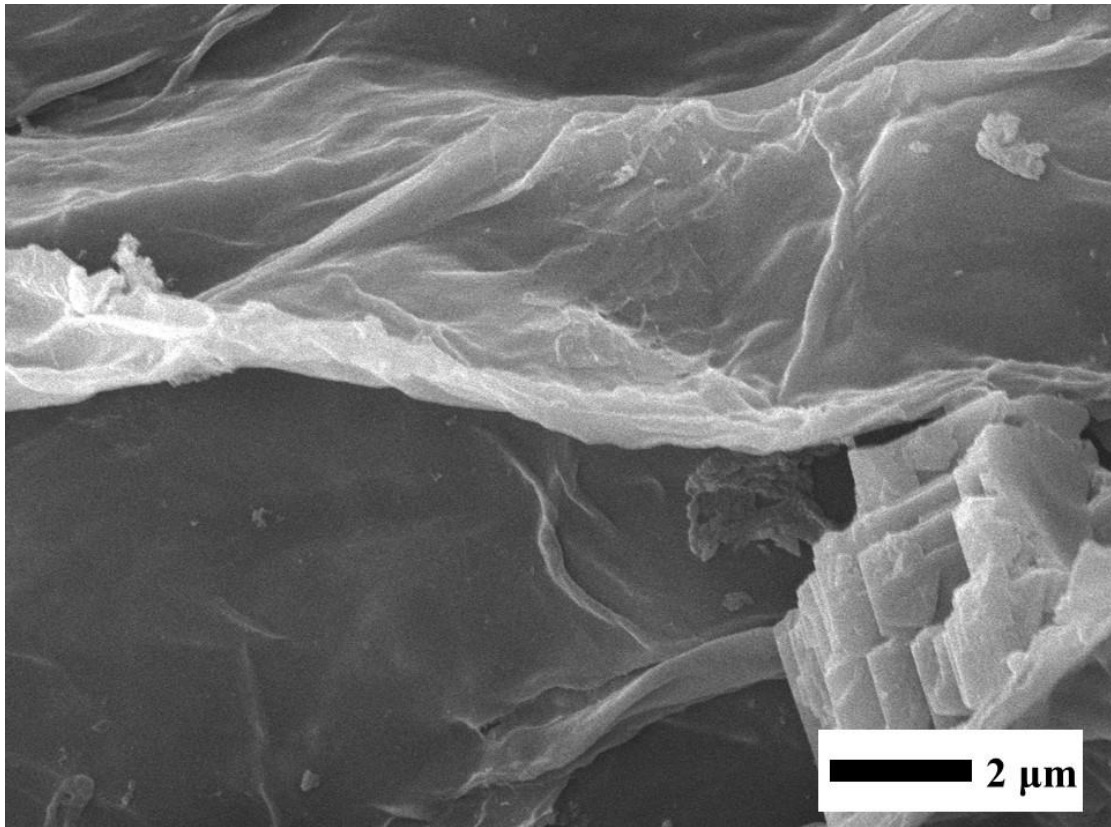
Figure 4-13 SEM images of activated carbon prepared using microwave irradiation for 3 min with potassium hydroxide to carbonized water hyacinth mass ratio of 6:1

4.5.2 Raman spectroscopy analysis

The surface structures of carbonized water hyacinth and activated carbon from potassium hydroxide activation with microwave irradiation in the range of 1-3 minutes together with potassium hydroxide to carbonized water hyacinth mass ratio of 1:1, 3:1, and 6:1 were studied using Raman scattering in the range of 1100 to 2000 cm^{-1} in order to confirm their graphitic and disorder carbon structure. As shown in **Figure 4-14** and **Figure 4-15**, carbonized water hyacinth and the activated carbons exhibited the Raman shift with detectable signals of disorder-induced D-band (1330 cm^{-1}) and in-plane graphitic vibrational G-band (1590 cm^{-1}) (Pimenta et al. 2007). D band represented the disordered carbonaceous structures which is linked to the breathing modes of

disordered graphite rings while G band represents vibrations of sp^2 carbon atoms found in graphitic materials and double bonds (Chia et al. 2012). Raman spectrum of each samples was fitted using two Lorentz functions and a linear baseline to achieve an adequate match to the experimental data. The match of activated carbon from potassium hydroxide activation with microwave irradiation for 1 minutes with potassium hydroxide to carbonized water hyacinth mass ratio in the range of 1:1, 3:1, 6:1 presented R^2 values at 0.96, 0.96 and 0.96 respectively.

Figure 4-14 (a) demonstrated the G-band peak of carbonizeded water hyacinth which are significantly stronger than the D-band with a higher intensity ratio of the D band to the G band (I_D/I_G) ratio of 0.81. This result indicated that there are both the disordered structures and graphitic structure in the structure of carbonized water hyacinth.

Figure 4-14 (b) demonstrated the G-band peak of activated carbon derived from potassium hydroxide activation with microwave irradiation at 1 minutes and potassium hydroxide to carbonized water hyacinth mass ratio of 1:1 which are significantly stronger than the D-band with a higher intensity ratio of the D band to the G band (I_D/I_G) ratio of 0.65. Activated carbon derived from potassium hydroxide activation with microwave irradiation at 1 minutes and potassium hydroxide to carbonized water hyacinth mass ratio of 1:1 possesed a lower I_D/I_G (0.65) than that of carbonized water hyacinth (0.81) indicating higher degree of graphitic ordering (Pimenta et al. 2007).

Figure 4-14 (c) demonstrated the G-band peak of activated carbon derived from potassium hydroxide activation with microwave irradiation at 1 minutes and

potassium hydroxide to carbonized water hyacinth mass ratio of 3:1   which are significantly stronger than the D-band with a higher intensity ratio of the D band to the G band (I_D/I_G) ratio of 0.74. Activated carbon derived from potassium hydroxide activation with microwave irradiation at 1 minutes and potassium hydroxide to carbonized water hyacinth mass ratio of 3:1 possesed a lower I_D/I_G (0.65) than that of carbonized water hyacinth (0.81) indicating higher degree of graphitic ordering (Pimenta et al. 2007). In addition, activated carbon derived from potassium hydroxide activation with microwave irradiation at 1 minutes and potassium hydroxide to carbonized water hyacinth mass ratio of 3:1 exhibited not sugnificantly different I_D/I_G (0.74) than that 1:1 (0.65) indicating no difference in degree of graphitic ordering (Pimenta et al. 2007).

Figure 4-14 (d) demonstrated the G-band peak of activated carbon derived from potassium hydroxide activation with microwave irradiation at 1 minutes and potassium hydroxide to carbonized water hyacinth mass ratio of 6:1 which are significantly stronger than the D-band with a higher intensity ratio of the D band to the G band (I_D/I_G) ratio of 0.67. Activated carbon derived from potassium hydroxide activation with microwave irradiation at 1 minutes and potassium hydroxide to carbonized water hyacinth mass ratio of 6:1 possesed a lower I_D/I_G (0.67) than that of carbonized water hyacinth (0.81) indicating higher degree of graphitic ordering (Pimenta et al. 2007). Moreover, experimental results demonstrated that activated carbon derived from potassium hydroxide activation with microwave irradiation at 1 minutes and potassium hydroxide to carbonized water hyacinth mass ratio of 6:1 exhabited not significantly differente I_D/I_G (0.87) than that of 1:1 (0.65) and 3:1 (0.74) indicating no different in degree of graphitic ordering (Pimenta et al. 2007). Difference

in degree of graphitic ordering could not be observed might owing to the irradiation period that not long enough to provide enough energy to make a change in carbon structure.

Figure 4-14 Raman spectrum and fitting results of (a) carbonized water hyacinth and activated carbon derived from potassium hydroxide activation with microwave irradiation for 1 minutes using mixture of potassium hydroxide to carbonized water hyacinth at mass ratio of (a) 1:1, (b) 3:1, and (c) 6:1

Raman spectrum of each samples was fitted using two Lorentz functions and a linear baseline to achieve an adequate match to the experimental data. The match of activated carbon prepared from potassium hydroxide activation with microwave irradiation for 3 minutes together with potassium hydroxide to carbonized water hyacinth mass ratio in the range of 1:1, 3:1, and 6:1 presented R^2 values at 0.95, 0.96, and 0.95 respectively.

Figure 4-15 (a) demonstrated the G-band peak of carbonizeded water hyacinth which are significantly stronger than the D-band with a higher intensity ratio of the D band to the G band (I_D/I_G) ratio of 0.81. This result indicated that there are both the disordered structures and graphitic structure in the structure of dried water hyacinth.

Figure 4-15 (b) demonstrated the G-band peak of activated carbon from potassium hydroxide activation with microwave irradiation at 3 minutes and potassium hydroxide to carbonized water hyacinth mass ratio of 1:1 which are significantly stronger than the D-band with a higher intensity ratio of the D band to the G band (I_D/I_G) ratio of 0.65. The activated carbon from potassium hydroxide activation with microwave radiaiton possesed a lower I_D/I_G (0.65) than that of carbonized water hyacinth (0.81) indicating higher degree of graphitic ordering (Pimenta et al. 2007). From this result, the resultant activated carbon can be expected to possess the high electric conductivity, which is necessary property for application of the capacitor.

Figure 4-15 (c) demonstrated the G-band peak of activated carbon derived from potassium hydroxide activation with microwave irradiation at 3 minutes and potassium hydroxide to carbonized water hyacinth mass ratio of 3:1 which are significantly stronger than the D-band with a higher intensity ratio of the D band to the

G band (I_D/I_G) ratio of 0.69. Activated carbon derived from potassium hydroxide activation with microwave irradiation at 3 minutes and potassium hydroxide to carbonized water hyacinth mass ratio of 3:1 possesed a lower I_D/I_G (0.69) than that of carbonized water hyacinth (0.81) indicating higher degree of graphitic ordering (Pimenta et al. 2007). In addition, activated carbon derived from potassium hydroxide activation with microwave irradiation at 3 minutes and potassium hydroxide to carbonized water hyacinth mass ratio of 3:1 exhibited not significantly different I_D/I_G (0.74) than that of 1:1 (0.65) indicating no difference in degree of graphitic ordering (Pimenta et al. 2007). **Figure 4-15 (d)** demonstrated the G-band peak of activated carbon derived from potassium hydroxide activation with microwave irradiation at 3 minutes and potassium hydroxide to carbonized water hyacinth mass ratio of 6:1 which are significantly stronger than the D-band with a higher intensity ratio of the D band to the G band (I_D/I_G) ratio of 0.65. Experimental results demonstrated that activated carbon derived from potassium hydroxide activation with microwave irradiation at 3 minutes and potassium hydroxide to carbonized water hyacinth mass ratio of 6:1 exhibited a lower I_D/I_G (0.65) than that of carbonized water hyacinth (0.81) indicating highher degree of graphitic ordering (Pimenta et al. 2007). Moreover, experimental results demonstrated that activated carbon derived from potassium hydroxide activation with microwave irradiation at 3 minutes and potassium hydroxide to carbonized water hyacinth mass ratio of 6:1 exhibited not significantly differente I_D/I_G (0.65) than that of 1:1 (0.65) and 3:1 (0.69) indicating no different in degree of graphitic ordering. Difference in degree of graphitic ordering could not be observed might owing to the irradiation period that not long enough to provide enough energy to make a change in carbon structure.
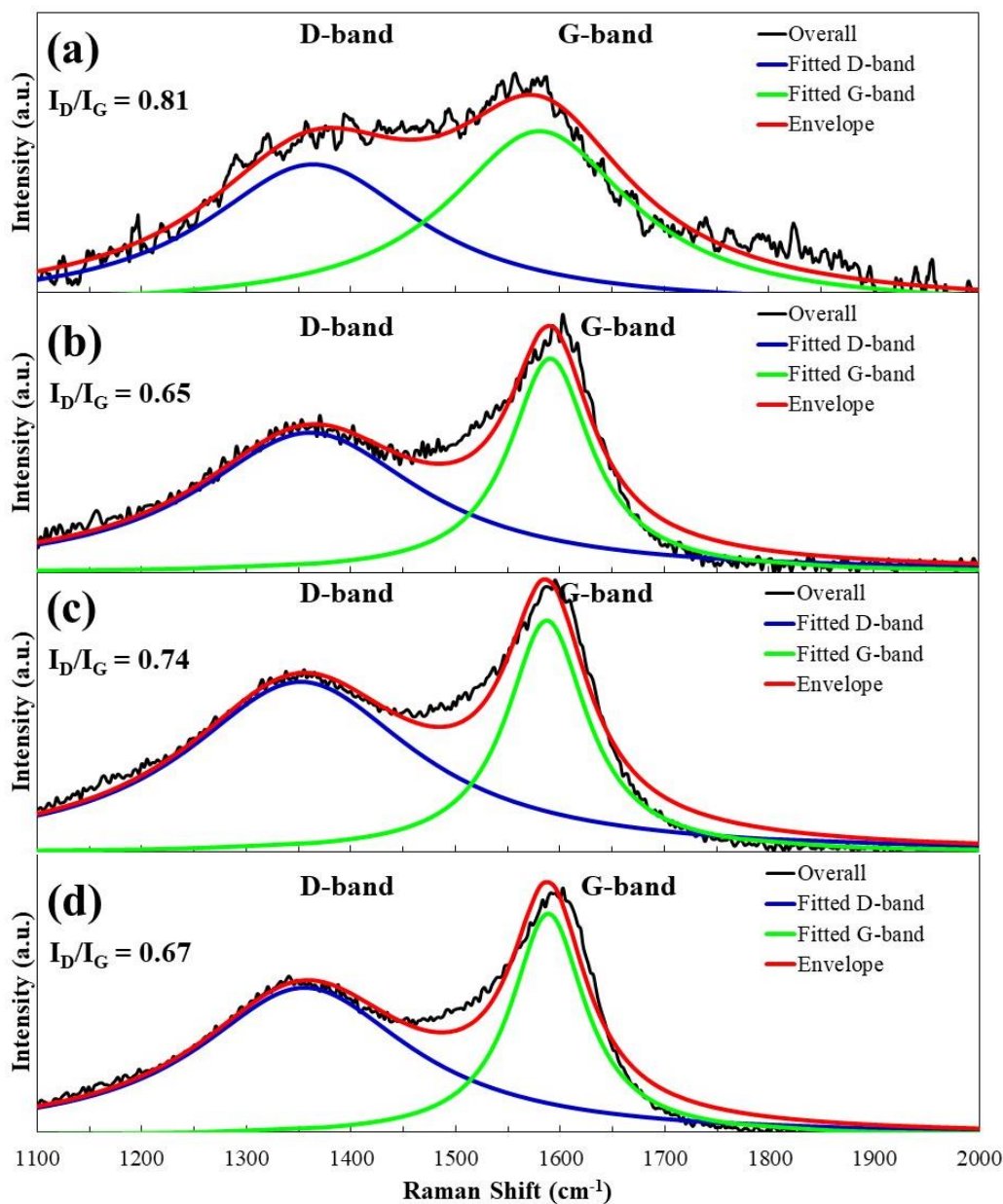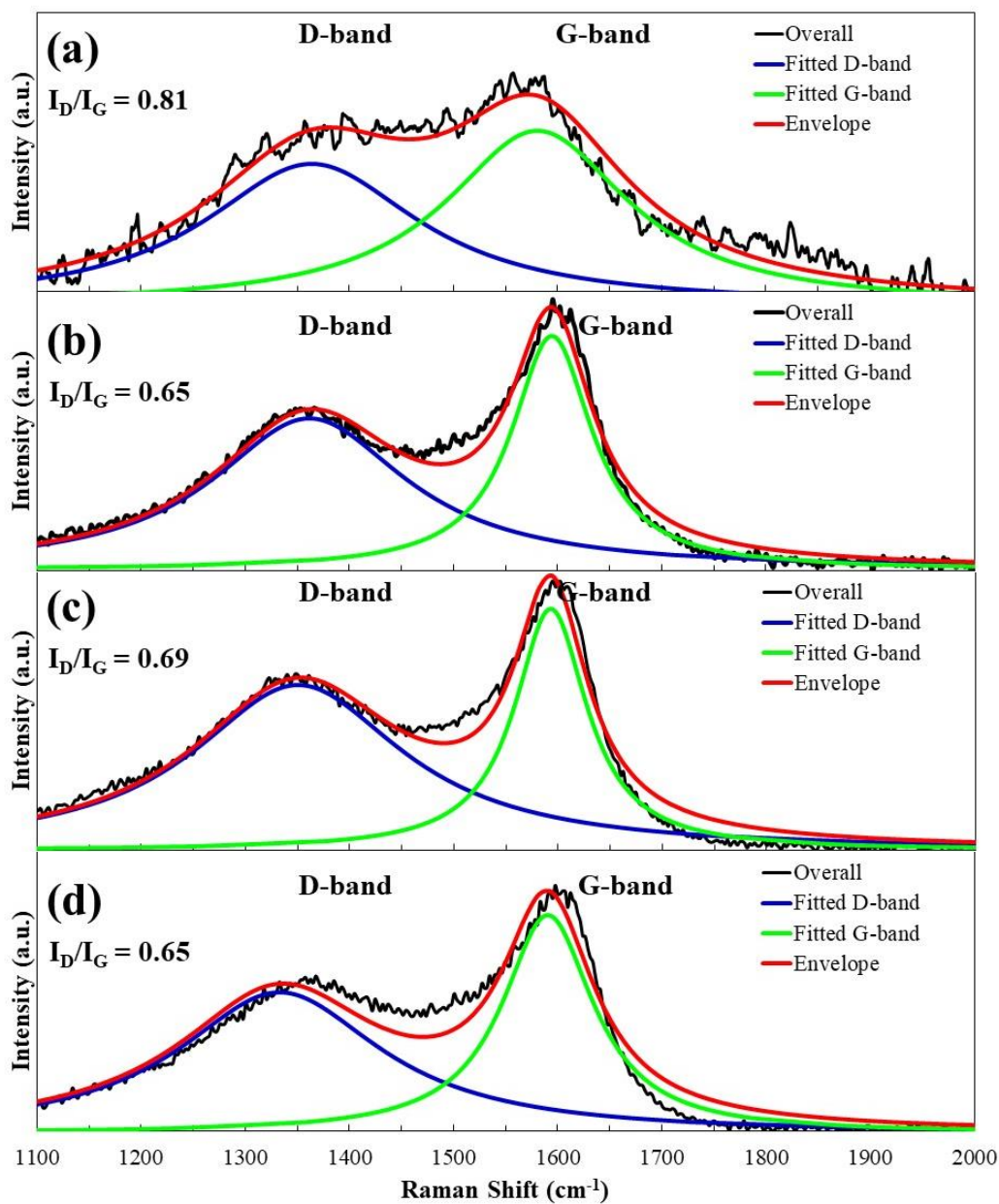
Figure 4-15 Raman spectrum and fitting results of (a) carbonized water hyacinth and activated carbon derived from potassium hydroxide activation with microwave irradiation for 3 minutes using mixture of potassium hydroxide to carbonized water hyacinth at mass ratio of (a) 1:1, (b) 3:1, and (c) 6:1

4.5.3 Elemental analysis

It found that the yield of activated carbon, which was calculated using **Equation 4-3**, and percentage of carbon content significantly decreased with an increasing of potassium hydroxide to carbonized water hyacinth mass ratio as shown in **Figure 4-13**. The reaction rate directly related to concentration of potassium hydroxide as described by Arrhenius equation in **Equation 2-3** and the mechanism stated in **Equation 4-4 to 4-12** resulting in decreased of carbon yield concentration of potassium hydroxide. This tendency could be observed when microwave irradiation time is in the range of 1-3 minutes as shown in **Figure 4-15** to **Figure 4-17**.
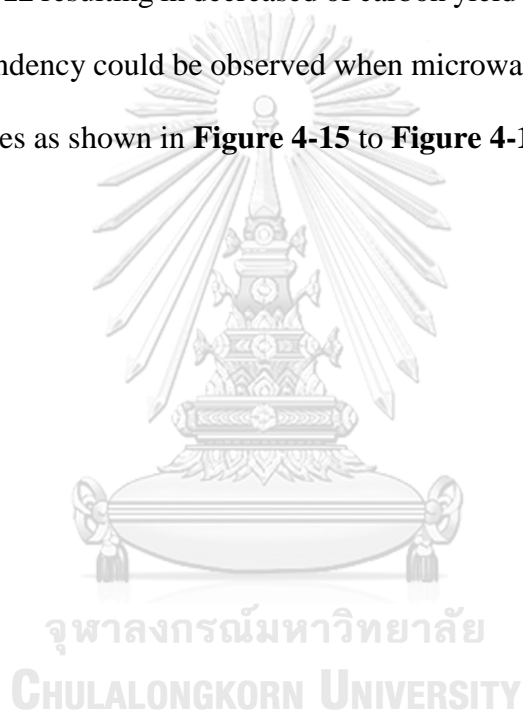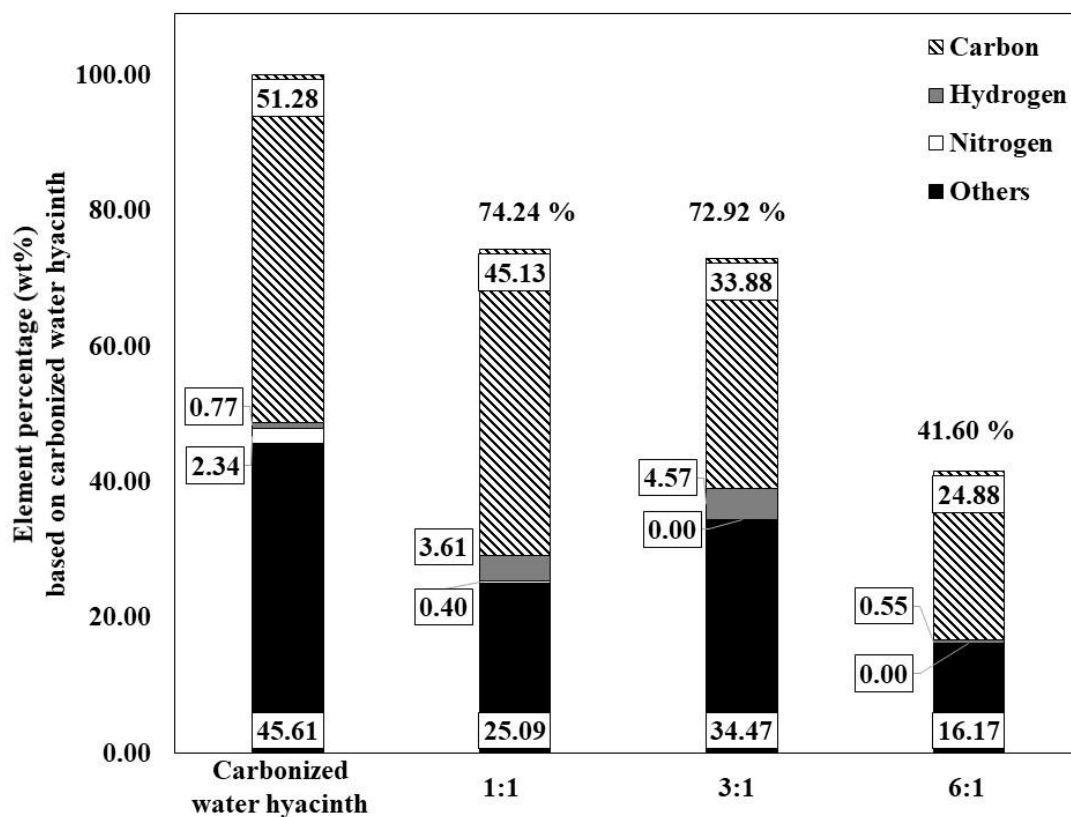
Figure 4-16 Elemental contents (in mass basis) of (a) carbonized water hyacinth and activated carbon derived from potassium hydroxide activation with microwave radiation at 1 minutes and potassium hydroxide to carbonized water hyacinth mass ratio of (a) 1:1, (b) 3:1, and (c) 6:1

Figure 4-17 Elemental contents (in mass basis) of carbonized water hyacinth and activated carbon derived from potassium hydroxide activation with microwave radiation at 2 minutes and potassium hydroxide to carbonized water hyacinth mass ratio of (a) 1:1, (b) 3:1, and (c) 6:1
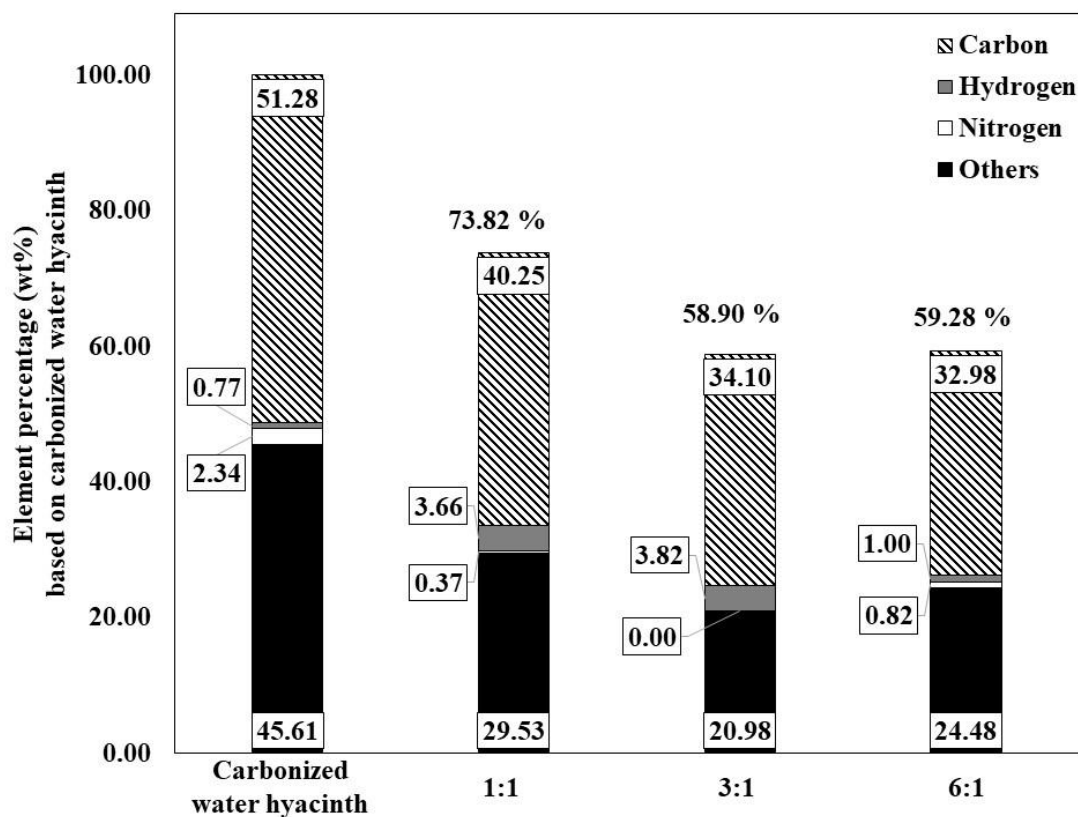
Figure 4-18 Elemental contents (in mass basis) of carbonized water hyacinth and activated carbon derived from potassium hydroxide activation with microwave radiation at 3 minutes and potassium hydroxide to carbonized water hyacinth mass ratio of (a) 1:1, (b) 3:1, and (c) 6:1

4.5.4 X-ray photoelectron spectroscopy analysis (XPS)

Due to limitation of elemental analysis used in this experiment, compositions of oxygen could not be determined directly. Compositions of oxygen can be obtained by XPS as shown in **Table 4-4**. The results shown that majority components in the activated carbon were carbon and oxygen which were consisted with elemental analysis results. XPS spectrum of the activated carbon were provided in **Figure D-3** to **Figure D-7** and **Table D-1.**

Table 4-3 Composition of activated carbon derived from potassium hydroxide activation with microwave radiation obtained from XPS

Activating Condition		% Composition by mole			% Composition by mass		
Potassium hydroxide to carbonized water hyacinth mass ratio	Radiation Time (min)	C	O	K	C	O	K
Carbonized Water Hyacinth		43.74	36.52	19.75	38.96	37.17	23.87
1:1	1	58.16	37.74	4.10	54.43	40.36	5.21
1:1	3	36.58	63.42	0.00	33.54	66.46	0.00
3:1	2	22.65	77.35	0.00	20.40	79.60	0.00
6:1	1	23.65	70.92	5.43	21.10	72.32	6.58
6:1	3	58.40	31.30	10.30	54.00	33.08	12.93

4.6 Effect of water adding method

This part of the research focused on method of adding water into activation. There are two methods was used in this study which are soaking carbonized water hyacinth with potassium hydroxide for 24 hours and wetting nitrogen gas before flowing in activation system. For comparison, activated carbon were derived from water hyacinth using potassium hydroxide activation with microwave radiation period of 1-3 minutes (800 watts) and potassium hydroxide to carbonized water hyacinth at mass ratio of 1:1, 3:1, and 6:1.

4.6.1 Scanning Electron Microscope (SEM)

      Figure 4-19 displays an SEM image of activated carbon, which were derived from potassium hydroxide activation using microwave radiation at 3 minutes and potass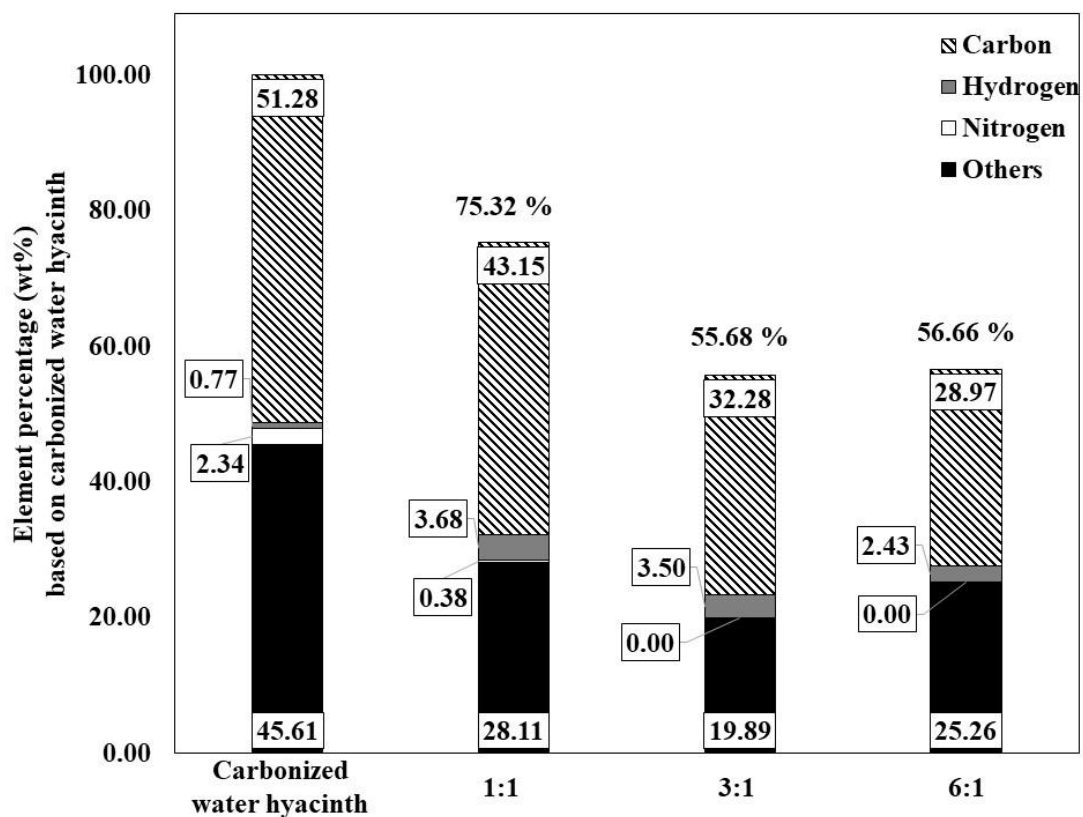ium hydroxide to carbonized water hyacinth mass ratio of 6:1 which is considered as the most severe condition studied in this thesis and adding water by wet impregnation together with wet nitrogen gas, and a sheet-like product with a large uniform surface was observed. After being activated, the morphology of the products' structure changed slightly compared with dried, hydrothermal, and carbonized water hyacinth's structures as presented in **Figure 4-1** to **Figure 4-3**.

2 µm
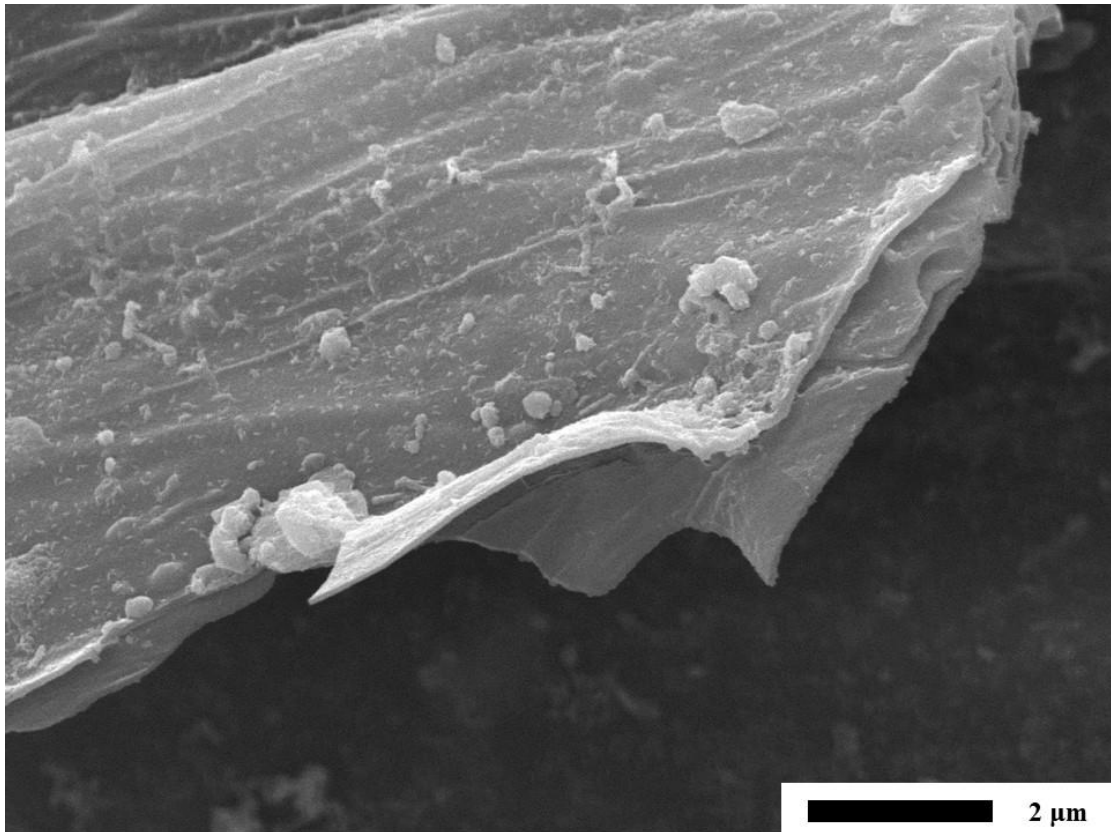
Figure 4-19 SEM images of activated carbon prepared using microwave irradiation for 3 min with potassium hydroxide to carbonized water hyacinth mass ratio of 6:1 and adding water by are wet impregnation together with wet nitrogen gas

4.6.3 Brunauer–Emmett–Teller (BET) analysis

According to the intercalation process of potassium metal (**Equation 4-8**) in the carbon lattices of the carbonized water hyacinth that volumetrically expands the carbon framework. After the intercalated potassium metal, K_2CO_3, and K_2O were removed by washing, a large nominal surface area with high micro- and meso-porosity can be observed in activated carbon prepared by adding water using wetting nitrogen gas, and

using both wetting nitrogen gas, and soaking in potassium hydroxide solution as presented in **Figure 4-20** respectively.
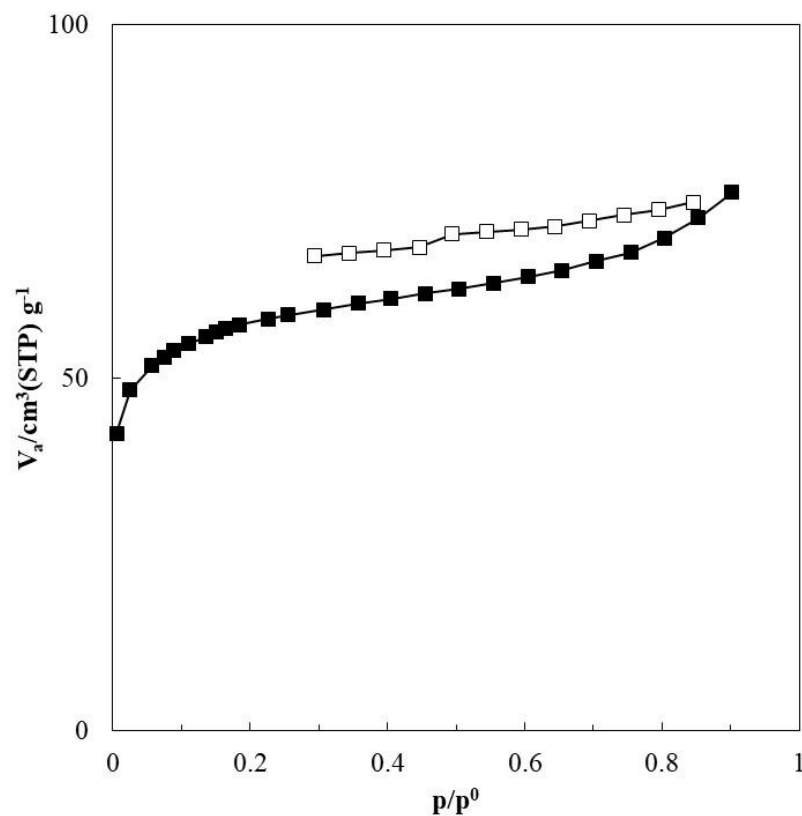
Figure 4-20 N$_2$ sorption isotherms (filled symbols mean adsorption isotherm, and open symbols mean desorption isotherm) of activated carbon derived from potassium hydroxide activation with microwave irradiation and using wet impregnation together with wet nitrogen gas

Specific surface area of activated carbon prepared by using only wetting nitrogen gas and using both wetting nitrogen gas and adding water by wet impregnation in potassium hydroxide solution possessed specific surface area of 131 m^2 g^{-1}-carbon. The experimental results show that degree of porosity of activated carbon wet impregnation in potassium hydroxide solution was lower than activated carbon

prepared without adding water (868 m^2 g^{-1}-carbon) because wetting carbonized water

hyacinth in potassium hydroxide solution causing water diffusing into the pores of

carbonized water hyacinth. When carbonized water hyacinth were activated, water in

the pores of carbonized water hyacinth were exposed and enlarged the pores size,

resulting in lower specific surface area.

4.6.4 Elemental analysis

It found that the yield of activated carbon obtained by adding water using wet

impregnation together with wet nitrogen gas, which was calculated using

Equation 4-3, and percentage of carbon content decreased with an increasing of

potassium hydroxide to carbonized water hyacinth mass ratio as shown in **Figure 4-21**.

The reaction rate directly related to concentration of potassium hydroxide as described

by Arrhenius equation in **Equation 2-3** and the mechanism stated in **Equation 4-4 to**

4-8 resulting in decreased of carbon yield with an increasing of concentration of

potassium hydroxide. This tendency can also be observed when adding water by only

wet impregnation in potassium hydroxide solution and only wet nitrogen gas as shown

in **Figure 4-22** and **Figure 4-23**.
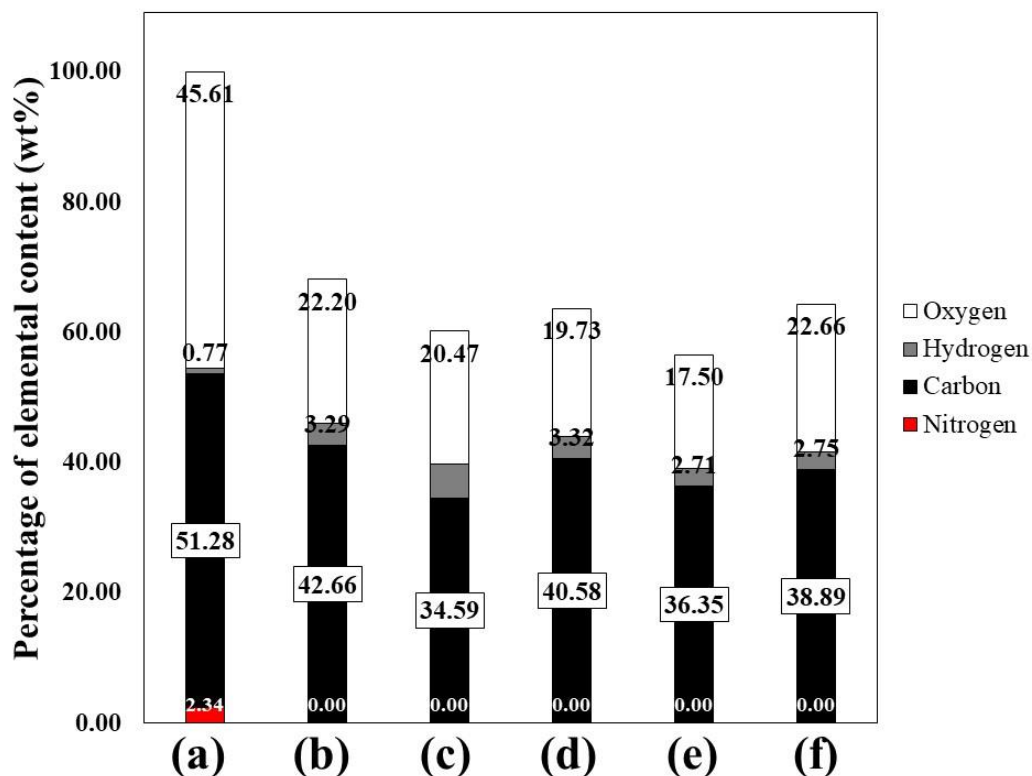
Figure 4-21 Elemental contents (in mass basis) of (a) carbonized water hyacinth and activated carbon derived from potassium hydroxide activation using microwave irradiation at 1 minutes and potassium hydroxide to carbonized water hyacinth mass ratio of (b) 1:1 and (c) 6:1, using microwave irradiation at 2 minutes and potassium hydroxide to carbonized water hyacinth mass ratio of (d) 3:1, and using microwave irradiation at 3 minutes and potassium hydroxide to carbonized water hyacinth mass ratio of (e) 1:1 and (f) 6:1 and adding water by wet impregnation together with wet nitrogen gas
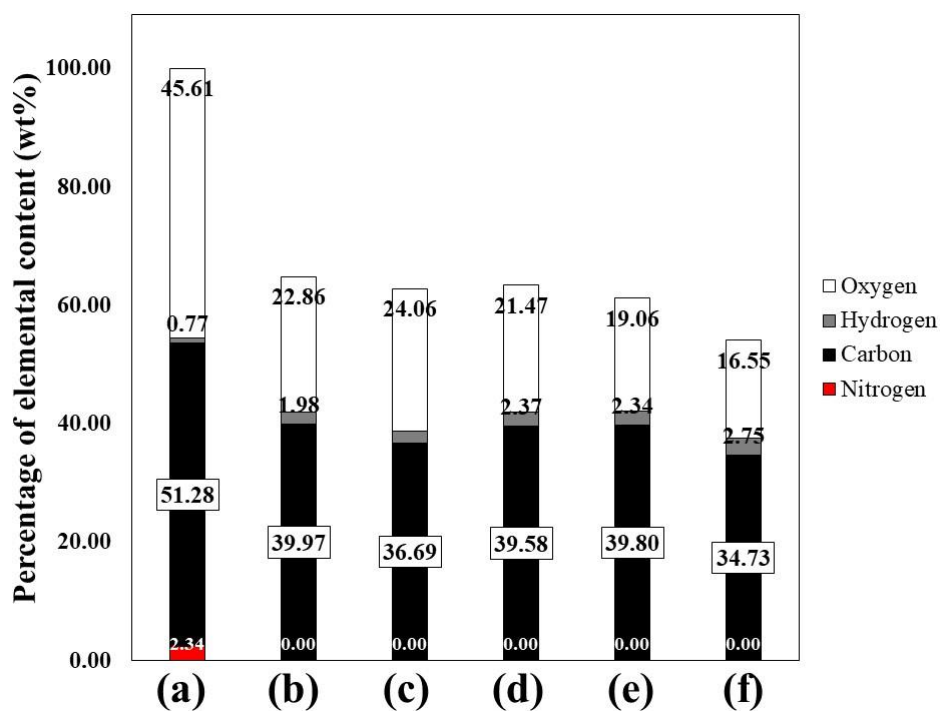
Figure 4-22 Elemental contents (in mass basis) of (a) carbonized water hyacinth and activated carbon derived from potassium hydroxide activation using microwave irradiation at 1 minutes and potassium hydroxide to carbonized water hyacinth mass ratio of (b) 1:1 and (c) 6:1, using microwave irradiation at 2 minutes and potassium hydroxide to carbonized water hyacinth mass ratio of (d) 3:1, and using microwave irradiation at 3 minutes and potassium hydroxide to carbonized water hyacinth mass ratio of (e) 1:1 and (f) 6:1 and adding water by only wet impregnation in potassium hydroxide solution
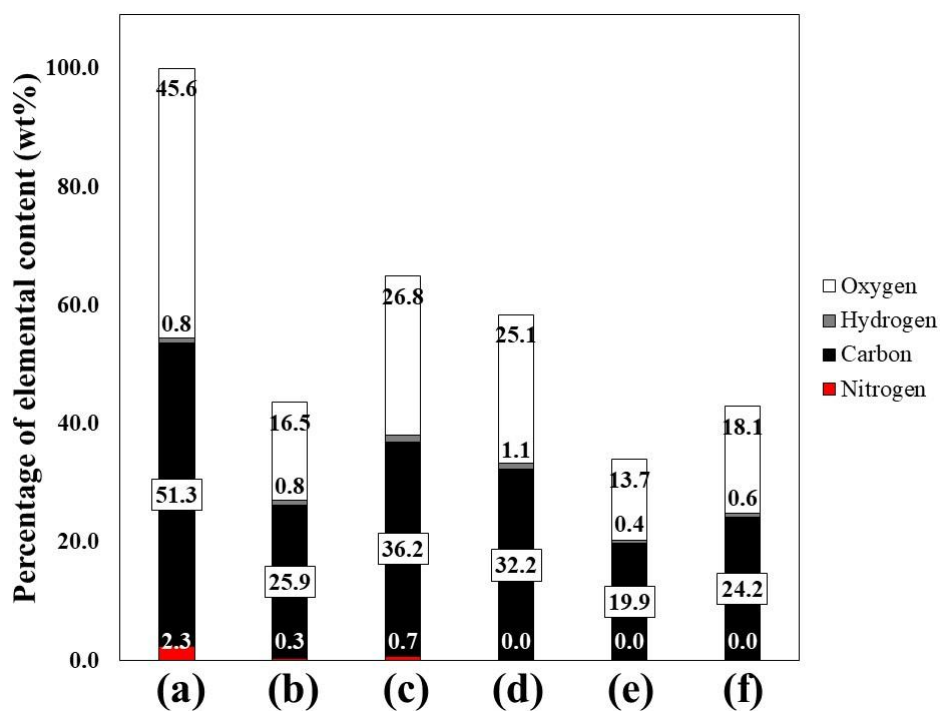
Figure 4-23 Elemental contents (in mass basis) of (a) carbonized water hyacinth and activated carbon derived from potassium hydroxide activation using microwave irradiation at 1 minutes and potassium hydroxide to carbonized water hyacinth mass ratio of (b) 1:1 and (c) 6:1, using microwave irradiation at 2 minutes and potassium hydroxide to carbonized water hyacinth mass ratio of (d) 3:1, and using microwave irradiation at 3 minutes and potassium hydroxide to carbonized water hyacinth mass ratio of (e) 1:1 and (f) 6:1 and adding water by only wetting nitrogen gas

4.6.5 X-ray photoelectron spectroscopy analysis (XPS)

Due to limitation of elemental analysis used in this experiment, compositions of oxygen could not be measured directly. Compositions of oxygen can be obtained by XPS as shown in **Table 4-4**. The results shown that majority components in activated carbon were carbon and oxygen which were consisted with elemental analysis results. XPS spectrum of activated carbon were provided in **Figure D-8** to **Figure D-17** and **Table D-1.**

Table 4-4 Composition of activated carbon obtained from XPS

| Activating Condition			% Composition by mole			% Composition by mass		
Methods of adding water	KOH:Carbon *	Radiation Time (min)	C	O	K	C	O	K
Carbonized Water Hyacinth			43.74	36.52	19.75	38.96	37.17	23.87
soaking	6:1	1	43.61	56.39	0	40.36	59.64	0.00
soaking	1:1	1	58.62	32.08	9.3	54.33	33.98	11.70
soaking	3:1	2	42.25	57.75	0	39.03	60.97	0.00
soaking	6:1	3	60.32	39.68	0	57.08	42.92	0.00
soaking	1:1	3	54.39	45.61	0	51.06	48.94	0.00
Soaking + wetting N_2	6:1	1	61.61	33.64	4.75	57.85	36.10	6.05
Soaking + wetting N_2	1:1	1	54.74	38.36	6.9	50.71	40.61	8.68
Soaking + wetting N_2	3:1	2	56.6	43.4	0	53.30	46.70	0.00
Soaking + wetting N_2	6:1	3	59.42	40.58	0	56.16	43.84	0.00
Soaking + wetting N_2	1:1	3	58.27	41.73	0	54.99	45.01	0.00

Note: KOH:Carbon* represented mass ratio of potassium hydroxide to carbonized water hyacinth

4.7 Application of activated carbon as capacitance electrode materials

For activated carbon prepared by carbon dioxide activation, the pellets of the consolidated water hyacinth powder could still be preserved after the carbonization and activation steps were conducted. It should be reminded that the weight of the dried water hyacinth could be reduced by carbonization, in which the volatile contents in water hyacinth were considered to be evaporated. It can be expected that these volatile components can become natural binders so that the addition of any chemical binders was not necessary to the consolidation of such water hyacinth powder. Accordingly, the as-formed disk pellets, which were prepared without addition of any blinder, were directly used as the electrodes in the investigation on electrical capacitive properties. To determine the electric capacitance of the activated carbon pellets with 6M KOH electrolyte, the direction of the constant current was switched in each cycle of the charge-discharge steps so that the inter-electrode voltage changed between the two programed values, 0 and 0.176 V. The time-dependency of the inter-electrode voltage when the current density was 1.26 mA g^{-1} is shown in **Figure 2-24 (a)**.

It should be noted that the charge-discharge cycle was asymmetric, where the fast rise and drop of the voltage when the current direction was switched are outstanding. Such fast changes could be caused by a limitation of the ionic diffusion rate for the exchange of the dominant polarity of the ions existing at adjacent zone nearby the electrode surface (Wu et al. 2016). These fast changes would become apparently significant because the voltage-scan was conducted in narrow range (0.0-0.176 V); nevertheless, the internal leakage current could be negligible in such conditions. Then, in the **Figure 2-24 (a)**, the range since the fast voltage-rise was terminated in charging step until the discharge step was initiated was used to calculate

the capacitance of the activated carbon electrode. As a result, the estimated capacitance of such typical sample was 32 F g^{-1}.

In addition, a multiple charge-discharge cycling operation was tested up to 425 cycles as shown in **Figure 2-24 (b)**. It was found that the capacitance of typical sample decreased to 33 % of the initial value after 200 charge-discharge cycles were conducted. Nevertheless, the capacitance of typical sample turned to rise up afterward and achieved the value of 190 % after 425 cycles were performed. The decrease in the capacitance would generally be attributed to the decrease in the specific surface area of electrode material (Chen et al. 2014). Such decrease in the capacitance would occur when weak structures generated by the activation step were destroyed by the multiple charge-discharge cycling process. On the other hand, the capacitance could be improved in the later cycles because amorphous carbons which would block the micropores could be eliminated during the multiple charge-discharge cycles (Pimenta et al. 2007). With all results discussed above, it would be reasonable to the activated carbon prepared from dried water hyacinth powder would be the promising electrode material for supercapacitor application.
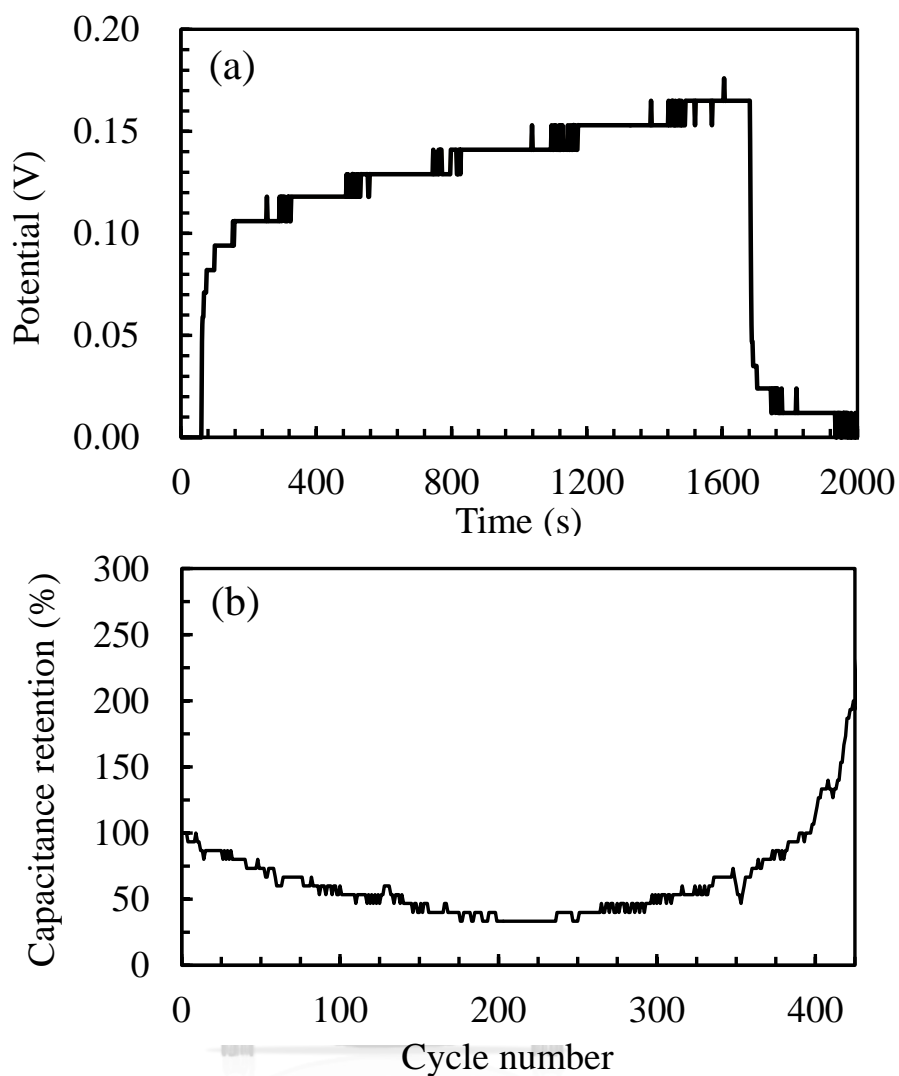
Figure 4-24 (a) Charge-discharge curve (one cycle) of activated carbon pellet electrode prepared from dried water hyacinth and (b) its cyclability

CHAPTER 5

CONCLUSIONS AND RECOMMENDATIONS

5.1 Conclusions

Activated carbon was successfully synthesized from dried water hyacinth using microwave irradiation and potassium hydroxide activation. As a beginning, dried water hyacinth was hydrothermally pretreated and carbonized before being activated. Hydrothermal pretreatment and carbonization can enhance carbon content of hydrothermal and carbonized water hyacinth from dried water hyacinth by reducing the hydrogen and oxygen contents according to chemical dehydration reaction during hydrothermal pretreatment and carbonization:

$$4(C_6H_{10}O_5)_n \rightarrow 2(C_{12}H_{10}O_5)_n + 10\ n \cdot (H_2O).$$

To study the effects of activating agent, activated carbon was prepared using potassium hydroxide and carbon dioxide activation. The results show that porosity of activated carbon derived from potassium hydroxide activation was larger than that of carbon dioxide activation because various activating agents i.e. K, K_2O, K_2CO_3, CO, CO_2, H_2O, and H_2 which could enhance activation process were generated in potassium hydroxide activation process.

To study the effects of heating method, activated carbon derived from potassium hydroxide activation were prepared by microwave irradiation and heat irradiation using electric furnace. Experimental results shown that activated carbon with nominal specific surface area can be synthesized from both heating methods. However, microwave irradiation (3 minutes) consumed less time than heat irradiation (1 hours)

because microwave irradiation can induce dipole rotation in atomic scale and create a frictional force between atoms and molecules within heated material so that volumetric heating inside the heated material is realized.

Effect of microwave radiation time on resultant activated carbon was studied. The results show that the yield of activated carbon and percentage of carbon content slightly decreased when microwave irradiation time was longer. The reasons are that the reaction rate relates to temperature, which increase when radiation time increase, resulting in decreased of carbon yield when radiation time is longer.

In addition, the yield of activated carbon and percentage of carbon content significantly decreased with an increase in potassium hydroxide to carbonized water hyacinth mass ratio. Since the reaction rate directly relates to concentration of potassium hydroxide, carbon yield decreased with increasing of potassium hydroxide concentration. This tendency could be observed when microwave irradiation time is in the range of 1-3 minutes. The BET analysis shows that activated carbon, which was activated with microwave irradiation for 3 minutes with mass radio of potassium hydroxide to carbonized water hyacinth at 6:1, possessed a nominal specific surface area of 867.39 m^2 g^{-1}-carbon.

Nowadays, water has been used as an activating agent to produce activated carbon. In this thesis, method of adding water into activation system was investigated. The experimental results show that the yield of activated carbon obtained by adding water using wetting nitrogen gas, soaking in potassium hydroxide solution and both soaking in potassium hydroxide solution and wetting nitrogen gas shown the same tendency that percentage of carbon content decreased with an increase in potassium hydroxide to carbonized water hyacinth mass ratio. Furthermore, activated carbon

prepared by using wet impregnation together with wet nitrogen gas and activated using potassium hydroxide activation with microwave irradiation for 1 minutes with mass radio of potassium hydroxide to carbonized water hyacinth at 1:1 possessed specific surface area of 208 m^2 g^{-1}-carbon.

The consolidated carbon pellets can be derived from water hyacinth using potassium hydroxide activation exhibited nominal electrical capacitance of 32 F g^{-1} when they were subjected to a direct electrical current of 1.26 mA g^{-1}. Observation of the capacitance retention with 425 charge-discharge cycles of the resultant activated carbon would suggested that it could be promising for supercapacitor application.

5.2 Recommendations

1. Improving specific surface area of activated carbon by increasing microwave radiation time used in activation step. To increasing the radiation time, activation system with microwave radiation much be improved e.g. a suitable container much has high thermal expansion coefficient.
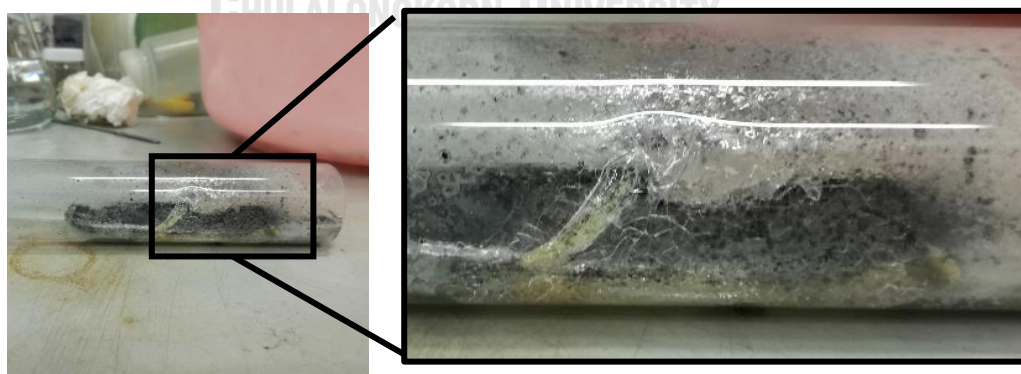

Figure 5-1 Broken quartz container

2. Improving microwave radiation in activation system to be more uniform

    distribution.

Figure 5-2 Insulation used in potassium hydroxide activation with microwave irradiation

จุฬาลงกรณ์มหาวิทยาลัย

CHULALONGKORN UNIVERSITY

REFERENCES

Abdul Khalil, H. P. S., P. Firoozian, I. O. Bakare, Hazizan Md Akil, and Ahmad Md
　　　　Noor. 2010. 'Exploring biomass based carbon black as filler in epoxy
　　　　composites: Flexural and thermal properties', *Materials & Design*, 31: 3419-
　　　　25.

Abechi, Stephen, Casimir Gimba, A. Uzairu, and Yakubu Dallatu. 2013. *Preparation
　　　　and characterization of activated carbon from Palm Kernel shell by chemical
　　　　activation*.

Ahmed, Muthanna J., and Samar K. Theydan. 2013. 'Microporous activated carbon
　　　　from Siris seed pods by microwave-induced KOH activation for
　　　　metronidazole adsorption', *Journal of Analytical and Applied Pyrolysis*, 99:
　　　　101-09.

Baccar, R., J. Bouzid, M. Feki, and A. Montiel. 2009. 'Preparation of activated carbon
　　　　from Tunisian olive-waste cakes and its application for adsorption of heavy
　　　　metal ions', *Journal of Hazardous Materials*, 162: 1522-29.

Chen, Haisheng, Thang Ngoc Cong, Wei Yang, Chunqing Tan, Yongliang Li, and
　　　　Yulong Ding. 2009. 'Progress in electrical energy storage system: A critical
　　　　review', *Progress in Natural Science*, 19: 291-312.

Chen, Shen-Ming, Rasu Ramachandran, Veerappan Mani, and Saraswathi Ramiah.
　　　　2014. *Recent Advancements in Electrode Materials for the High-performance
　　　　Electrochemical Supercapacitors: A Review*.

Chia, Chee H., Bin Gong, Stephen D. Joseph, Christopher E. Marjo, Paul Munroe,
　　　　and Anne M. Rich. 2012. 'Imaging of mineral-enriched biochar by FTIR,
　　　　Raman and SEM–EDX', *Vibrational Spectroscopy*, 62: 248-57.

Dai, Leilei, Chao He, Yunpu Wang, Yuhuan Liu, Zhenting Yu, Yue Zhou, Liangliang
　　　　Fan, Dengle Duan, and Roger Ruan. 2017. 'Comparative study on microwave
　　　　and conventional hydrothermal pretreatment of bamboo sawdust: Hydrochar
　　　　properties and its pyrolysis behaviors', *Energy Conversion and Management*,
　　　　146: 1-7.

El-Wakil, A. M., and F. S. Awad. 2014. *Removal of Lead from Aqueous Solution on
　　　　Activated Carbon and Modified Activated Carbon Prepared from Dried Water
　　　　Hyacinth Plant*.

Ergun, Sabri. 1956. 'Kinetics of the Reaction of Carbon with Carbon Dioxide', *The
　　　　Journal of Physical Chemistry*, 60: 480-85.

Foo, K. Y., and B. H. Hameed. 2011. 'Preparation of oil palm (Elaeis) empty fruit
　　　　bunch activated carbon by microwave-assisted KOH activation for the
　　　　adsorption of methylene blue', *Desalination*, 275: 302-05.

Frackowiak, Elzbieta. 2007. 'Carbon materials for supercapacitor application',
　　　　Physical Chemistry Chemical Physics, 9: 1774-85.

Funke, Axel, and Felix Ziegler. 2010. 'Hydrothermal carbonization of biomass: A
　　　　summary and discussion of chemical mechanisms for process engineering',
　　　　Biofuels, Bioproducts and Biorefining, 4: 160-77.

Gao, Ying, Xianhua Wang, Jun Wang, Xiangpeng Li, Jianjun Cheng, Haiping Yang,
　　　　and Hanping Chen. 2013. 'Effect of residence time on chemical and structural

properties of hydrochar obtained by hydrothermal carbonization of water hyacinth', *Energy*, 58: 376-83.

Hsieh, Chien-To, and Hsisheng Teng. 2002. 'Influence of oxygen treatment on electric double-layer capacitance of activated carbon fabrics', *Carbon*, 40: 667-74.

Hu, Zhifeng, Xiaoqian Ma, and Longjun Li. 2015. 'Optimal conditions for the catalytic and non-catalytic pyrolysis of water hyacinth', *Energy Conversion and Management*, 94: 337-44.

Huang, Yang, Shunxing Li, Jianhua Chen, Xueliang Zhang, and Yiping Chen. 2014. 'Adsorption of Pb(II) on mesoporous activated carbons fabricated from water hyacinth using H3PO4 activation: Adsorption capacity, kinetic and isotherm studies', *Applied Surface Science*, 293: 160-68.

Huang, Yu-Fong, Pei-Te Chiueh, and Shang-Lien Lo. 2016. 'A review on microwave pyrolysis of lignocellulosic biomass', *Sustainable Environment Research*, 26: 103-09.

Hulicova, Denisa, Masaya Kodama, and Hiroaki Hatori. 2006. 'Electrochemical Performance of Nitrogen-Enriched Carbons in Aqueous and Non-Aqueous Supercapacitors', *Chemistry of Materials*, 18: 2318-26.

Ji, Yongbin, Tiehu Li, Li Zhu, Xiaoxian Wang, and Qilang Lin. 2007. 'Preparation of activated carbons by microwave heating KOH activation', *Applied Surface Science*, 254: 506-12.

Kierzek, K., E. Frackowiak, G. Lota, G. Gryglewicz, and J. Machnikowski. 2004. 'Electrochemical capacitors based on highly porous carbons prepared by KOH activation', *Electrochimica Acta*, 49: 515-23.

Kubota, Mitsuhiro, Atsushi Hata, and Hitoki Matsuda. 2009. 'Preparation of activated carbon from phenolic resin by KOH chemical activation under microwave heating', *Carbon*, 47: 2805-11.

Lam, Su Shiung, Rock Keey Liew, Yee Mun Wong, Peter Nai Yuh Yek, Nyuk Ling Ma, Chern Leing Lee, and Howard A. Chase. 2017. 'Microwave-assisted pyrolysis with chemical activation, an innovative method to convert orange peel into activated carbon with improved properties as dye adsorbent', *Journal of Cleaner Production*, 162: 1376-87.

Li, Guizhen, Jiaxiong Li, Wei Tan, Hai Jin, Huaixian Yang, Jinhui Peng, Colin J. Barrow, Min Yang, Hongbin Wang, and Wenrong Yang. 2016. 'Preparation and characterization of the hydrogen storage activated carbon from coffee shell by microwave irradiation and KOH activation', *International Biodeterioration & Biodegradation*, 113: 386-90.

Lillo-Ródenas, M. A., D. Cazorla-Amorós, and A. Linares-Solano. 2003. 'Understanding chemical reactions between carbons and NaOH and KOH: An insight into the chemical activation mechanism', *Carbon*, 41: 267-75.

Lin, Yuhan, Nana Zhao, Wei Nie, and Xiangling Ji. 2008. 'Synthesis of Ruthenium Dioxide Nanoparticles by a Two-Phase Route and Their Electrochemical Properties', *The Journal of Physical Chemistry C*, 112: 16219-24.

Molina-Sabio, M., M. T. Gonzalez, F. Rodriguez-Reinoso, and A. Sepúlveda-Escribano. 1996. 'Effect of steam and carbon dioxide activation in the micropore size distribution of activated carbon', *Carbon*, 34: 505-09.

Pandolfo, A. G., and A. F. Hollenkamp. 2006. 'Carbon properties and their role in supercapacitors', *Journal of Power Sources*, 157: 11-27.

Pimenta, M. A., G. Dresselhaus, M. S. Dresselhaus, L. G. Cancado, A. Jorio, and R. Saito. 2007. 'Studying disorder in graphite-based systems by Raman spectroscopy', *Phys Chem Chem Phys*, 9: 1276-91.

Raymundo-Piñero, E., K. Kierzek, J. Machnikowski, and F. Béguin. 2006. 'Relationship between the nanoporous texture of activated carbons and their capacitance properties in different electrolytes', *Carbon*, 44: 2498-507.

Rezania, Shahabaldin, Mohanadoss Ponraj, Mohd Fadhil Md Din, Ahmad Rahman Songip, Fadzlin Md Sairan, and Shreeshivadasan Chelliapan. 2015. 'The diverse applications of water hyacinth with main focus on sustainable energy and production for new era: An overview', *Renewable and Sustainable Energy Reviews*, 41: 943-54.

Russell, Alan D., Evangelia I. Antreou, Su Shiung Lam, Carlos Ludlow-Palafox, and Howard A. Chase. 2012. 'Microwave-assisted pyrolysis of HDPE using an activated carbon bed', *RSC Advances*, 2: 6756.

Sayğılı, Hasan, Fuat Güzel, and Yunus Önal. 2015. 'Conversion of grape industrial processing waste to activated carbon sorbent and its performance in cationic and anionic dyes adsorption', *Journal of Cleaner Production*, 93: 84-93.

Smith, J.M., and H.C. Van Ness. 1987. *Introduction to Chemical Engineering Thermodynamics* (McGraw-Hill).

Sodtipinta, Jedsada, Chanoknan Ieosakulrat, Natchapol Poonyayant, Pinit Kidkhunthod, Narong Chanlek, Taweechai Amornsakchai, and Pasit Pakawatpanurut. 2017. 'Interconnected open-channel carbon nanosheets derived from pineapple leaf fiber as a sustainable active material for supercapacitors', *Industrial Crops and Products*, 104: 13-20.

Wang, Yong-Gang, Zi-Dong Wang, and Yong-Yao Xia. 2005. 'An asymmetric supercapacitor using RuO2/TiO2 nanotube composite and activated carbon electrodes', *Electrochimica Acta*, 50: 5641-46.

Wu, Kai, Biao Gao, Jianjun Su, Xiang Peng, Xuming Zhang, Jijiang Fu, Shunjin Peng, and Paul K. Chu. 2016. 'Large and porous carbon sheets derived from water hyacinth for high-performance supercapacitors', *RSC Advances*, 6: 29996-30003.

Yan, Jun, Tong Wei, Wenming Qiao, Zhuangjun Fan, Lijun Zhang, Tianyou Li, and Qiankun Zhao. 2010. 'A high-performance carbon derived from polyaniline for supercapacitors', *Electrochemistry Communications*, 12: 1279-82.

Yang, Zusing, Chia-Ying Chen, and Huan-Tsung Chang. 2011. 'Supercapacitors incorporating hollow cobalt sulfide hexagonal nanosheets', *Journal of Power Sources*, 196: 7874-77.

Zhang, Lili, Zhibin Lei, Jintao Zhang, Xiaoning Tian, and X. S. Zhao. 2011. *Supercapacitors: Electrode Materials Aspects*.

APPENDIX

Appendix A   Elemental analysis

Table A- 1 Elemental analysis on mass basis

Operating variables used for the activation			% Yield	Composition (%wt)			
Adding water methods	Microwave radiation time (min)	KOH:Carbon *		N	C	H	O
Dried water hyacinth			-	2.16	33.95	4.85	58.96
Hydrothermal water hyacinth			-	2.51	37.73	5.12	54.52
Carbonized water hyacinth			100	2.34	51.28	0.77	45.61
No	3	6:1	59.28	1.39	55.63	1.69	41.29
No	2	6:1	56.66	0.00	51.12	4.30	44.58
No	1	6:1	41.60	0.00	59.80	1.33	38.87
No	3	1:1	73.82	0.51	54.53	4.96	40.00
No	1	1:1	74.24	0.54	60.79	4.87	33.80
No	2	1:1	75.32	0.51	57.29	4.89	37.32
No	1	3:1	72.92	0.00	46.46	6.27	47.27
No	2	3:1	55.68	0.00	57.98	6.29	35.73
No	3	3:1	58.90	0.00	57.89	6.49	35.62
Soaking and Wetting N_2 gas	1	6:1	60.18	0.00	57.47	8.51	34.02
Soaking and Wetting N_2 gas	1	1:1	68.14	0.00	62.60	4.82	32.58
Soaking and Wetting N_2 gas	2	3:1	63.64	0.00	63.77	5.22	31.01
Soaking and Wetting N_2 gas	3	6:1	64.30	0.00	60.48	4.28	35.24
Soaking and Wetting N_2 gas	3	1:1	56.56	0.00	64.27	4.79	30.94
Soaking	1	6:1	62.80	0.00	58.42	3.27	38.31
Soaking	1	1:1	64.82	0.00	61.67	3.06	35.27
Soaking	2	3:1	63.42	0.00	62.41	3.73	33.86
Soaking	3	6:1	54.04	0.00	64.28	5.09	30.63
Soaking	3	1:1	61.76	0.00	64.45	4.69	30.87

Table A- 1 Elemental analysis on mass basis (continuous)

Operating variables used for the activation			%Yield	Composition (%wt)			
Adding water methods	Microwave radiation time (min)	KOH:Carbon *		N	C	H	O
No water (same KOH left after soaking)	1	6:1	48.20	1.11	66.43	0.71	31.76
No water (same KOH left after soaking)	1	1:1	61.60	1.40	57.08	1.40	40.12
No water (same KOH left after soaking)	2	3:1	52.00	0.55	57.53	1.04	40.88
No water (same KOH left after soaking)	3	6:1	49.20	0.55	52.91	1.50	45.05
No water (same KOH left after soaking)	3	1:1	53.82	0.47	55.85	1.32	42.37
Wetting N_2 gas	1	6:1	43.60	0.69	59.45	1.92	37.95
Wetting N_2 gas	1	1:1	64.86	1.15	55.80	1.67	41.37
Wetting N_2 gas	2	3:1	58.36	0.00	55.22	1.81	42.96
Wetting N_2 gas	3	6:1	33.98	0.00	58.42	1.28	40.30
Wetting N_2 gas	3	1:1	42.88	0.00	56.51	1.35	42.14
KOH in furnace		6:1	55.92	0.00	50.48	0.23	49.29
CO_2 in furnace		6:1	40.70	0.00	34.46	0.39	65.15

Note: KOH:Carbon* represented mass ratio of potassium hydroxide to carbonized water hyacinth

Appendix B   Particle size distribution
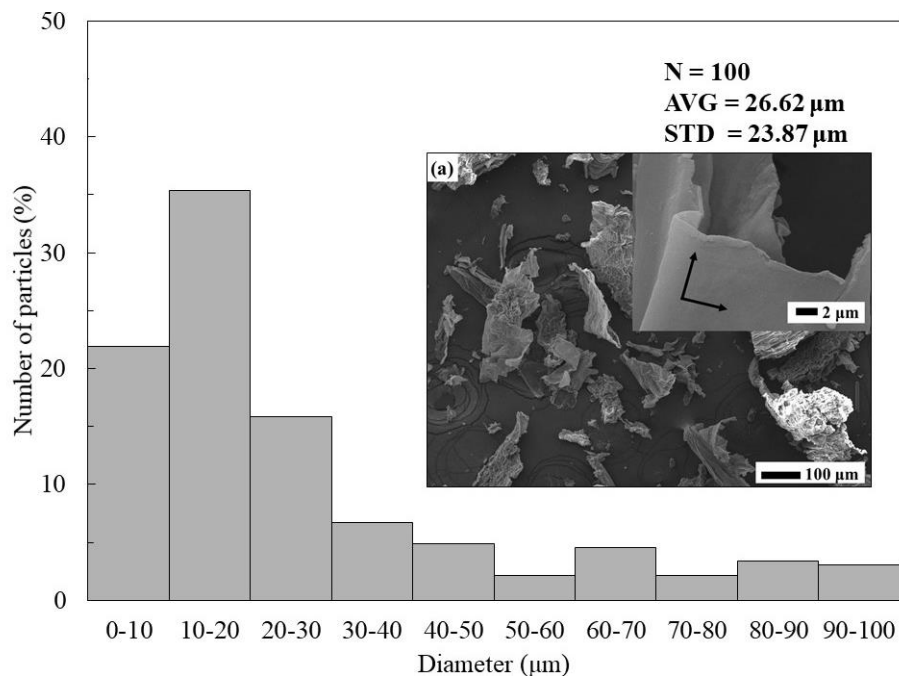
Figure B- 1 (a) SEM images and (b) particle size distribution of dried water hyacinth
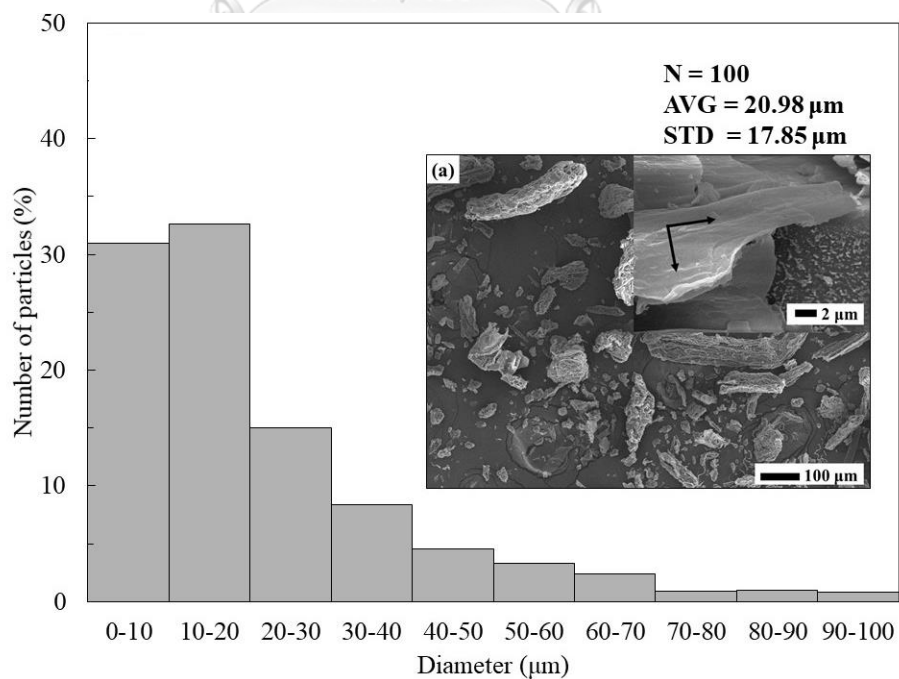
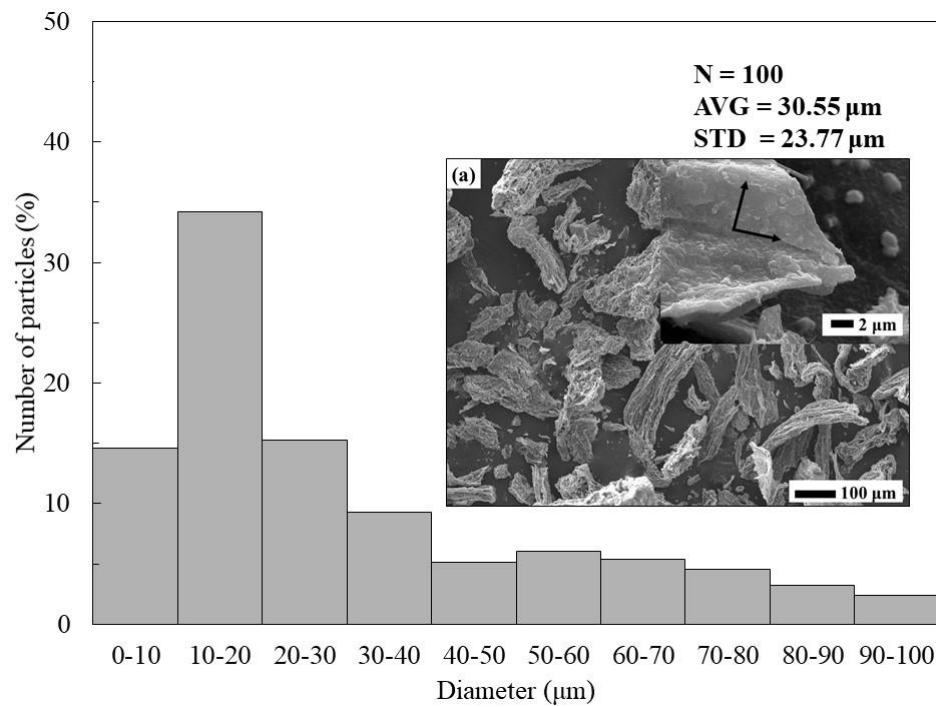**Figure B- 2 (a) SEM images and (b) particle size distribution of hydrothermal water hyacinth**

Figure B- 3 (a) SEM images and (b) particle size distribution of carbonized water hyacinth
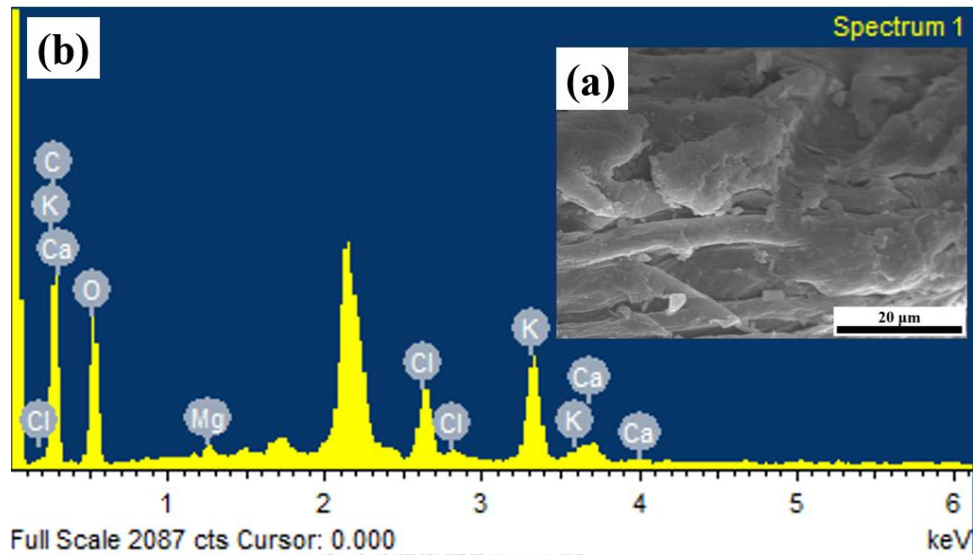
Appendix C   EDS Spectrum

Figure C- 1 (a) SEM image and EDS spectrum of dried water hyacinth

Appendix D   XPS spectrum

Table D- 1 Deconvoluted results from the C1s peak presented in XPS spectrum

Operating condition			Metal carbide	C-C	C-O	C=O
Adding water methods	Microwave radiation time (min)	KOH:Carbon *				
Hydrothermal Water Hyacinth			20.37	20.53	48.98	10.12
Carbonized Water Hyacinth			17.81	61.09	13.50	7.60
No	3	1:1	12.37	67.31	16.86	3.46
No	1	1:1	11.75	65.39	12.53	10.33
No	2	3:1	43.26	27.51	14.54	14.69
No	3	6:1	18.24	53.43	20.31	8.02
No	1	6:1	32.03	45.99	19.97	2.02
soaking	1	9.3	57.32	15.02	18.36	9.3
soaking	1	9.36	68.55	14.68	7.4	9.36
soaking	2	22.46	43.9	23.03	10.6	22.46
soaking	3	3.76	70.97	15.25	10.02	3.76
soaking	3	16.62	55.84	19.58	7.96	16.62
Soaking + wetting N2	1	15.61	62.27	12.75	9.37	15.61
Soaking + wetting N2	1	9.52	62.64	19.45	8.39	9.52
Soaking + wetting N2	2	6.24	65.24	20.41	8.11	6.24
Soaking + wetting N2	3	46.27	25.81	20.2	7.72	46.27
Soaking + wetting N2	3	70.85	7.97	15.61	5.58	70.85

Note: KOH:Carbon* represented mass ratio of potassium hydroxide to carbonized water hyacinth
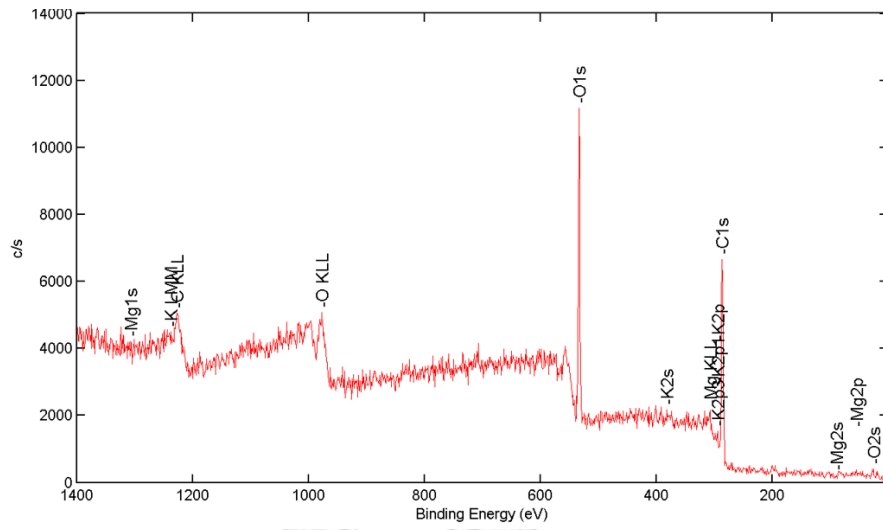
Figure D- 1 Full-scan XPS spectrum of hydrothermal water hyacinth
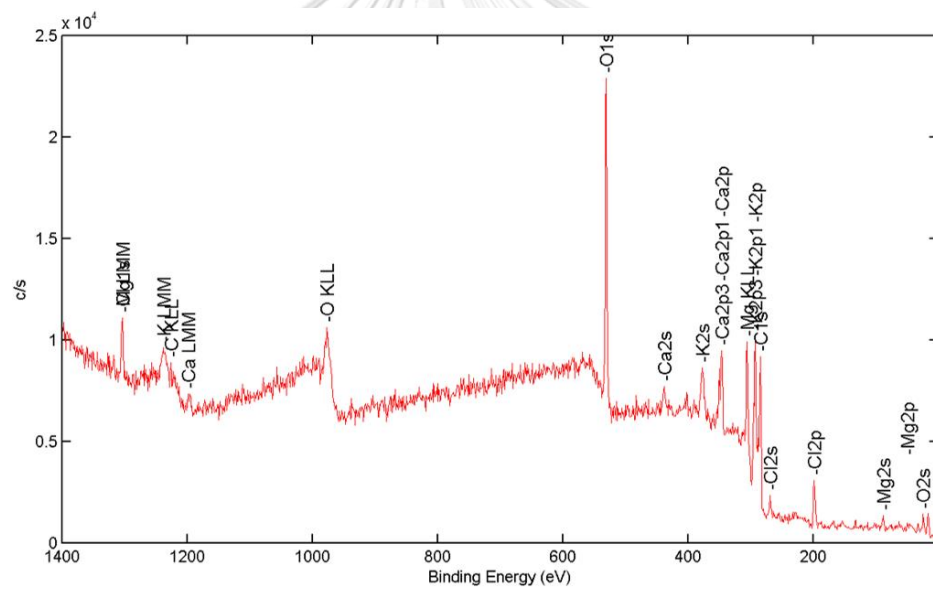
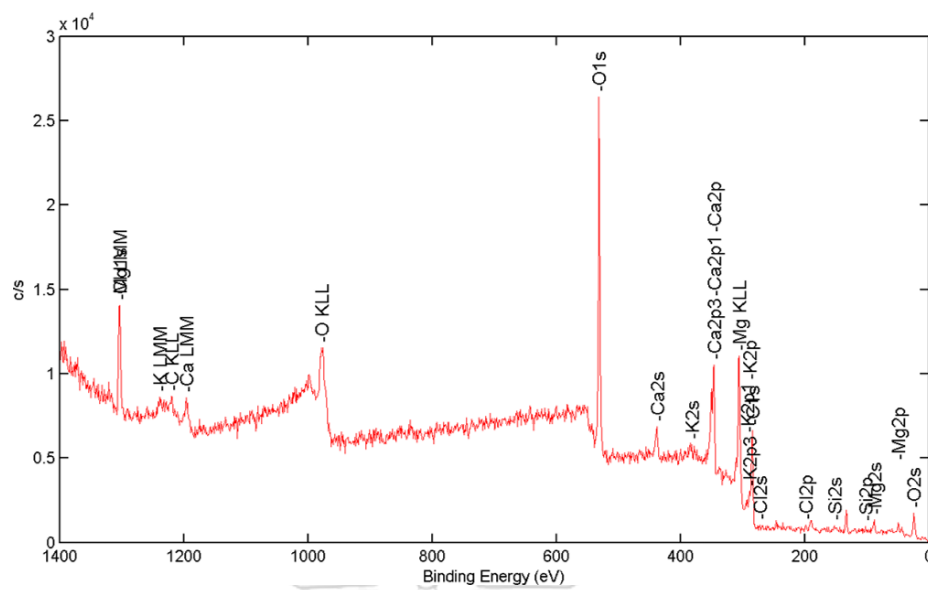**Figure D- 2 Full-scan XPS spectrum of carbonized water hyacinth**

Figure D- 3 Full-scan XPS spectrum of activated carbon derived from potassium hydroxide activation with microwave radiation at 3 minutes and potassium hydroxide to carbonized water hyacinth mass ratio of 1:1
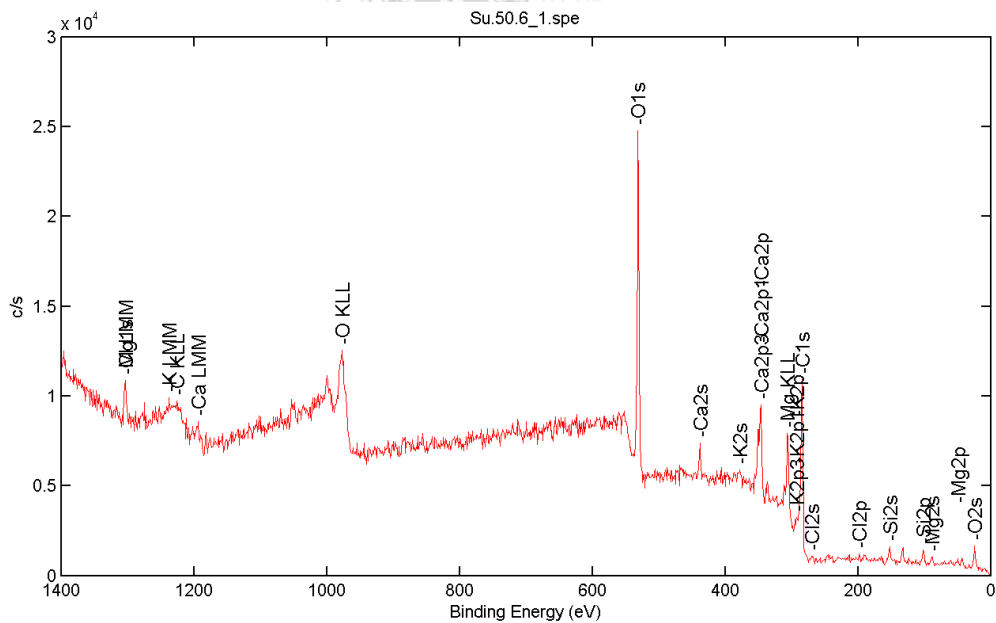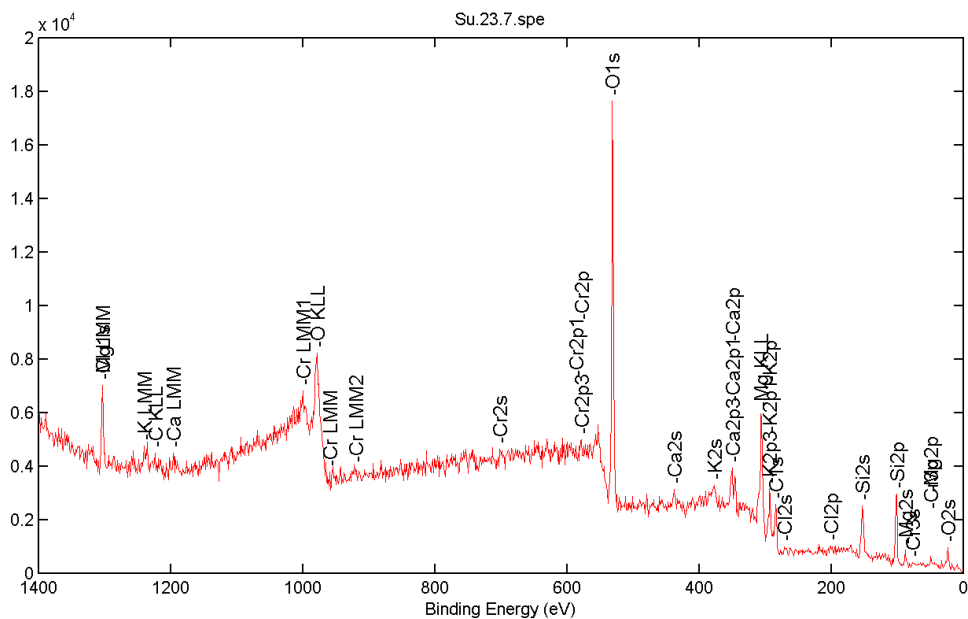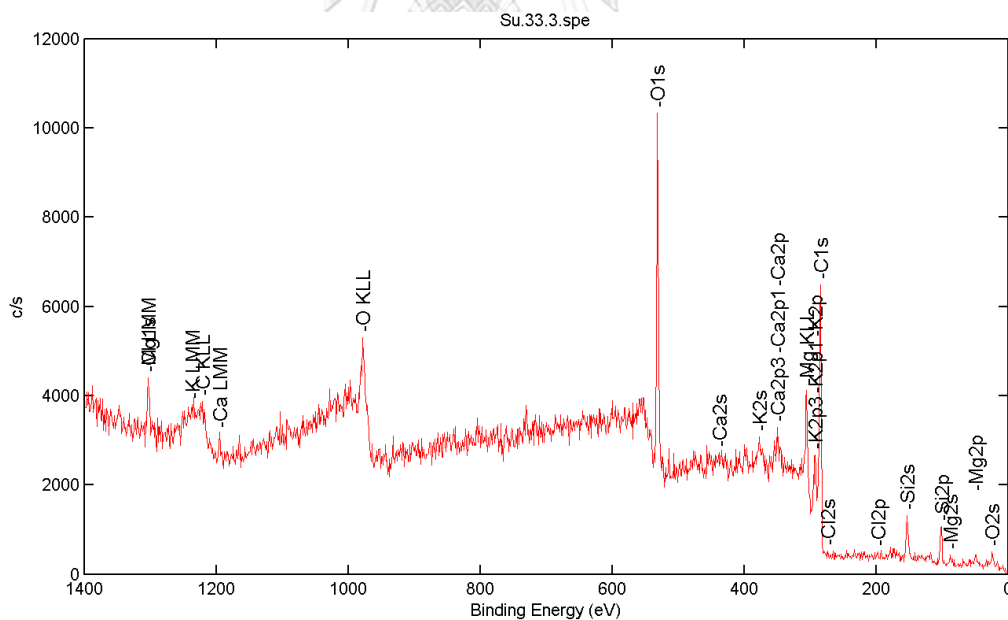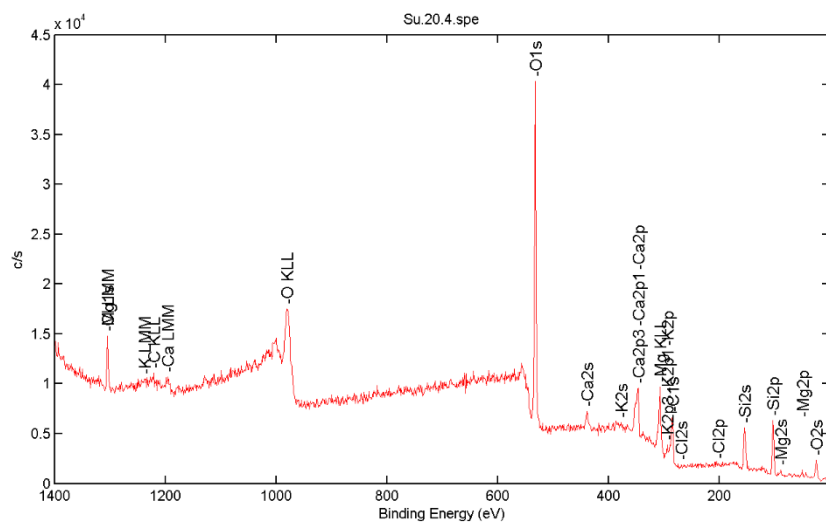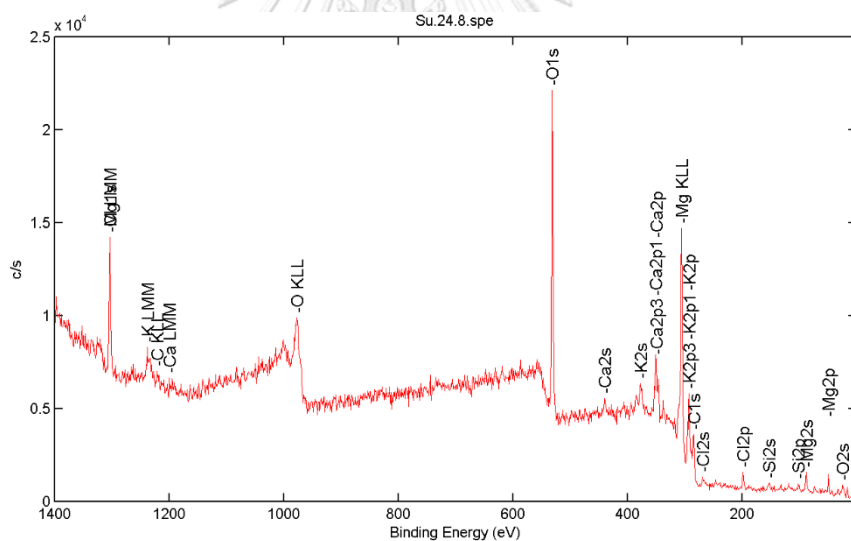

Figure D- 4 Full-scan XPS spectrum of activated carbon derived from potassium hydroxide activation with microwave radiation at 1 minutes and potassium hydroxide to carbonized water hyacinth mass ratio of 1:1

Figure D- 5 Full-scan XPS spectrum of activated carbon derived from potassium hydroxide activation with microwave radiation at 2 minutes and potassium hydroxide to carbonized water hyacinth mass ratio of 3:1
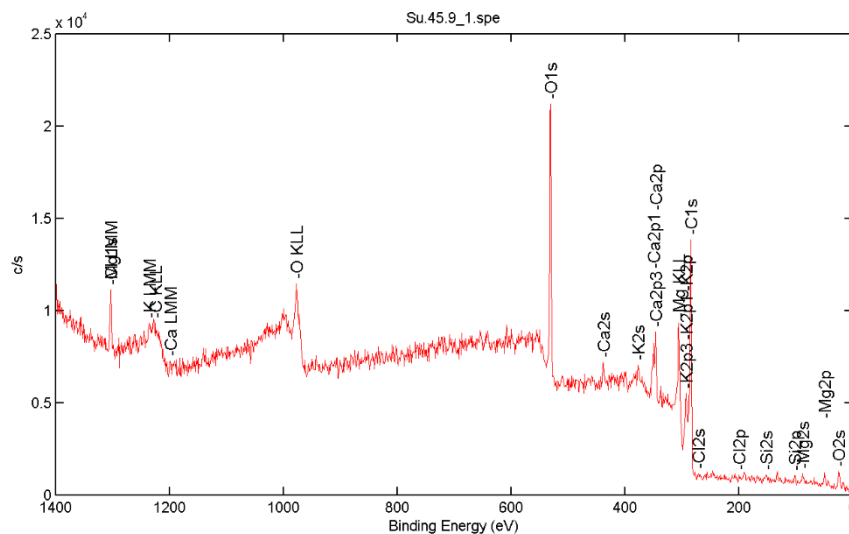

Figure D- 6 Full-scan XPS spectrum of activated carbon derived from potassium hydroxide activation with microwave radiation at 3 minutes and potassium hydroxide to carbonized water hyacinth mass ratio of 6:1

Figure D- 7 Full-scan XPS spectrum of activated carbon derived from potassium hydroxide activation with microwave radiation at 1 minutes and potassium hydroxide to carbonized water hyacinth mass ratio of 6:1

Figure D- 8 Full-scan XPS spectrum of activated carbon derived from potassium hydroxide activation with microwave radiation at 1 minutes and potassium hydroxide to carbonized water hyacinth mass ratio of 1:1 and adding water by soaking with potassium hydroxide solution
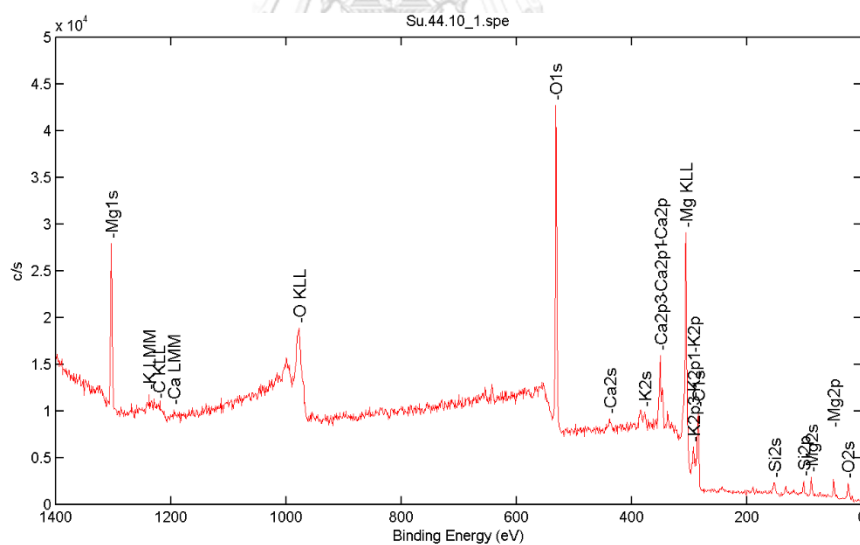
Figure D- 9 Full-scan XPS spectrum of activated carbon derived from potassium hydroxide activation with microwave radiation at 1 minutes and potassium hydroxide to carbonized water hyacinth mass ratio of 6:1 and adding water by soaking with potassium hydroxide solution
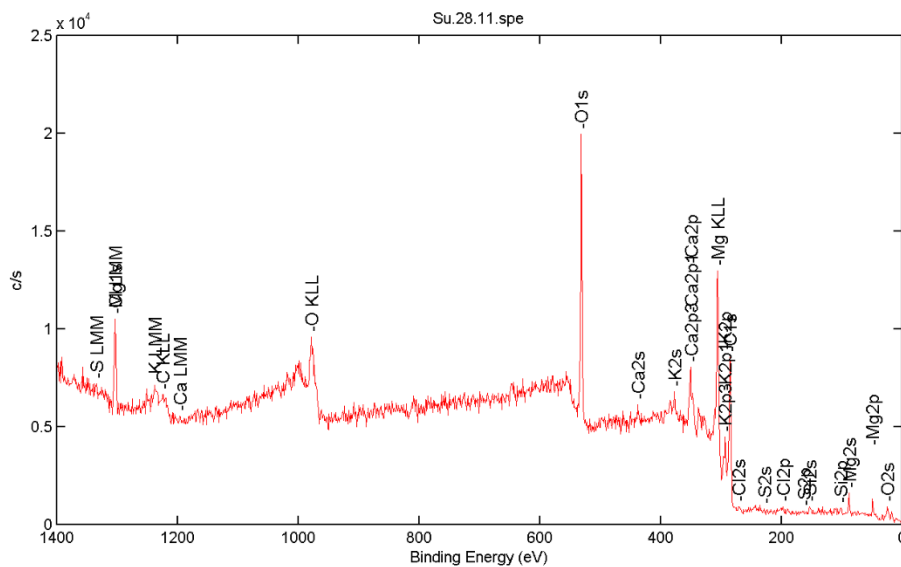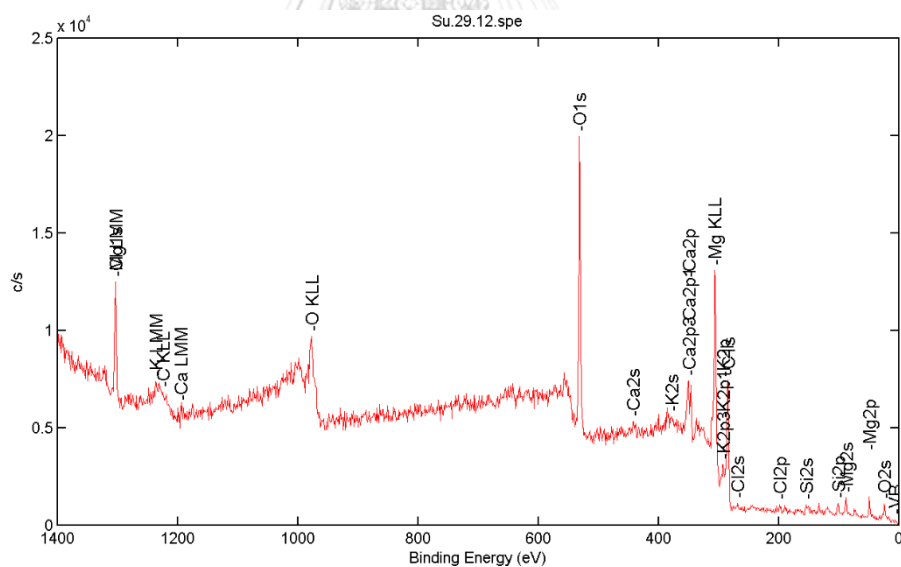

Figure D- 10 Full-scan XPS spectrum of activated carbon derived from potassium hydroxide activation with microwave radiation at 2 minutes and potassium hydroxide to carbonized water hyacinth mass ratio of 3:1 and adding water by soaking with potassium hydroxide solution

Figure D- 11 Full-scan XPS spectrum of activated carbon derived from potassium hydroxide activation with microwave radiation at 3 minutes and potassium hydroxide to carbonized water hyacinth mass ratio of 1:1 and adding water by soaking with potassium hydroxide solution
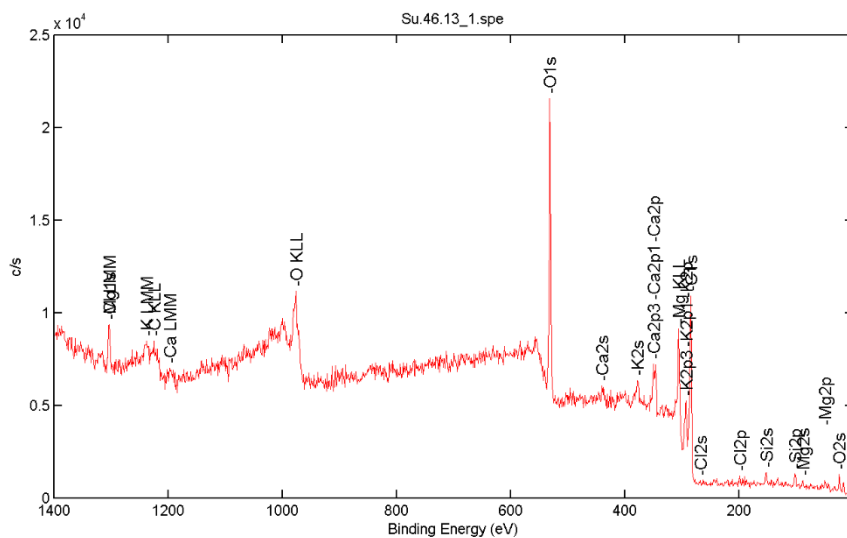

Figure D- 12 Full-scan XPS spectrum of activated carbon derived from potassium hydroxide activation with microwave radiation at 3 minutes and potassium hydroxide to carbonized water hyacinth mass ratio of 6:1 and adding water by soaking with potassium hydroxide solution

Figure D- 13 Full-scan XPS spectrum of activated carbon derived from potassium hydroxide activation with microwave radiation at 1 minutes and potassium hydroxide to carbonized water hyacinth mass ratio of 1:1 and adding water by soaking with potassium hydroxide solution together with wetting nitrogen gas
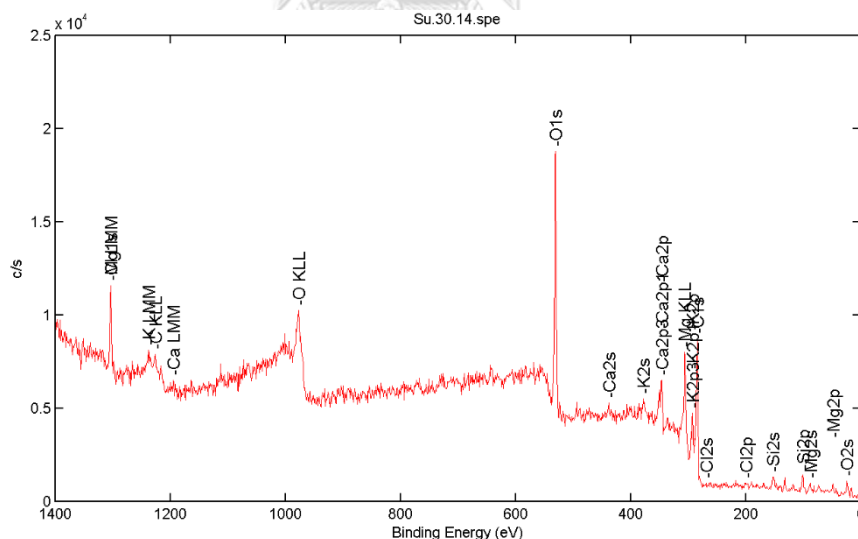

Figure D- 14 Full-scan XPS spectrum of activated carbon derived from potassium hydroxide activation with microwave radiation at 1 minutes and potassium hydroxide to carbonized water hyacinth mass ratio of 6:1 and adding water by soaking with potassium hydroxide solution together with wetting nitrogen gas
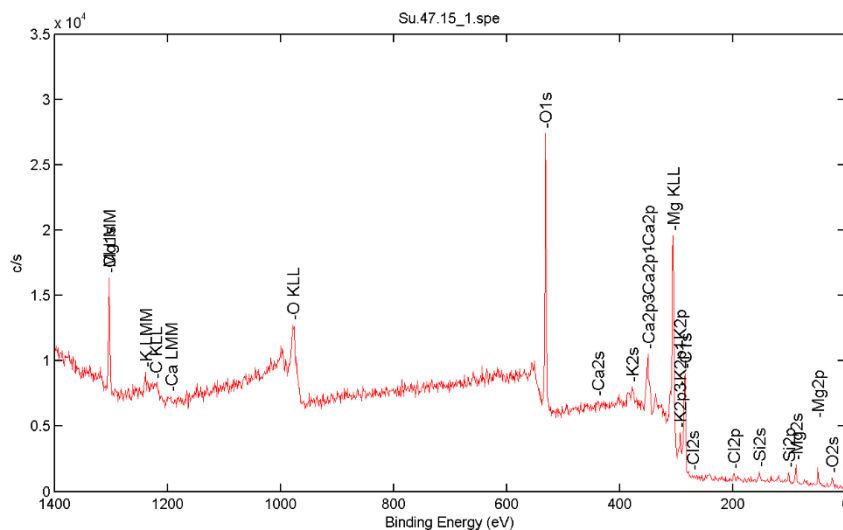
Figure D- 15 Full-scan XPS spectrum of activated carbon derived from potassium hydroxide activation with microwave radiation at 2 minutes and potassium hydroxide to carbonized water hyacinth mass ratio of 3:1 and adding water by soaking with potassium hydroxide solution together with wetting nitrogen gas
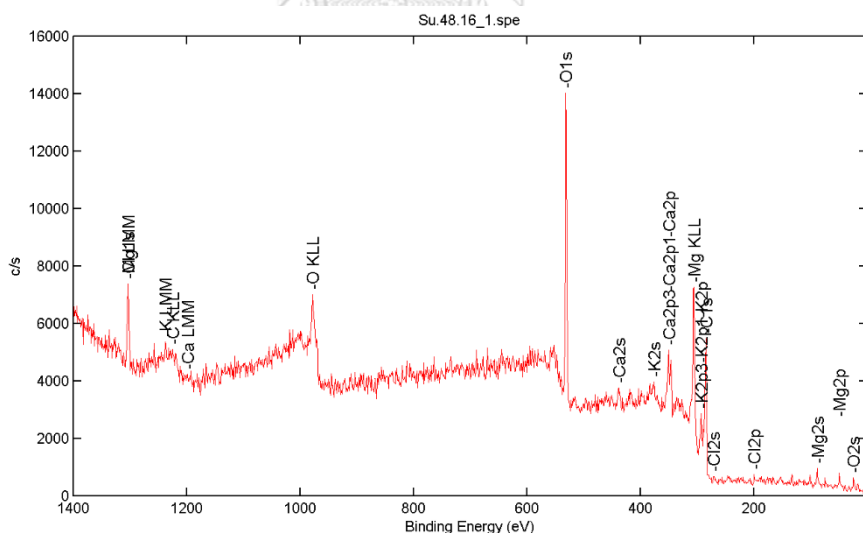

Figure D- 16 Full-scan XPS spectrum of activated carbon derived from potassium hydroxide activation with microwave radiation at 3 minutes and potassium hydroxide to carbonized water hyacinth mass ratio of 1:1 and adding water by soaking with potassium hydroxide solution together with wetting nitrogen gas
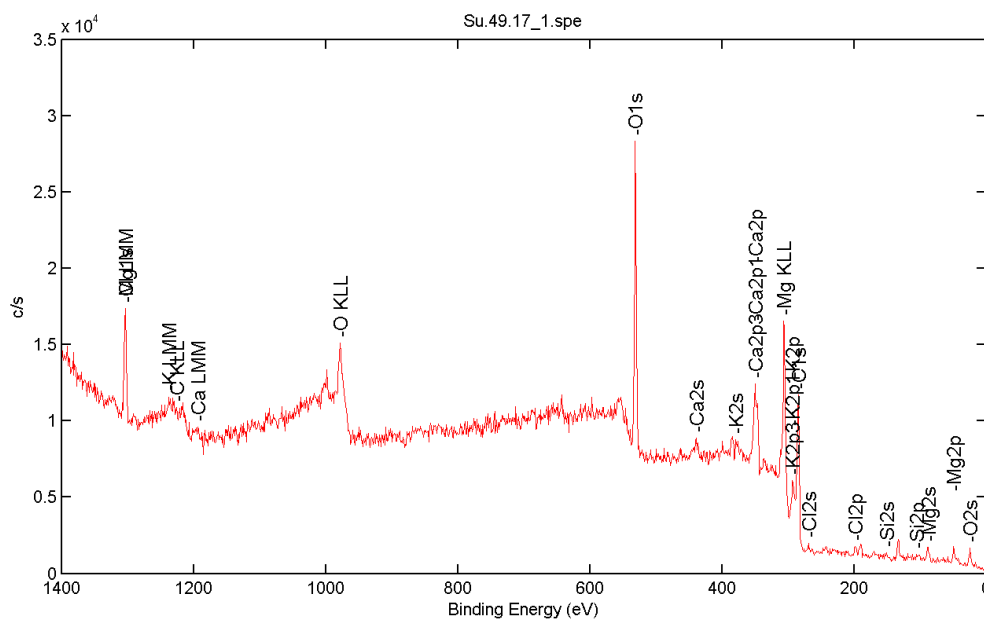
Figure D- 17 Full-scan XPS spectrum of activated carbon derived from potassium hydroxide activation with microwave radiation at 3 minutes and potassium hydroxide to carbonized water hyacinth mass ratio of 6:1 and adding water by soaking with potassium hydroxide solution together with wetting nitrogen gas

VITA

Purichaya Kuptajit was born on December 23th, 1993 in Bangkok, Thailand. She earned a Bachelor of Engineering Degree from the Department of Chemical Engineering, Chulalongkorn University., Thailand, in 2015. She then subsequently fulfilled the requirements for a Master of Engineering Degree at the Department of Chemical Engineering, Faculty of Engineering, Chulalongkorn University, Thailand in 2017.